Efficiency of Heat Engine of a Single Quantum Dot

Author: Yap Han Hoe

Supervisor: Prof. Wang Jian-Sheng

A thesis submitted in partial fulfilment of the requirements for the degree of Bachelor of Science with Honours in Physics

Department of Physics

Academic Year 2015/16

Abstract

We model a single-level quantum system connected to two reservoirs as a heat engine. A typical angle of attack is to assume weak system-bath coupling, so that one can study the system using a master equation. In this project, we follow Esposito [1] and use the non-equilibrium Green's function (NEGF) combined with first order gradient expansion to study this model. In so doing, no weak-coupling assumption is invoked and we obtain a quantum kinetic equation (QKE). From there, we discuss Esposito's definitions of energy, heat, entropy and external work. We then solve the QKE and study steady-state thermoelectric engine. Finally, we propose protocols for driven cyclic heat engine.

Acknowledgement

First and foremost, my heartfelt gratitude goes to Prof. Wang Jian-Sheng for providing me with this opportunity to explore NEGF and relearn thermodynamics. I also thank him for sharing with us his other expertises in mathematics and computing, as well as his experience of life as researcher.

Secondly, I am indebted to Prof. Gong Jiangbin and Prof. Christian Miniatura for the fruitful discussions we had regarding thermodynamic entropy, Dyson equation and my project in general.

Next, I am grateful to my mentor Dr. Juzar Thingna for his kind words of encouragement, for pointing out the problems of my mindset, and for teaching me to be open-minded to critiques.

I would also like to thank my fellow group members Mr. Xu Xiansong for his little library and advice, as well as Mr. Chen Ruofan for sharing his knowledge in physics. Throughout my life as a student, I benefited from discussions with my friends Mr. Sim Jun Yan and Ms. Sonya Maslovskaya in physics and mathematics. I sincerely acknowledge my high school teacher Mr. Low Meng Wha for igniting my passion in science.

Last but not least, I would like to thank my family for their unconditional love and support.

Contents

Introduction

Classical thermodynamics allows us to characterize a system consisting of 10^{23} particles with just a few variables [2]. Thanks to statistical mechanics, we now understand that this large number of particles is exactly what allows us to speak of the energy, volume of the system as averaged quantities. When we shrink the size of the system, a different approach should be adopted, and this falls under the scope of stochastic [3] or quantum [4] thermodynamics. Among the various topics in (stochastic or quantum) thermodynamics, one persistent question is the exchange of energy in strong coupling. Indeed, this was probably what initiated Esposito [5] to work on his new formalism of strongly (or non-weakly)-coupled quantum thermodynamics.

In the nineteenth century, the desire to improve steam engines was what motivated the pioneers (Carnot, Clausius, Joule among others) to establish the groundwork for thermodynamics. Indeed heat engines and thermodynamics are intimately connected: with Carnot cycles one can define a temperature scale [6], and in some idealized situations, it is even possible to formulate classical thermodynamics using Carnot cycles [7][8]. Naturally, with small-scale systems, one wishes to do the same: to harness our knowledge in constructing energy conversion devices, and reciprocally, to improve our understanding of thermodynamics with nano-heat engines.

Classical thermodynamics enjoys a certain universality similar to special relativity. To see this, compare Carnot's statement [7][9]:

> *Independently* of the working fluid, there is an *upper bound* to the efficiency of cyclic heat engines working between two thermal reservoirs.

with the following statement in special relativity [14]:

> In *any* inertial frame, the speed of light is the *same*.

On the other hand, sometimes, the studies on (stochastic or quantum) heat engines can be very model-dependent. For instance, one can consider a Brownian particle in a harmonic potential [10], a particle in a box [11], an interacting Bose gas [12], a chiral multiferroic chain [13] etc. Our project is of no exception. More precisely, we use a single-level quantum dot as our model and consider a steady-state thermoelectric engine and protocols for driven cyclic heat engine.

For ease of reading, here is the synopsis of this thesis: Chapter 1 sets the stage for a discussion of non-equilibrium Green's function (NEGF). More precisely, we begin with equilibrium Green's function and discuss how contour naturally arises. In Chapter 2, we first revisit NEGF applied to thermal transport. Supplemented with first-order gradient expansion, we obtain the expression for the retarded Green's function and a quantum kinetic equation describing the occupation of the single-level system. In Chapter 3, we provide motivations for the proposed definitions of thermodynamics that are not included in the original article. Chapter 4 discusses aspects of the quantum kinetic equation, as well as its exact and perturbative solution. With these, we consider steady-state regime in Chapter 5 and solve for the thermodynamic quantities and check its consistencies with linear irreversible thermodynamics. One important application of our model as a thermoelectric engine is then presented. Finally, Chapter 6 deals with the case of driven quantum dot and proposes protocols for cyclic heat engine.

The first two chapters constitute a large part of this project. For research articles, it would have been more appropriate to put them in Appendices, or simply not write them at all. However, these are indispensable for a thorough understanding of the backgrounds. For instance, by going through the derivations we see why this treatment does not require weak-coupling, and by observing the spectral function we see how energy level-broadening is being taken into account. The reader may wish to skip these technical details and start directly from Chapter 3, where extra thermodynamical aspects are discussed.

Chapter 1

Equilibrium Green's Function

As advocated by Haug and Jauho [15], NEGF is "structurally equivalent" to its equilibrium counterpart. Therefore, in the hope to highlight their similarities and to justify the need for NEGF, we first discuss equilibrium Green's function, which we divide into two cases: free-electron and general. In the former case, we introduce the notion of time-ordering and obtain the Green's function equation associated to the time-dependent Schrödinger equation. For the general case, by switching between pictures, we discuss how the need for contour naturally arises and how this can be avoided in the equilibrium case.

1.1 The Free-electron case

We have in mind a non-interacting thermal particle reservoir[1] at temperature T and chemical potential μ, whose Hamiltonian is given by

$$H = \sum_k \epsilon_k a_k^\dagger a_k. \tag{1.1}$$

As usual, a_k and $a_k^\dagger$ are the fermionic annihilation and creation operators for the k-th state. We thus define the $k-$th state free-electron Green's function as:

$$g_k(t_1, t_2) = -\frac{i}{\hbar} \left\langle \mathcal{T}_t\{a_k(t_1)a_k^\dagger(t_2)\} \right\rangle_0 . \tag{1.2}$$

In passing, we remark that, putting the $\mathcal{T}_t$ aside, this definition is similar to a two-point correlation function in statistics.

We shall now explain the notations involved. First of all, $\mathcal{T}_t$ is the time-ordering operator:

$$\mathcal{T}_t\{A(t_1)B(t_2)\} = \begin{cases} A(t_1)B(t_2) & \text{, if } t_1 > t_2, \\ -B(t_2)A(t_1) & \text{, if } t_2 > t_1, \\ A(t)B(t) & \text{, if } t_1 = t_2 = t. \end{cases} \tag{1.3}$$

[1] A thermal particle reservoir is one which can exchange energy and particle with the system, while keeping its energy and particle number practically unchanged.

where A, B are fermionic operators[2]. In Appendix C we elaborate further on the action of $\mathcal{T}_t$ on more than two operators.

We now proceed to define the averaging bracket:

$$\langle \dots \rangle_0 = \mathrm{Tr}[\rho_0 \dots] \tag{1.4}$$

where ρ_0 is the equilibrium density matrix describing the system or reservoir, given by:

$$\rho_0 = \frac{e^{-\beta(H-\mu N)}}{Z}. \tag{1.5}$$

Here and below $\beta = \frac{1}{k_B T}$ always denotes the inverse temperature. Z is the grand canonical partition function:

$$Z = \mathrm{Tr}[e^{-\beta(H-\mu N)}] \tag{1.6}$$

and N is the particle number operator:

$$N = \sum_k a_k^\dagger a_k. \tag{1.7}$$

Finally, we note that it is possible to expand the time-ordering operator in (1.2) as:

$$g_k(t_1, t_2) = -\frac{i}{\hbar}\left[\theta(t_1 - t_2)\left\langle\{a_k(t_1)a_k^\dagger(t_2)\}\right\rangle_0 - \theta(t_2 - t_1)\left\langle\{a_k^\dagger(t_2)a_k(t_1)\}\right\rangle_0\right]. \tag{1.8}$$

Given the above expression, we have the following equations of motion for the free-electron Green's function:

$$\begin{aligned}\left(i\hbar\frac{\partial}{\partial t_1} - \epsilon_k\right) g_k(t_1, t_2) &= \delta(t_1 - t_2),\\ \left(-i\hbar\frac{\partial}{\partial t_2} - \epsilon_k\right) g_k(t_1, t_2) &= \delta(t_2 - t_1).\end{aligned} \tag{1.9}$$

In equilibrium, one enjoys time-translational invariance: the free-electron Green's function depends on just one argument rather than two:

$$g_k(t_1, t_2) \xrightarrow{\text{equilibrium}} g_k(t_1 - t_2). \tag{1.10}$$

With $t = t_1 - t_2$, we thus obtain

$$\left(i\hbar\frac{\partial}{\partial t} - \epsilon_k\right) g_k(t) = \delta(t). \tag{1.11}$$

The moral of the story is that, in equilibrium, the time-ordering operator allows us to essentially recover the Green's function equation associated to the free-particle Schrödinger equation.

[2]A fermionic operator is an operator that can be expressed in terms of sums and products of fermionic creation and annihilation operators.

1.2 The General case

We now introduce a more general system whose Hamiltonian is given by:

$$\mathcal{H} = H_0 + V, \tag{1.12}$$

where H_0, like (1.1), is the reservoir (or unperturbed) Hamiltonian, V is an interaction term that renders the problem insoluble. Let $\left|\Phi_g\right\rangle$ denote the (second-quantized) ground state of the interacting system (1.12). Then, we define the Green's function for a $k-$state electron, when the ground state of (1.12) is $\left|\Phi_g\right\rangle$, as:

$$G_\Phi(t_1, t_2) = -\frac{i}{\hbar} \left\langle \Phi_g \right| \mathcal{T}_t\{a_\mathcal{H}(t_1) a^\dagger_\mathcal{H}(t_2)\} \left| \Phi_g \right\rangle \tag{1.13}$$

where we suppressed the state index k for notational brevity.

In definition (1.13), everything is in Heisenberg picture: the wavefunction $\left|\Phi_g\right\rangle$ is frozen in time, the subscript $\mathcal{H}$ of an operator O means that:

$$O_\mathcal{H}(t) = U^\dagger_\mathcal{H}(t, t_0) O(t) U_\mathcal{H}(t, t_0) \tag{1.14}$$

with $U_\mathcal{H}(t_1, t_2)$ the Heisenberg evolution operator[3]:

$$U_\mathcal{H}(t_1, t_2) = \mathcal{T}_t \exp\left[-\frac{i}{\hbar} \int_{t_1}^{t_2} \mathcal{H}(s)\, \mathrm{d}s \right]. \tag{1.15}$$

In (1.14), t_0 is the synchronization time[4] where all three (Schrödinger, Heisenberg, interaction) pictures coincide.

It is worthwhile to mention that, for the most general case, where the interacting ground state is not pure but described by a density matrix[5]:

$$\rho_g = \sum_\Phi p_\Phi \left|\Phi_g\right\rangle \left\langle \Phi_g \right|, \tag{1.16}$$

one would then calculate the Green's function using:

$$G = \sum_\Phi p_\Phi G_\Phi, \tag{1.17}$$

recovering thus the more familiar expression:

$$G(t_1, t_2) = -\frac{i}{\hbar} \mathrm{Tr}\left\{ \rho_g \mathcal{T}_t\{a_\mathcal{H}(t_1) a^\dagger_\mathcal{H}(t_2)\} \right\}. \tag{1.18}$$

[3] In equilibrium the Hamiltonian $\mathcal{H}$ has no explicit time-dependence, so there is no need for time-ordering since at each time it commutes with itself. However for consistency of notation to NEGF we shall keep $\mathcal{T}_t$ here.

[4] For the two time instants t_1, t_2 in (1.13), it is a common practice to choose $t_0 \leq \min(t_1, t_2)$: all time instants of interest are ulterior to the synchronization time.

[5] In other words, the interacting system is prepared in a classical statistical mixture.

The problem then is to calculate each G_Φ as in (1.13) which contains valuable information (spectral function, particle density, etc) of the system[6]. However, in its definition (1.13), we need to calculate the quantum-mechanical average of some operators (whose time-evolution we do not know) in the interacting ground state $\left|\Phi_g\right\rangle$ (which we do not know).

Thus in order to have an operational definition of the Green's function, we must perform a series of transformations. More precisely, we are going to put it in a form ready for perturbation expansion. First, we recall the definition of an operator in interaction picture:

$$O_I(t) = U_{H_0}^\dagger(t, t_0) O(t) U_{H_0}(t, t_0) \tag{1.19}$$

with $U_{H_0}(t_1, t_2)$ the evolution operator in interaction picture:

$$U_{H_0}(t_1, t_2) = \mathcal{T}_t \exp\left[-\frac{i}{\hbar}\int_{t_1}^{t_2} H_0(s)\,\mathrm{d}s\right]. \tag{1.20}$$

Combining (1.14) and (1.19), we obtain a relation connecting an operator in Heisenberg and interaction picture:

$$O_{\mathcal{H}}(t) = S^\dagger(t, t_0) O_I(t) S(t, t_0), \tag{1.21}$$

where the scattering matrix (or $S-$matrix) is defined as:

$$S(t_1, t_2) = U_{H_0}^\dagger(t_1, t_2) U_{\mathcal{H}}(t_1, t_2). \tag{1.22}$$

The Green's function then becomes:

$$G_\Phi(t_1, t_2) = -\frac{i}{\hbar}\left\langle\Phi_g\right| \mathcal{T}_t\Big\{[S^\dagger(t_1, t_0) a_I(t_1) S(t_1, t_0)][S^\dagger(t_2, t_0) a_I^\dagger(t_2) S(t_2, t_0)]\Big\}\left|\Phi_g\right\rangle. \tag{1.23}$$

By the properties of time-evolution operators (U and S), we thus have:

$$G_\Phi(t_1, t_2) = -\frac{i}{\hbar}\left\langle\Phi_g\right| \mathcal{T}_t\Big\{S(t_0, t_1) a_I(t_1) S(t_1, t_2) a_I^\dagger(t_2) S(t_2, t_0)\Big\}\left|\Phi_g\right\rangle. \tag{1.24}$$

A connection to NEGF is in place. Observing the terms inside the time-ordering operator, one could regard the operators as acting successively from $t_0 \longrightarrow t_2 \longrightarrow t_1$ then back to t_0. That is, they follow a contour on the time axis:

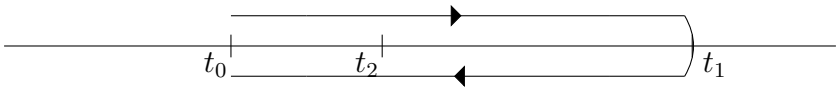

Figure 1.1: The contour followed by the operators in (1.24).

There is however no need for such contour in equilibrium: by a series of transformations, we can "deform" the contour so that it runs through the entire time-axis instead of turning around.

[6]Since by virtue of (1.17), the total Green's function would simply be a weighted average of each individual G_Φ.

We first exploit a clever trick of switching between the pictures. Since at the synchronization time all pictures coincide, we have:

$$\big|\Phi_g\big\rangle = \big|\Phi_I(t_0)\big\rangle$$

where the LHS is in Heisenberg picture, RHS in interaction picture. By construction, wavefunctions in the latter picture satisfy:

$$\big|\Phi_I(t_1)\big\rangle = S(t_1,t_2)\,\big|\Phi_I(t_2)\big\rangle\,. \tag{1.25}$$

Thus, by introducing two additional reference time instants: the distant past ($t=-\infty$) and far future ($t=+\infty$), we have:

$$\begin{aligned}\big|\Phi_I(t_0)\big\rangle &= S(t_0,-\infty)\,\big|\Phi_I(-\infty)\big\rangle\,,\\ \big\langle\Phi_I(t_0)\big| &= \big\langle\Phi_I(+\infty)\big|\,S(+\infty,t_0),\end{aligned} \tag{1.26}$$

which when inserted into (1.24) yields:

$$\begin{aligned}&G_\Phi(t_1,t_2)\\ &=-\frac{i}{\hbar}\,\big\langle\Phi_I(+\infty)\big|\,S(+\infty,t_0)\mathcal{T}_t\Big\{S(t_0,t_1)a_I(t_1)S(t_1,t_2)a_I^\dagger(t_2)S(t_2,t_0)\Big\}S(t_0,-\infty)\,\big|\Phi_I(-\infty)\big\rangle\,.\end{aligned} \tag{1.27}$$

In Appendix A we demonstrate that it is safe to include the two scattering matrices sandwiching the time-ordering operator $\mathcal{T}_t\Big\{\,\ldots\,\Big\}$ inside it:

$$\begin{aligned}&G_\Phi(t_1,t_2)\\ &=-\frac{i}{\hbar}\,\big\langle\Phi_I(+\infty)\big|\,\mathcal{T}_t\Big\{S(+\infty,t_1)a_I(t_1)S(t_1,t_2)a_I^\dagger(t_2)S(t_2,-\infty)\Big\}\,\big|\Phi_I(-\infty)\big\rangle\,.\end{aligned} \tag{1.28}$$

For an even more compact notation, we group the $S-$matrices together[7], writing:

$$G_\Phi(t_1,t_2)=-\frac{i}{\hbar}\,\big\langle\Phi_I(+\infty)\big|\,\mathcal{T}_t\Big\{a_I(t_1)a_I^\dagger(t_2)S(+\infty,-\infty)\Big\}\,\big|\Phi_I(-\infty)\big\rangle\,. \tag{1.29}$$

In order to proceed, we adopt a procedure called adiabatic switching-on-off [16], in which the Hamiltonian (1.12) is replaced by:

$$\mathcal{H}_\eta = H_0 + e^{-\eta|t-t_0|}V. \tag{1.30}$$

Here, $\eta>0$ is a number that will eventually be taken to be zero.

[7]In so doing, we have assumed that the interaction Hamiltonian in the interaction picture V_I contains only even powers of fermionic operators, so that when permuted around, the minus signs incurred always cancel out to leave the final result unchanged in sign.

Let us investigate the consequence of such replacement. First of all, for $\eta \longrightarrow 0$, we recover $\mathcal{H}$:

$$\lim_{\eta \to 0} \mathcal{H}_\eta = \mathcal{H}. \tag{1.31}$$

Next, for η small but not equal to zero:

$$\mathcal{H}_\eta = \begin{cases} H_0 & \text{when } t = -\infty, \\ H_0 + V & \text{when } t = t_0, \\ H_0 & \text{when } t = +\infty. \end{cases} \tag{1.32}$$

Since the rate of transition, η, is a small positive number, we deduce that $\mathcal{H}_\eta$ effectively represents a Hamiltonian where we adiabatically switch from H_0 to $H_0 + V$ then to H_0 again. Symbolically, the Green's function (1.29) becomes:

$$G^\eta_\Phi(t_1, t_2) = -\frac{i}{\hbar} \left\langle \Phi^\eta_I(+\infty) \right| \mathcal{T}_t \Big\{ a^\eta_I(t_1) a^{\eta\dagger}_I(t_2) S^\eta(+\infty, -\infty) \Big\} \left| \Phi^\eta_I(-\infty) \right\rangle \tag{1.33}$$

where we put a superscript η to remind ourselves that we replaced the Hamiltonian: $\mathcal{H} \longrightarrow \mathcal{H}_\eta$. Therefore, the interacting (Hamiltonian $H_0 + e^{-\eta|t-t_0|}V$) ground state at $t = -\infty$ is identical to the non-interacting (Hamiltonian H_0) ground state (denoted by $|\Phi_0\rangle$):

$$\left| \Phi^\eta_I(-\infty) \right\rangle = |\Phi_0\rangle \,. \tag{1.34}$$

Furthermore, the adiabatic switching-on-off ensures [17] that:

$$\left| \Phi^\eta_I(+\infty) \right\rangle = S^\eta(+\infty, -\infty) \left| \Phi^\eta_I(-\infty) \right\rangle \tag{1.35}$$

only differs from $\left| \Phi^\eta_I(-\infty) \right\rangle$ by a phase factor:

$$\left| \Phi^\eta_I(+\infty) \right\rangle = e^{i\Theta} \left| \Phi^\eta_I(-\infty) \right\rangle \tag{1.36}$$

with $\Theta \in \mathbb{R}$. By multiplying both sides by $\left\langle \Phi^\eta_I(-\infty) \right|$, we obtain:

$$e^{i\Theta} = \left\langle \Phi^\eta_I(-\infty) \right| S^\eta(+\infty, -\infty) \left| \Phi^\eta_I(-\infty) \right\rangle . \tag{1.37}$$

To sum up, we obtain:

$$\left\langle \Phi^\eta_I(+\infty) \right| = \frac{\left\langle \Phi^\eta_I(-\infty) \right|}{\left\langle \Phi^\eta_I(-\infty) \right| S^\eta(+\infty, -\infty) \left| \Phi^\eta_I(-\infty) \right\rangle} \tag{1.38}$$

which when plugged back into (1.33) gives:

$$G^\eta_\Phi(t_1, t_2) = -\frac{i}{\hbar} \frac{\left\langle \Phi^\eta_I(-\infty) \right| \mathcal{T}_t \Big\{ a^\eta_I(t_1) a^{\eta\dagger}_I(t_2) S^\eta(+\infty, -\infty) \Big\} \left| \Phi^\eta_I(-\infty) \right\rangle}{\left\langle \Phi^\eta_I(-\infty) \right| S^\eta(+\infty, -\infty) \left| \Phi^\eta_I(-\infty) \right\rangle} \tag{1.39}$$

and finally, using (1.34):

$$G^\eta_\Phi(t_1, t_2) = -\frac{i}{\hbar} \frac{\langle \Phi_0 | \, \mathcal{T}_t \Big\{ a^\eta_I(t_1) a^{\eta\dagger}_I(t_2) S^\eta(+\infty, -\infty) \Big\} | \Phi_0 \rangle}{\langle \Phi_0 | \, S^\eta(+\infty, -\infty) | \Phi_0 \rangle}. \tag{1.40}$$

By taking the limit $\eta \longrightarrow 0$, we simply drop the η indices, obtaining:

$$G_\Phi(t_1, t_2) = -\frac{i}{\hbar} \frac{\langle \Phi_0 | \, \mathcal{T}_t \Big\{ a_I(t_1) a^\dagger_I(t_2) S(+\infty, -\infty) \Big\} | \Phi_0 \rangle}{\langle \Phi_0 | \, S(+\infty, -\infty) | \Phi_0 \rangle} \tag{1.41}$$

where we have an expression of the equilibrium time-ordered Green's function which is ready for a perturbation expansion.

Chapter 2

Non-equilibrium Green's Function

Having discussed briefly the equilibrium Green's function, we now turn to NEGF proper. We first elaborate on the model, before the bread and butter of NEGF—the contour-ordered Green's function [18]—is defined. We then discuss the notion of contour [19], accompanied by a procedure called adiabatic switching-on, to obtain an expression of the contour-ordered Green's function ready for perturbation expansion. Next, we outline several consequences of Wick's theorem and Feynman diagrammatics that allow us to arrive at the Dyson equation. From there we show how to obtain Kadanoff-Baym equations [15]. Then, we introduce Wigner transform and gradient expansion [20], which will be applied to Kadanoff-Baym equations to solve for the retarded Green's function and obtain the equation of motion for the occupation probability of the single-level system.

2.1 The Model

Throughout this project, the terms "bath" and "reservoir", "single-level system" and "quantum dot" will be used interchangeably. We will be using the following simple model: a single-level (at energy ε) quantum system connected to two thermal electronic reservoirs (at chemical potentials $\mu_{L/R}$ and temperatures $T_{L/R}$).

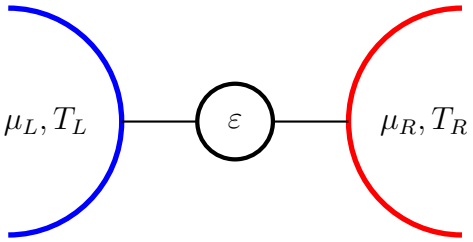

Figure 2.1: A single-level quantum system connected to two baths individually kept in equilibrium.

used prevalently in quantum transport and open quantum systems. The total Hamiltonian of the dot+bath is given by:

$$\mathcal{H} = H_d + H_B + H_T \tag{2.1}$$

where the Hamiltonian of the single-level quantum system is given by:

$$H_d = \varepsilon d^\dagger d, \tag{2.2}$$

the sum of the Hamiltonian of left (right) reservoir being:

$$\begin{aligned} H_B &= H_L + H_R \\ &= \sum_k \varepsilon_k c_k^\dagger c_k + \sum_j \varepsilon_j a_j^\dagger a_j \end{aligned} \tag{2.3}$$

and the tunneling Hamiltonian:

$$H_T = \sum_k [\gamma_k c_k^\dagger d + \gamma_k^* d^\dagger c_k] + \sum_j [\lambda_j a_j^\dagger d + \lambda_j^* d^\dagger a_j], \tag{2.4}$$

where we have used index k to indicate states in the left bath, j to indicate those in the right.

Normally, one has to specify how the energy levels (ε_k and ε_j) are being distributed, as well as the tunneling amplitudes (γ_k and λ_j). However, these details become unimportant under the wide-band approximation as we shall see later. Suffice it to say that, kept in chemical potentials $\mu_{L/R}$ and temperatures $T_{L/R}$, the electrons in the baths are non-interacting, and that the system-bath couplings are described quadratically in creation/annihilation operators. Finally, we stress that the terms $\varepsilon, \varepsilon_k, \varepsilon_j, V_k, V_j$ can all admit explicit time-dependences. In other words, they can be driven externally.

Since we will be doing perturbation expansion later, let us regroup the Hamiltonian (2.1) as:

$$\mathcal{H} = \underbrace{H_d + H_B}_{H_0} + \underbrace{H_T}_{V}. \tag{2.5}$$

For a closer look to H_0, we shall first introduce the Fock space describing the system and bath, which is split into three parts:

$$\mathscr{F}_{\text{total}} = \mathscr{F}_L \otimes \mathscr{F}_d \otimes \mathscr{F}_R \tag{2.6}$$

with $\mathscr{F}_{L(R)}$ the Fock space of left (right) bath, $\mathscr{F}_d$ the Fock space of the dot. Let us now consider H_0:

$$\begin{aligned} H_0 &= H_L + H_d + H_R \\ &= \sum_k \varepsilon_k c_k^\dagger c_k + \varepsilon d^\dagger d + \sum_j \varepsilon_j a_j^\dagger a_j. \end{aligned} \tag{2.7}$$

In this context, we should understand these terms as:

$$\begin{aligned} H_L &= \sum_k \varepsilon_k c_k^\dagger c_k \otimes \mathbb{1}_d \otimes \mathbb{1}_R, \\ H_d &= \mathbb{1}_L \otimes \varepsilon d^\dagger d \otimes \mathbb{1}_R, \\ H_R &= \mathbb{1}_L \otimes \mathbb{1}_d \otimes \sum_j \varepsilon_j a_j^\dagger a_j. \end{aligned} \tag{2.8}$$

We thus infer that H_0 simply describes the Hamiltonian of the baths and the single-level quantum system, treated as one composite but decoupled system.

2.2 Contour-ordered Green's function

Given the model, we can now define the contour-ordered Green's function. Before that, we recall that already in equilibrium theory, when switching from Heisenberg to interaction picture, one finds that, when read from right to left, the operators can be regarded as acting on a contour. We have seen that after some manipulations, such contour can be "deformed" to the entire real-time axis. One key recipe is the Gell-Mann and Low theorem [17], which exploits the fact that systems in equilibrium must also be in ground state. This is evidently not the case when studying non-equilibrium problems. Therefore, the necessity of a contour seems to be unavoidable, if a Green's function is to be defined for non-equilibrium problems.

2.2.1 Contour and Contour-ordering

In equilibrium, one major component in the definition of Green's function is the time-ordering operator $\mathcal{T}_t$. However, on a contour, time-ordering alone does not suffice to determine the precedence, as we can see in the Figure below[1]:

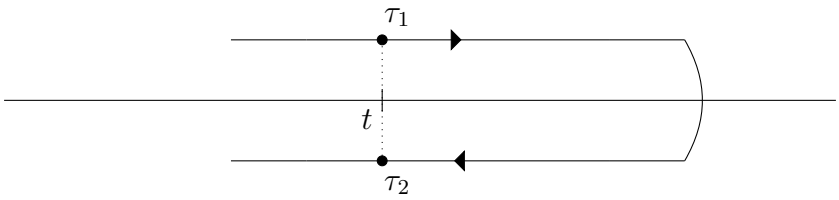

Figure 2.2: One real-time corresponds to two points on a contour.

Therefore, before we discuss contour precedence, let us consider a generic contour C:

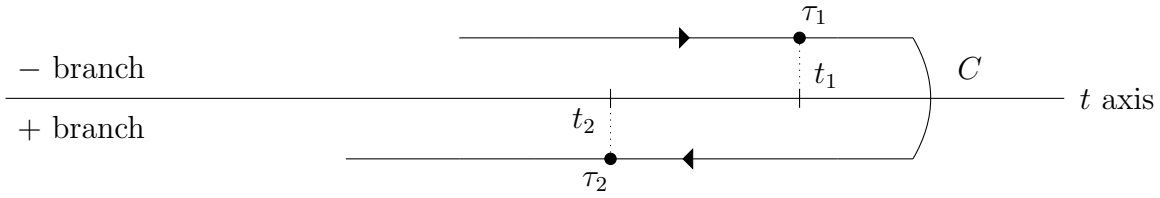

Figure 2.3: A generic contour in NEGF.

which describes an oriented path on the real-time axis. Each point on the contour C assumes a value[2] on $\mathbb{R} \times \{+1, -1\}$. For example:

$$\begin{aligned} \tau_1 &:= (t_1, \sigma_1) = (t_1, -), \\ \tau_2 &:= (t_2, \sigma_2) = (t_2, +), \end{aligned} \tag{2.9}$$

if the upper (lower) branch is assigned to be $-$ $(+)$, and we have written $\mp$ in place of ∓ 1.

[1] We only draw the contour off the real-time axis for illustration purpose. All contours should be understood as always staying on the real-time axis.

[2] Some authors define the contour on $\mathbb{C}$. A contour-time is then given by $\tau = t + i\eta$ with $t, \eta \in \mathbb{R}$ and η small. When one is done with contour, one would then take $\eta \longrightarrow 0$ to return to real-time.

With this consideration, we can define a binary relation $\succ$ to order contour times. Let $\tau = (t, \sigma)$ and $\tilde{\tau} = (\tilde{t}, \tilde{\sigma})$. We say that

$$\tau \succ \tilde{\tau}, \tag{2.10}$$

read as "τ succeeds $\tilde{\tau}$"[3], if

$$(\sigma > \tilde{\sigma}) \text{ or } (\sigma = \tilde{\sigma} \text{ and } t > \tilde{t}). \tag{2.11}$$

Using this relation, we see that $\tau_2 \succ \tau_1$ for both Figure 2.2 and Figure 2.3. Notice that in (2.11), we exclude the case where $\sigma = \tilde{\sigma}$ and $t = \tilde{t}$, that is, a contour time τ is not comparable with itself using the relation $\succ$. Next, we replace the real-time arguments by contour-times:

$$A(t) \longrightarrow A(\tau) \tag{2.12}$$

and define a contour-ordering operator $\mathcal{T}_\tau$ which arranges the later operators[4] to the left, obeying the anticommutation rule in case of fermionic operators. Using Figure 2.3 as example[5], let $A(\tau_1), B(\tau_2)$ be fermionic operators. We have:

$$\mathcal{T}_t\Big\{A(\tau_1)B(\tau_2)\Big\} = -B(\tau_2)A(\tau_1) \tag{2.13}$$

since $\tau_2 \succ \tau_1$.

2.2.2 Contour-ordered Green's function

With the above considerations in mind, we now define the contour-ordered Green's function of the system of interest (the dot):

$$G(\tau_1, \tau_2) = -\frac{i}{\hbar}\left\langle \mathcal{T}_\tau\Big\{d_{\mathcal{H}}(\tau_1)d^\dagger_{\mathcal{H}}(\tau_2)\Big\}\right\rangle_0, \tag{2.14}$$

where, as before, operators are in Heisenberg picture with respect to the fully-interacting Hamiltonian $\mathcal{H}$, and the averaging bracket is with respect to the frozen density matrix, ρ_0, at synchronization contour-time τ_0:

$$\langle \ldots \rangle_0 = \mathrm{Tr}[\rho_0 \ldots]. \tag{2.15}$$

With the same reasons as in the case of equilibrium, it is difficult, if not impossible, to calculate any term in definition (2.14). A series of transformations is then in place but before that, we observe that there is no mention of any contour in the definition. Thus, let us picture the general shape of contour on which $\mathcal{T}_\tau$ acts in (2.14). For that, we first switch to interaction picture:

$$\begin{aligned} d_{\mathcal{H}}(\tau_1) &= \mathcal{S}(\tau_0^+, \tau_1)d_I(\tau_1)\mathcal{S}(\tau_1, \tau_0^-), \\ d^\dagger_{\mathcal{H}}(\tau_2) &= \mathcal{S}(\tau_0^+, \tau_2)d^\dagger_I(\tau_2)\mathcal{S}(\tau_2, \tau_0^-), \end{aligned} \tag{2.16}$$

with

$$\tau_0^\pm = (t_0, \pm). \tag{2.17}$$

Notice that we have used the symbol $\mathcal{S}$ in place of S to refer to contour-time scattering matrices. We defer the discussion of what such object mean to Appendix C.

[3] Also "$\tilde{\tau}$ precedes τ", or "$\tilde{\tau}$ is earlier than τ" or "τ is later than $\tilde{\tau}$".

[4] That is, operators whose contour argument is later.

[5] We refer to Appendix B for more examples on contour-ordering.

The contour-ordered Green's function (2.14) then becomes:

$$G(\tau_1,\tau_2) = -\frac{i}{\hbar}\left\langle \mathcal{T}_\tau\Big\{\mathcal{S}(\tau_0^+,\tau_1)d_I(\tau_1)\mathcal{S}(\tau_1,\tau_2)d_I^\dagger(\tau_2)\mathcal{S}(\tau_2,\tau_0^-)\Big\}\right\rangle_0 . \tag{2.18}$$

We now see how a general contour[6] in (2.18) must look like[7]:

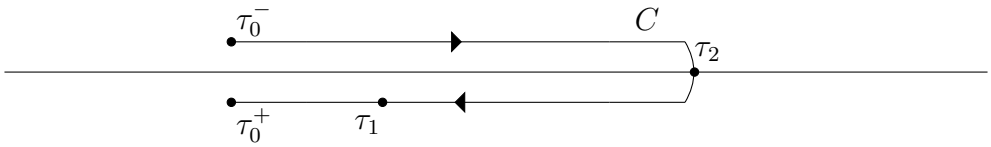

Figure 2.4: A general contour C involved in (2.18).

We now proceed with other transformations to obtain a calculable expression for the contour-ordered Green's function. Let us group the scattering matrices[8] into one, and write

$$\begin{aligned}&\mathcal{T}_\tau\Big\{\mathcal{S}(\tau_0^+,\tau_1)d_I(\tau_1)\mathcal{S}(\tau_1,\tau_2)d_I^\dagger(\tau_2)\mathcal{S}(\tau_2,\tau_0^-)\Big\}\\ =&\mathcal{T}_\tau\Big\{d_I(\tau_1)d_I^\dagger(\tau_2)\mathcal{S}_C(\tau_0^+,\tau_0^-)\Big\}\end{aligned} \tag{2.19}$$

where

$$\mathcal{S}_C(\tau_0^+,\tau_0^-) = \mathcal{T}_\tau \exp\left[-\frac{i}{\hbar}\int_C V_I(\tau)\,\mathrm{d}\tau\right]. \tag{2.20}$$

We show in Appendix C that as far as (2.19) is concerned, we can extend the contour in Figure 2.4 to the following one:

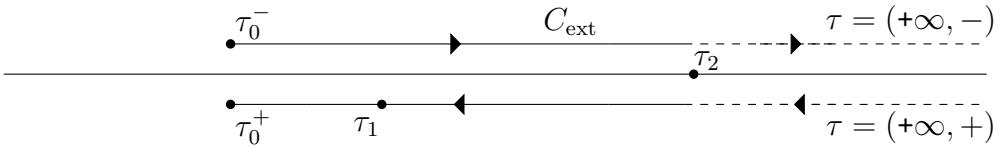

Figure 2.5: An extended contour C_{ext} from Figure 2.4.

resulting in:

$$G(\tau_1,\tau_2) = -\frac{i}{\hbar}\left\langle \mathcal{T}_\tau\Big\{d_I(\tau_1)d_I^\dagger(\tau_2)\mathcal{S}_{C_{\text{ext}}}(\tau_0^+,\tau_0^-)\Big\}\right\rangle_0 \tag{2.21}$$

with

$$\mathcal{S}_{C_{\text{ext}}}(\tau_0^+,\tau_0^-) = \mathcal{T}_\tau \exp\left[-\frac{i}{\hbar}\int_{C_{\text{ext}}} V_I(\tau)\,\mathrm{d}\tau\right]. \tag{2.22}$$

The motivation for extending C to C_{ext} is: when brought back to real-time, for contour C, one would have to write $\max(t_1,t_2)$ for the upper bounds of integrals, whereas for contour C_{ext} it would simply be $t = +\infty$.

[6]Of course, Figure 2.4 is only for illustration purpose: τ_1,τ_2 need not be ordered this way in general.

[7]In drawing Figure 2.4, we placed τ_2 on the real-time axis without distinguishing whether it is on the upper or lower branch, but it does not matter since $\tau_1 \succ \tau_2$ for both cases.

[8]Since the tunneling Hamiltonian $V = H_T$ (cf. (2.4)) is quadratic in fermionic operators, permuting the scattering matrices does not result in any minus sign.

Next, we attack the averaging bracket $\langle \dots \rangle_0$. In the spirit of perturbation theory, it would be desirable to average with respect to H_0:

$$\langle \dots \rangle_{\text{-}\infty} \stackrel{?}{=} \mathrm{Tr}[\rho_{\text{-}\infty} \dots] \tag{2.23}$$

where the composite decoupled system has separable equilibrium density matrix[9]:

$$\begin{aligned} \rho_{\text{-}\infty} &= \rho_L \otimes \rho_d \otimes \rho_R \\ &= \frac{e^{\beta_L(H_L - \mu_L N_L)}}{Z_L} \otimes \left[p_d \left|0\right\rangle \left\langle 0\right| + (1-p_d) \left|1\right\rangle \left\langle 1\right| \right] \otimes \frac{e^{\beta_R(H_R - \mu_R N_R)}}{Z_R} \end{aligned} \tag{2.24}$$

with p_d the occupation probability of the single-level quantum dot, N, β, μ, Z the usual quantities (cf. Section 1.1).

In order for (2.23) to be realised, analogous to the equilibrium case, we adopt an adiabatic switching-on (not on-off) procedure. For the sake of discussion we revert to real-time. The Hamiltonian $\mathcal{H}$ is replaced by:

$$\mathcal{H}_\eta = \begin{cases} H_0 + e^{\eta|t-t_0|}V & \text{if } t \leq t_0 \\ H_0 + V & \text{if } t > t_0 \end{cases} \tag{2.25}$$

Hence, for $t = \text{-}\infty$, the tunneling term V is turned off, and the density matrix (in all pictures) describing the Hamiltonian $\mathcal{H}_\eta(\text{-}\infty) = H_0$ will be given by (2.24). Using the same trick that at the synchronization time t_0, all pictures coincide, the frozen Heisenberg density matrix ρ_0 is related to the interaction-picture density matrix $\rho_I(t)$ by[10]:

$$\rho_0 = S(t_0, t)\rho_I(t)S(t, t_0). \tag{2.26}$$

Thus by taking $t = \text{-}\infty$ we have:

$$\begin{aligned} \rho_0 &= S(t_0, \text{-}\infty)\rho_I(\text{-}\infty)S(\text{-}\infty, t_0) \\ &= S(t_0, \text{-}\infty)\rho_{\text{-}\infty}S(\text{-}\infty, t_0). \end{aligned} \tag{2.27}$$

Referring back to (2.21), we have:

$$\begin{aligned} &\left\langle \mathcal{T}_\tau \Big\{ d_I(\tau_1) d_I^\dagger(\tau_2) \mathcal{S}_{C_{\text{ext}}}(\tau_0^+, \tau_0^-) \Big\} \right\rangle_0 \\ =&\mathrm{Tr}\left[\rho_0 \mathcal{T}_\tau \Big\{ d_I(\tau_1) d_I^\dagger(\tau_2) \mathcal{S}_{C_{\text{ext}}}(\tau_0^+, \tau_0^-) \Big\} \right] \\ =&\mathrm{Tr}\left[\Big[S(t_0, \text{-}\infty)\rho_{\text{-}\infty}S(\text{-}\infty, t_0) \Big] \mathcal{T}_\tau \Big\{ d_I(\tau_1) d_I^\dagger(\tau_2) \mathcal{S}_{C_{\text{ext}}}(\tau_0^+, \tau_0^-) \Big\} \right] \\ =&\mathrm{Tr}\left[\rho_{\text{-}\infty}S(\text{-}\infty, t_0) \mathcal{T}_\tau \Big\{ d_I(\tau_1) d_I^\dagger(\tau_2) \mathcal{S}_{C_{\text{ext}}}(\tau_0^+, \tau_0^-) \Big\} S(t_0, \text{-}\infty) \right] \end{aligned} \tag{2.28}$$

[9]The density matrix ρ_S of a composite system $S = S_1 \cup S_2$ is separable if it can be factored into density matrices ρ_1, ρ_2 describing the constituent systems which make up the total one: $\rho_S = \rho_1 \otimes \rho_2$.

[10]Unlike in the equilibrium case (cf. Equation (1.33) onwards), we do not put η superscript for simpler notation.

where for the last line we exploited the cyclic property of trace. The next step is to promote the real-time $S-$matrices to contour-time $\mathcal{S}-$matrices[11]:

$$\begin{aligned} S(t_0, \text{-}\infty) &\longrightarrow \mathcal{S}(\tau_0^-, \text{-}\infty^-), \\ S(\text{-}\infty, t_0) &\longrightarrow \mathcal{S}(\text{-}\infty^+, \tau_0^+), \end{aligned} \tag{2.30}$$

so that the last line in (2.28) becomes:

$$\mathrm{Tr}\left[\rho_{\text{-}\infty}\mathcal{S}(\text{-}\infty^+, \tau_0^+)\mathcal{T}_\tau\Big\{d_I(\tau_1)d_I^\dagger(\tau_2)\mathcal{S}_{C_{\text{ext}}}(\tau_0^+, \tau_0^-)\Big\}\mathcal{S}(\tau_0^-, \text{-}\infty^-)\right]. \tag{2.31}$$

We have encountered similar expression in the equilibrium case (cf. Equation (1.27)), and by a same argument as in Appendix A, the sandwiching $\mathcal{S}-$matrices can be combined into the $\mathcal{T}_\tau\Big\{\ \dots\ \Big\}$ term, giving:

$$\mathrm{Tr}\left[\rho_{\text{-}\infty}\mathcal{T}_\tau\Big\{\mathcal{S}(\text{-}\infty^+, \tau_0^+)d_I(\tau_1)d_I^\dagger(\tau_2)\mathcal{S}_{C_{\text{ext}}}(\tau_0^+, \tau_0^-)\mathcal{S}(\tau_0^-, \text{-}\infty^-)\Big\}\right]. \tag{2.32}$$

Since the $\mathcal{S}-$matrices involve even powers of fermionic operators, they can be permuted around freely under the $\mathcal{T}_\tau$ sign without incurring change of sign. Thus we group them together into one term:

$$\mathcal{S}_{\mathcal{C}}(\text{-}\infty^+, \text{-}\infty^-) \tag{2.33}$$

where $\mathcal{C}$ is the following Schwinger-Keldysh contour:

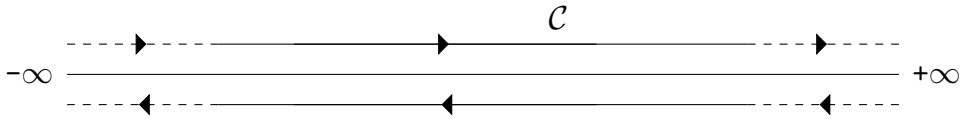

Figure 2.6: Schwinger-Keldysh contour: a loop over the entire real axis.

Finally for the contour-ordered Green's function we have:

$$G(\tau_1, \tau_2) = -\frac{i}{\hbar}\mathrm{Tr}\left[\rho_{\text{-}\infty}\mathcal{T}_\tau\Big\{d_I(\tau_1)d_I^\dagger(\tau_2)\mathcal{S}_{\mathcal{C}}(\text{-}\infty^+, \text{-}\infty^-)\Big\}\right]. \tag{2.34}$$

The transformation is not yet finished: in the next section we will be drawing Feynman diagrams, and we will need a denominator to cancel disconnected diagrams. We return to (2.24) and write:

$$\rho_{\text{-}\infty} = \frac{e^{\beta_L(H_L - \mu_L N_L)} \otimes \left[p_d \left|0\right\rangle\left\langle 0\right| + (1-p_d)\left|1\right\rangle\left\langle 1\right|\right] \otimes e^{\beta_R(H_R - \mu_R N_R)}}{Z_L Z_R} \tag{2.35}$$

[11] There are, of course, several ways for this to be done, for example:

$$\begin{aligned} S(t_0, \text{-}\infty) &\longrightarrow \mathcal{S}(\tau_0^+, \text{-}\infty^+) \\ S(\text{-}\infty, t_0) &\longrightarrow \mathcal{S}(\text{-}\infty^-, \tau_0^-) \end{aligned} \tag{2.29}$$

but (2.29) is certainly the most useful one.

where we have exploited the multilinearity of $\otimes$. On the other hand, since

$$\mathrm{Tr}\Big[p_d \left|0\right\rangle \left\langle 0\right| + (1-p_d)\left|1\right\rangle \left\langle 1\right|\Big] = 1, \tag{2.36}$$

the product of partition function Z_L and Z_R can be written as

$$\begin{aligned} Z_L Z_R &= \mathrm{Tr}\Big[e^{\beta_L(H_L-\mu_L N_L)}\Big]\ \mathrm{Tr}\Big[p_d \left|0\right\rangle \left\langle 0\right| + (1-p_d)\left|1\right\rangle \left\langle 1\right|\Big]\ \mathrm{Tr}\Big[e^{\beta_R(H_R-\mu_R N_R)}\Big] \\ &= \mathrm{Tr}\Big[e^{\beta_L(H_L-\mu_L N_L)} \otimes \big[p_d \left|0\right\rangle \left\langle 0\right| + (1-p_d)\left|1\right\rangle \left\langle 1\right|\big] \otimes e^{\beta_R(H_R-\mu_R N_R)}\Big] \end{aligned} \tag{2.37}$$

because $\mathrm{Tr}[A\otimes B] = \mathrm{Tr}[A]\ \mathrm{Tr}[B]$. We now write

$$\tilde{\rho}_{\text{-}\infty} = e^{\beta_L(H_L-\mu_L N_L)} \otimes \big[p_d \left|0\right\rangle \left\langle 0\right| + (1-p_d)\left|1\right\rangle \left\langle 1\right|\big] \otimes e^{\beta_R(H_R-\mu_R N_R)} \tag{2.38}$$

so that we have

$$\rho_{\text{-}\infty} = \frac{\tilde{\rho}_{\text{-}\infty}}{\mathrm{Tr}[\tilde{\rho}_{\text{-}\infty}]}. \tag{2.39}$$

We now multiply from left by $S(t_0, \text{-}\infty)$, from right by $S(\text{-}\infty, t_0)$. By virtue of (2.27), we obtain:

$$\rho_0 = S(t_0, \text{-}\infty)\frac{\tilde{\rho}_{\text{-}\infty}}{\mathrm{Tr}[\tilde{\rho}_{\text{-}\infty}]} S(\text{-}\infty, t_0). \tag{2.40}$$

We now move the denominator to the LHS and promote the operators to contour time:

$$\rho_0(\tau_0)\mathrm{Tr}[\tilde{\rho}_{\text{-}\infty}] = \mathcal{S}(\tau_0, \text{-}\infty^-)\tilde{\rho}_{\text{-}\infty}\mathcal{S}(\text{-}\infty^+, \tau_0). \tag{2.41}$$

Recall that ρ_0 is the density matrix associated to $\mathcal{H}_\eta$ at time t_0. Despite its unknown complexity, being a density matrix, ρ_0 must be normalised: $\mathrm{Tr}[\rho_0] = 1$. Therefore it follows that

$$\mathrm{Tr}[\tilde{\rho}_{\text{-}\infty}] = \mathrm{Tr}\left[\mathcal{S}(\tau_0, \text{-}\infty^-)\tilde{\rho}_{\text{-}\infty}\mathcal{S}(\text{-}\infty^+, \tau_0)\right]. \tag{2.42}$$

Using the cyclicity of trace, we have:

$$\mathrm{Tr}[\tilde{\rho}_{\text{-}\infty}] = \mathrm{Tr}[\tilde{\rho}_{\text{-}\infty}\mathcal{S}_{\mathcal{C}}(\text{-}\infty^+, \text{-}\infty^-)]. \tag{2.43}$$

With (2.39), this becomes:

$$\mathrm{Tr}[\rho_{\text{-}\infty}\mathcal{S}_{\mathcal{C}}(\text{-}\infty^+, \text{-}\infty^-)] = 1. \tag{2.44}$$

Referring back to (2.34), we obtain:

$$G(\tau_1, \tau_2) = -\frac{i}{\hbar}\frac{\mathrm{Tr}\left[\rho_{\text{-}\infty}\mathcal{T}_\tau\Big\{d_I(\tau_1)d_I^\dagger(\tau_2)\mathcal{S}_{\mathcal{C}}(\text{-}\infty^+, \text{-}\infty^-)\Big\}\right]}{\mathrm{Tr}\left[\rho_{\text{-}\infty}\mathcal{S}_{\mathcal{C}}(\text{-}\infty^+, \text{-}\infty^-)\right]} \tag{2.45}$$

where we now have a denominator which allows us to cancel disconnected diagrams later on.

2.3 Dyson equation

Having expressed the contour-ordered Green's function as:

$$G(\tau,\tau') = -\frac{i}{\hbar}\frac{\left\langle \mathcal{T}_\tau\Big\{ d_I(\tau) d_I^\dagger(\tau')\mathcal{S}_\mathcal{C}(-\infty^+,-\infty^-)\Big\}\right\rangle}{\left\langle \mathcal{S}_\mathcal{C}(-\infty^+,-\infty^-)\right\rangle}, \tag{2.46}$$

where $\langle \dots \rangle$ means average in decoupled system+bath, $\mathrm{Tr}[\rho_{-\infty}\dots]$, we shall now begin with the perturbation expansion. First and foremost, we will suppress the I subscripts, while being fully aware that all operators are in interaction picture. For convenience we rewrite the expression for the $\mathcal{S}-$matrix:

$$\begin{aligned}\mathcal{S}_\mathcal{C}(-\infty^+,-\infty^-) &= \mathcal{T}_\tau \exp\left[-\frac{i}{\hbar}\int_\mathcal{C} V_I(\tau)\,\mathrm{d}\tau\right] \\ &= \mathcal{T}_\tau\left\{\sum_{n=0}^{+\infty}\frac{1}{n!}\left(-\frac{i}{\hbar}\int_\mathcal{C} V_I(\tau)\,\mathrm{d}\tau\right)^n\right\}.\end{aligned} \tag{2.47}$$

Therefore we have for the numerator of (2.46):

$$\begin{aligned}-\frac{i}{\hbar}\left\langle \mathcal{T}_\tau\Big\{ d_I(\tau) d_I^\dagger(\tau')\mathcal{S}_\mathcal{C}(-\infty^+,-\infty^-)\Big\}\right\rangle &= -\frac{i}{\hbar}\left\langle \mathcal{T}_\tau\left\{ dd^{\dagger\prime}\sum_{n=0}^{+\infty}\frac{1}{n!}\left(-\frac{i}{\hbar}\int_\mathcal{C} V_I(\tau)\,\mathrm{d}\tau\right)^n\right\}\right\rangle \\ &= G_0 + G_1 + G_2 + G_3 + G_4 + \dots\end{aligned} \tag{2.48}$$

where each G_n indicates the $n-$th power of the exponential expansion. We recall as well the interaction term:

$$V = H_T = \sum_k [\gamma_k c_k^\dagger d + \gamma_k^* d^\dagger c_k] + \sum_j [\lambda_j a_j^\dagger d + \lambda_j^* d^\dagger a_j]. \tag{2.49}$$

2.3.1 Wick's theorem

An expression like (2.48) is impossible to evaluate, not without Wick's theorem. We shall use the following shorthand notation[12]:

$$\begin{aligned} d &= d(\tau), \\ d^{\dagger\prime} &= d^\dagger(\tau'), \\ V_n &= V(\tau_n), \\ A_n \ \text{ or } \ A(n) &= A(\tau_n), \end{aligned} \tag{2.50}$$

where A is any of $c, d, a, c^\dagger, d^\dagger, a^\dagger$. Returning to the expansion (2.48), clearly,

$$G_0 = -\frac{i}{\hbar}\langle \mathcal{T}_\tau\{dd^{\dagger\prime}\}\rangle \tag{2.51}$$

[12] As a reminder, index n labels the contour time, whereas indices k (j) refer to the electron state in left (right) reservoir.

is the free Green's function of the system when it is decoupled from the baths. The original statement of Wick's theorem is of combinatoric nature. We refer to Fetter and Walecka [21] for an excellent exposition and we shall only state its consequences[13] as we go along with examples. First of all, we have:

Consequence 1. *All odd orders in* (2.48) *vanish, i.e.* $G_{2n+1} = 0$ *for* $n \in \mathbb{N}$.

We thus begin with the calculation of G_2. The multiplication between two V would normally mix the left $c, c^\dagger$ and right $a, a^\dagger$ operators, however we have

Consequence 2. *Under the action of* $\langle \mathcal{T}_\tau\{\dots\}\rangle$*, each operator must be paired with its adjoint for a non-vanishing contribution to* G_n.

to the rescue. That is, terms such as $\langle dd^{\dagger\prime} c_1^\dagger d_1 d_2^\dagger a_2\rangle$ vanish because $c_1^\dagger$ and a_2 are unpaired with their respective adjoints.

Hence, for G_2 at least, we can concentrate on one bath, say the left, and add up the right one to obtain the total G_2:

$$G_2 = G_2^{\text{left}} + G_2^{\text{right}} \tag{2.52}$$

We have:

$$G_2^{\text{left}} = \frac{1}{2}\left(-\frac{i}{\hbar}\right)^3 \sum_{k_i,k_j} \int_{\mathcal{C}}\int_{\mathcal{C}} \Big\langle \mathcal{T}_\tau \Big\{ dd^{\dagger\prime}\Big[\gamma_{k_i}(1)c_{k_i}^\dagger(1)d_1 + \gamma_{k_i}^*(1)d_1^\dagger c_{k_i}(1)\Big] \times \Big[\gamma_{k_j}(2)c_{k_j}^\dagger(2)d_2 + \gamma_{k_j}^*(2)d_2^\dagger c_{k_j}(2)\Big]\Big\}\Big\rangle \,\mathrm{d}\tau_1\mathrm{d}\tau_2 \tag{2.53}$$

Thanks to Consequence 2 again, terms like $\langle dd^{\dagger\prime} c_{k_i}^\dagger(1) d_1 d_2^\dagger c_{k_j}(2)\rangle$ vanish for $k_i \neq k_j$. Therefore the summation over different states k_i, k_j essentially reduces to just one:

$$G_2^{\text{left}} = \frac{1}{2}\left(-\frac{i}{\hbar}\right)^3 \sum_{k} \int_{\mathcal{C}}\int_{\mathcal{C}} \Big\langle \mathcal{T}_\tau \Big\{ dd^{\dagger\prime}\Big(\Big[\gamma_k(1)c_k^\dagger(1)d_1\Big]\Big[\gamma_k^*(2)d_2^\dagger c_k(2)\Big] + \Big[\gamma_k^*(1)d_1^\dagger c_k(1)\Big]\Big[\gamma_k(2)c_k^\dagger(2)d_2\Big]\Big)\Big\}\Big\rangle \,\mathrm{d}\tau_1\mathrm{d}\tau_2 \tag{2.54}$$

We shall consider only the first term inside the round bracket, as the treatment for the other is exactly the same. Let us focus on the braket $\langle \mathcal{T}_\tau\{\dots\}\rangle$ by moving the scalar tunneling amplitudes γ aside, and arrange the operators into two groups, one of d and another of c:

$$\Big\langle \mathcal{T}_\tau \Big\{ \Big[dd^{\dagger\prime} d_1 d_2^\dagger\Big]\Big[-c_k(2)c_k^\dagger(1)\Big]\Big\}\Big\rangle \tag{2.55}$$

Thus far, we have only used the fact that fermionic operators anticommute inside $\mathcal{T}_\tau\{\dots\}$. We next introduce

[13] Together with the fact that averaging is done with respect to the decoupled system+bath density matrix, as well as several other that we will highlight whenever necessary.

Consequence 3. *Under $\langle \mathcal{T}_\tau\{\dots\}\rangle$, the chain of operators rearrange and split into sum of products of $\langle \mathcal{T}_\tau\{c_k c_k^\dagger\}\rangle$, $\langle \mathcal{T}_\tau\{dd^\dagger\}\rangle$, $\langle \mathcal{T}_\tau\{a_j a_j^\dagger\}\rangle$ only*[14].

To illustrate,

$$\begin{aligned}
&-\left\langle \mathcal{T}_\tau\left\{dd^{\dagger\prime}d_1d_2^\dagger c_k(2)c_k^\dagger(1)\right\}\right\rangle \\
&=-\left\langle \mathcal{T}_\tau\{dd^{\dagger\prime}\}\right\rangle\left\langle \mathcal{T}_\tau\{d_1d_2^\dagger\}\right\rangle\left\langle \mathcal{T}_\tau\{c_k(2)c_k^\dagger(1)\}\right\rangle \\
&+\left\langle \mathcal{T}_\tau\{dd_2^\dagger\}\right\rangle\left\langle \mathcal{T}_\tau\{d_1d^{\dagger\prime}\}\right\rangle\left\langle \mathcal{T}_\tau\{c_k(2)c_k^\dagger(1)\}\right\rangle
\end{aligned} \tag{2.56}$$

For notational simplicity, let us drop the k index. We also adopt the following notation:

$$-\frac{i}{\hbar}\left\langle \mathcal{T}_\tau\{\dots\}\right\rangle = \langle\dots\rangle \tag{2.57}$$

As an example, by multiplying both sides by the cube of $-\frac{i}{\hbar}$, the RHS of (2.56) will be written as:

$$-\langle dd^{\dagger\prime}\rangle\langle d_1d_2^\dagger\rangle\langle c_2c_1^\dagger\rangle+\langle dd_2^\dagger\rangle\langle d_1d^{\dagger\prime}\rangle\langle c_2c_1^\dagger\rangle \tag{2.58}$$

If we repeat the procedure for the other term in (2.54), we obtain:

$$\begin{aligned}
G_2^{\text{left}}=\frac{1}{2}\sum\int_{\mathcal{C}}\int_{\mathcal{C}}\Bigg\{&\gamma_1\gamma_2^*\Big[-\langle dd^{\dagger\prime}\rangle\langle d_1d_2^\dagger\rangle\langle c_2c_1^\dagger\rangle+\langle dd_2^\dagger\rangle\langle d_1d^{\dagger\prime}\rangle\langle c_2c_1^\dagger\rangle\Big] \\
&+\gamma_1^*\gamma_2\Big[-\langle dd^{\dagger\prime}\rangle\langle d_2d_1^\dagger\rangle\langle c_1c_2^\dagger\rangle+\langle dd_1^\dagger\rangle\langle d_2d^{\dagger\prime}\rangle\langle c_1c_2^\dagger\rangle\Big]\Bigg\}\,\mathrm{d}\tau_1\mathrm{d}\tau_2
\end{aligned} \tag{2.59}$$

where the summation is over the states assumed by c, whose k subscript is suppressed. We remark that the expression above is symmetric when we permute $1\leftrightarrow 2$. Indeed, the contour times τ_1,τ_2, being integration variables, are dummy in the sense that it does not matter if we change their names: $\tau_1\leftrightarrow\tau_2$, since we will be performing the contour integral $\int_{\mathcal{C}}\int_{\mathcal{C}}\dots d\tau_1 d\tau_2$. Therefore, the second line is actually identical to the first, which sums up to cancel the one-half factor in front:

$$G_2^{\text{left}}=\sum\int_{\mathcal{C}}\int_{\mathcal{C}}\gamma_1\gamma_2^*\Big[-\langle dd^{\dagger\prime}\rangle\langle d_1d_2^\dagger\rangle\langle c_2c_1^\dagger\rangle+\langle dd_2^\dagger\rangle\langle d_1d^{\dagger\prime}\rangle\langle c_2c_1^\dagger\rangle\Big]\,\mathrm{d}\tau_1\mathrm{d}\tau_2 \tag{2.60}$$

Similarly, for the contribution from right bath, we have:

$$G_2^{\text{right}}=\sum\int_{\mathcal{C}}\int_{\mathcal{C}}\lambda_1\lambda_2^*\Big[-\langle dd^{\dagger\prime}\rangle\langle d_1d_2^\dagger\rangle\langle a_2a_1^\dagger\rangle+\langle dd_2^\dagger\rangle\langle d_1d^{\dagger\prime}\rangle\langle a_2a_1^\dagger\rangle\Big]\,\mathrm{d}\tau_1\mathrm{d}\tau_2 \tag{2.61}$$

In fact the above is also true for higher order terms, when we focus on only one bath. More precisely, for a generic even term G_{2n}, let us write

$$G_{2n}=G_{2n}^{\text{left}}+G_{2n}^{\text{mixed}}+G_{2n}^{\text{right}} \tag{2.62}$$

where for example G_{2n}^{left} contains only $c,d,c^\dagger,d^\dagger$ but not $a,a^\dagger$. Then we have:

Consequence 4. *For G_{2n}^{left} and G_{2n}^{right}, except for τ,τ', all contour arguments τ_n can be permuted freely to cancel the $\frac{1}{n!}$ in expansion* (2.48).

[14]This "only" is to emphasize that we need only to split the operators in such a way that each c,d,a is paired with its adjoint and none else. For instance, adopting notation (2.57), in (2.56) there is no $\langle dd_1\rangle\langle d^{\dagger\prime}d_2^\dagger\rangle\langle c_2c_1^\dagger\rangle$ as the first two brackets vanish, cf. Consequence 2.

2.3.2 Feynman diagram

In our perturbation expansion, for each interaction term V there is a sum of four quadratic operators[15]. Evidently the higher order terms become all the more complicated. To handle them efficiently, let us introduce the celebrated bookkeeping device called Feynman diagram. We draw Feynman diagrams using the following rules [22]:

$\langle dd^{\dagger\prime}\rangle =$ 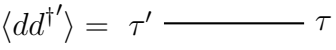

$\langle c_i c_j^\dagger\rangle =$ 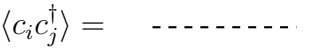

$\langle a_k a_\ell^\dagger\rangle =$ 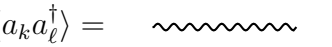

In words: d operators are connected by solid line, c operators by dashed line, a operators by wiggly line. They all are unoriented. When drawing the diagrams, except for τ, τ', we can drop the contour labels since they are integrated anyway. We notice in passing that the diagrams correspond respectively to the free Green's function of system, left bath, right bath. Using these rules, we have:

$\langle dd^{\dagger\prime}\rangle \langle d_1 d_2^\dagger\rangle \langle c_2 c_1^\dagger\rangle =$ 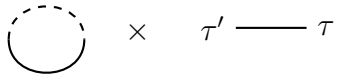

(2.63)

Diagram of the above kind is said to be disconnected. It can be factored into the free Green's function multiplied by another diagram, without being connected by any line. When collected and summed up, these diagrams become the so-called vacuum diagram and is exactly the denominator in (2.46). Therefore, we have

Consequence 5. *Disconnected diagrams factor out and get cancelled by the denominator in* (2.46)*.*

Thus disconnected diagrams will not contribute to the series expansion (2.48) and we shall only focus on connected diagrams. For the second order term, the connected diagrams are from the left and right bath:

$\langle dd_2^\dagger\rangle \langle c_2 c_1^\dagger\rangle \langle d_1 d^{\dagger\prime}\rangle =$ 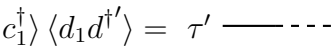

$\langle dd_2^\dagger\rangle \langle a_2 a_1^\dagger\rangle \langle d_1 d^{\dagger\prime}\rangle =$ 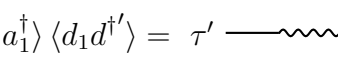

(2.64)

Therefore, G_2 is given by the sum of the above, multiplied by appropriate tunneling amplitudes $\gamma_1\gamma_2^*$ and $\lambda_1\lambda_2^*$, and integrated over τ_1, τ_2. We stress that there is a summation over the centre dashed and wiggly lines[16].

Let us list the fourth order connected diagrams:

$\langle dd_2^\dagger\rangle \langle c_2 c_3^\dagger\rangle \langle d_3 d_4^\dagger\rangle \langle c_4 c_1^\dagger\rangle \langle d_1 d^{\dagger\prime}\rangle =$ 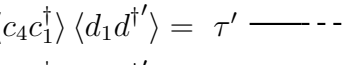

(2.65)

$\langle dd_2^\dagger\rangle \langle a_2 a_3^\dagger\rangle \langle d_3 d_4^\dagger\rangle \langle a_4 a_1^\dagger\rangle \langle d_1 d^{\dagger\prime}\rangle =$ 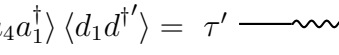

(2.66)

[15]These then need to be summed over the states of left/right bath.

[16]This corresponds to summing the different states k, j in the left and right bath.

Again, there is an implicit multiplication with tunneling amplitudes, integration, and summation over states. Then, (2.65) and (2.66) are respectively G_4^{left} and G_4^{right} in (2.62). We now turn to G_4^{mixed}. The only non-vanishing diagram is:

$$\langle dd_2^\dagger\rangle \langle c_2 c_1^\dagger\rangle \langle d_1 d_4^\dagger\rangle \langle a_4 a_3^\dagger\rangle \langle d_3 d^{\dagger\prime}\rangle =$$

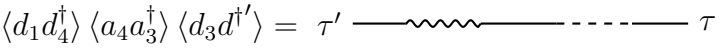

(2.67)

Unlike G_4^{left} and G_4^{right}, G_4^{mixed} is twice the above diagram. We mentioned time and again that the order of $1, 2, 3, 4$ does not matter as they are integration variables. Therefore, there is a corresponding diagram:

$$\langle dd_4^\dagger\rangle \langle a_4 a_3^\dagger\rangle \langle d_3 d_2^\dagger\rangle \langle c_2 c_1^\dagger\rangle \langle d_1 d^{\dagger\prime}\rangle =$$

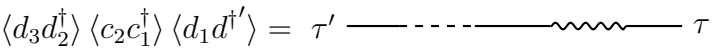

(2.68)

which is identical to (2.67) after integration. Thus, instead of writing

$$G_4^{\text{mixed}} = 2 \times$$

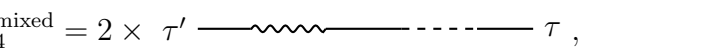

(2.69)

let us write

$$G_4^{\text{mixed}} =$$

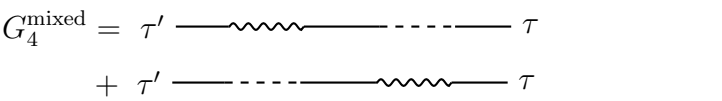

(2.70)

To summarize, up to fourth order we have:

$$G(\tau,\tau') =$$

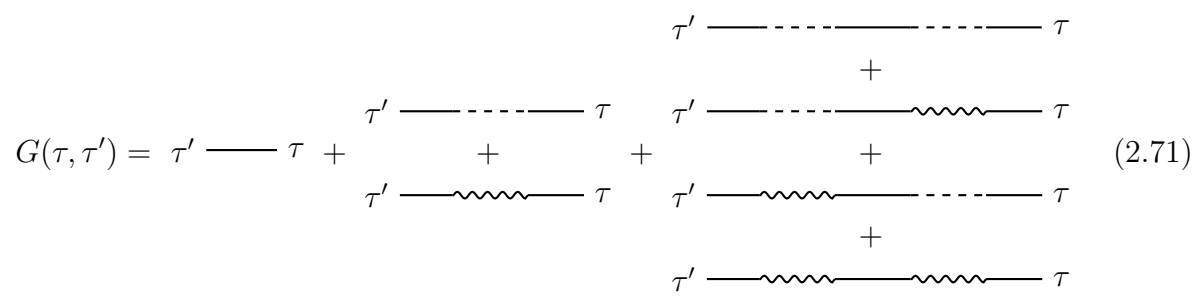

(2.71)

Alternatively, dropping the τ, τ' for simplicity:

$$G =$$

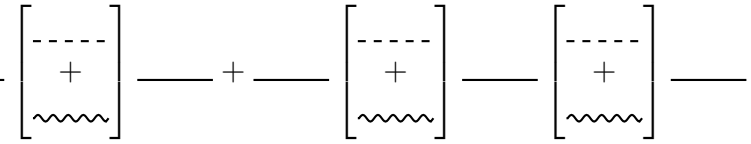

(2.72)

The above shows us the usefulness of Feynman diagram: it allows for a clearer representation of expansion (2.48), rather than chains of brackets. We proceed to define the self energy:

$$\Sigma(\tau,\tau') =$$

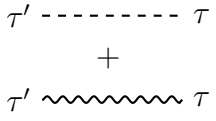

(2.73)

Recalling that solid line is just the decoupled system Green's function, we can write (2.72) in a more compact manner:

$$G = g + g\Sigma g + g\Sigma g\Sigma g. \tag{2.74}$$

We stopped at fourth order, but if we continue the expansion, the combinatorics magically work out [21][22] to give the following:

$$\begin{aligned} G &= g + g\Sigma g + g\Sigma g\Sigma g + g\Sigma g\Sigma g\Sigma g + \dots \\ &= g + g\Sigma\Big(g + g\Sigma g + g\Sigma g\Sigma g + \dots\Big) \\ &= g + g\Sigma G. \end{aligned} \tag{2.75}$$

We have chosen one particular way, but the other is equally valid:

$$\begin{aligned} \cdots + g\Sigma g\Sigma g\Sigma g + g\Sigma g\Sigma g + g\Sigma g + g &= G \\ \Big(\cdots + g\Sigma g\Sigma g + g\Sigma g\Big)\Sigma g + g &= \\ .G\Sigma g + g &= \end{aligned} \tag{2.76}$$

The above two symbolic equations, (2.75) and (2.76), are called Dyson equation. What they really mean is:

$$\begin{aligned} G(\tau,\tau') &= g(\tau,\tau') + \int_{\mathcal{C}}\int_{\mathcal{C}} \mathrm{d}\tau_1\mathrm{d}\tau_2\; g(\tau,\tau_1)\Sigma(\tau_1,\tau_2)G(\tau_2,\tau'), \\ G(\tau,\tau') &= g(\tau,\tau') + \int_{\mathcal{C}}\int_{\mathcal{C}} \mathrm{d}\tau_1\mathrm{d}\tau_2\; G(\tau,\tau_1)\Sigma(\tau_1,\tau_2)g(\tau_2,\tau'), \end{aligned} \tag{2.77}$$

with the total self energy being the sum of that of the left and right bath:

$$\Sigma(\tau_1,\tau_2) = \Sigma_L(\tau_1,\tau_2) + \Sigma_R(\tau_1,\tau_2). \tag{2.78}$$

Here,

$$\Sigma_L(\tau_1,\tau_2) = \sum_k \gamma_k(\tau_1) g_k^c(\tau_1,\tau_2)\gamma_k^*(\tau_2) \tag{2.79}$$

with the left reservoir $k-$th state free electron Green's function:

$$g_k^c(\tau_1,\tau_2) = -\frac{i}{\hbar}\left\langle \mathcal{T}_\tau\{c_k(\tau_1)c_k^\dagger(\tau_2)\}\right\rangle. \tag{2.80}$$

For completeness, at the expense of brevity we provide the analogous expressions for the right self energy:

$$\Sigma_R(\tau_1,\tau_2) = \sum_j \lambda_j(\tau_1) g_j^a(\tau_1,\tau_2)\lambda_j^*(\tau_2) \tag{2.81}$$

and the right reservoir $j-$th state free electron Green's function:

$$g_j^a(\tau_1,\tau_2) = -\frac{i}{\hbar}\left\langle \mathcal{T}_\tau\{a_j(\tau_1)a_j^\dagger(\tau_2)\}\right\rangle. \tag{2.82}$$

Let us briefly recap what happened: we started with the definition of contour-ordered Green's function, then performed a series of transformations so that we could series-expand it. With Wick's theorem and Feynman diagram analysis, we obtained Dyson equation which we would like to solve. We shall devote the following sections to that end.

2.4 Projections of Dyson equation

The Dyson equation (2.77) is a pair of integral equations, the integrals being defined on a contour. To understand better what exactly does a contour integral[17] mean, we must discuss the precedence of the two contour times τ_1, τ_2.

2.4.1 Greater and lesser Green's functions

Thus, we return to the contour-ordered Green's function $G(\tau_1, \tau_2)$, cf. (2.46). As usual let σ_1, σ_2 be the branch index of τ_1, τ_2. Thanks to the contour-ordering operator $\mathcal{T}_\tau$, the Green's function can be one of the two[18]:

$$G(\tau_1, \tau_2) = \begin{cases} -\frac{i}{\hbar} \left\langle d(\tau_1) d^\dagger(\tau_2) \right\rangle & \text{, if } \sigma_1 > \sigma_2 \\ +\frac{i}{\hbar} \left\langle d^\dagger(\tau_2) d(\tau_1) \right\rangle & \text{, if } \sigma_2 > \sigma_1. \end{cases} \tag{2.83}$$

For the first one, contour time τ_1 (τ_2) lies on lower (upper) branch and the second one is the reverse. When the contour-times are brought back to real-times, their frequent appearances have earned them definitions, known respectively as greater Green's function $G^>$ and lesser Green's function $G^<$:

$$\begin{aligned} G^>(t_1, t_2) &= -\frac{i}{\hbar} \left\langle d(\tau_1) d^\dagger(\tau_2) \right\rangle, \\ G^<(t_1, t_2) &= +\frac{i}{\hbar} \left\langle d^\dagger(\tau_2) d(\tau_1) \right\rangle. \end{aligned} \tag{2.84}$$

Of course, such definitions are not limited to G: every function defined based on $\mathcal{T}_\tau$ [19] shares these so-called greater and lesser projections.

2.4.2 Lesser projection of a double product

Since the terms involved in the integrand: g, Σ, G all contain contour-ordering operators, it follows that Dyson equation (2.77) can be projected into greater or lesser component, depending on the precedence of τ_1, τ_2. In order to study the projection of triple product, we need to start with double product. In particular, we first discuss its lesser projection. Suppose we have contour-ordered functions A, B, C, with the symbolic relation $C = AB$, meaning:

$$C(\tau_1, \tau_2) = \int_{\mathcal{C}} \mathrm{d}\tau \; A(\tau_1, \tau) B(\tau, \tau_2). \tag{2.85}$$

Recall that the Schwinger-Keldysh contour $\mathcal{C}$ was obtained by extending from $\max(t_1, t_2)$ to $+\infty$. Here for simplicity let us return to the original contour[20] $\mathscr{C}$. If $\tau_2 \succ \tau_1$, to fix idea, let us set $t_1 > t_2$. Graphically:

[17] In the sense of NEGF, not complex analysis.

[18] There are actually two more cases associated to $\sigma_1 = \sigma_2$ which will give us time and anti time-ordered Green's functions but we will not be needing them in this project.

[19] As well as those defined based on $\mathcal{T}_t$ in the equilibrium case.

[20] This will not affect the contour-ordered functions A, B, C, cf. Appendix C

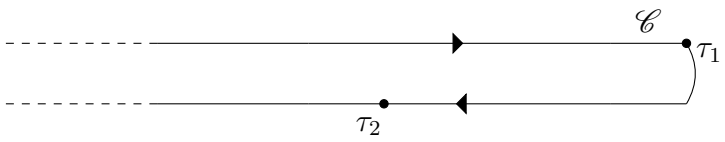

Figure 2.7: The contour $\mathscr{C}$ involved in (2.85).

Notice that much like in ordinary integrals, we can deform $\mathscr{C}$ into the following:

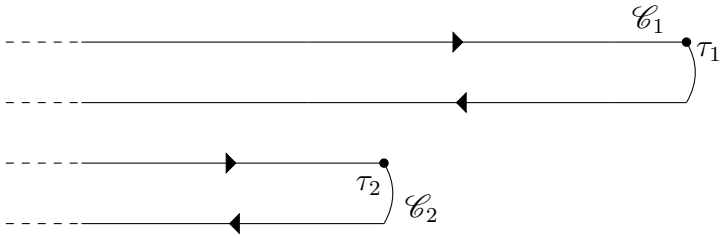

Figure 2.8: Deformed contour $\mathscr{C}_1 \cup \mathscr{C}_2$ from $\mathscr{C}$.

without changing the result of the contour integral AB. The advantage in so doing is the following: on $\mathscr{C}_1$, as the integration variable τ runs, it is always earlier than τ_2. Therefore[21] $B(\tau, \tau_2) = B^<(\tau, \tau_2)$ on $\mathscr{C}_1$. Similarly, on $\mathscr{C}_2$, τ is always later than τ_1 so $A(\tau_1, \tau) = A^<(\tau_1, \tau)$. Combining, we have:

$$\int_{\mathcal{C}} \mathrm{d}\tau\ A(\tau_1,\tau)B(\tau,\tau_2) = \int_{\mathscr{C}_1} \mathrm{d}\tau\ A(\tau_1,\tau)B^<(\tau,\tau_2) + \int_{\mathscr{C}_2} \mathrm{d}\tau\ A^<(\tau_1,\tau)B(\tau,\tau_2). \tag{2.86}$$

Let us now focus on the first term on the RHS. We have, upon splitting: $\mathscr{C}_1 = (-\infty^-, t_1^-) \cup (t_1^+, -\infty^+)$, and considering the precedence to project A into $A^<$ or $A^>$:

$$\begin{aligned}\int_{\mathscr{C}_1} \mathrm{d}\tau\ A(\tau_1,\tau)B^<(\tau,\tau_2) &= \int_{-\infty}^{t_1} \mathrm{d}t\ A^>(t_1,t)B^<(t,t_2) + \int_{t_1}^{-\infty} \mathrm{d}t\ A^<(t_1,t)B^<(t,t_2) \\ &= \int_{-\infty}^{t_1} \mathrm{d}t\ \Big(A^>(t_1,t) - A^<(t_1,t)\Big)B^<(t,t_2) \\ &= \int_{-\infty}^{+\infty} \mathrm{d}t\ \Big[\theta(t_1,t)\Big(A^>(t_1,t) - A^<(t_1,t)\Big)\Big]B^<(t,t_2).\end{aligned} \tag{2.87}$$

We shall not repeat the case for $\mathscr{C}_2$ but only provide the result here:

$$\int_{\mathscr{C}_2} \mathrm{d}\tau\ A^<(\tau_1,\tau)B(\tau,\tau_2) = \int_{-\infty}^{+\infty} \mathrm{d}t\ A^<(t_1,t)\Big[-\theta(t_2-t)\Big(B^>(t,t_2) - B^<(t,t_2)\Big)\Big]. \tag{2.88}$$

We studied the case ($\tau_2 \succ \tau_1$ and $t_1 > t_2$). The other case ($\tau_2 \succ \tau_1$ and $t_2 > t_1$) gives the same result and we have:

$$\begin{aligned}C^<(t_1,t_2) = &\int_{-\infty}^{+\infty} \mathrm{d}t\ \Big[\theta(t_1,t)\Big(A^>(t_1,t) - A^<(t_1,t)\Big)\Big]B^<(t,t_2) \\ &+ \int_{-\infty}^{+\infty} \mathrm{d}t\ A^<(t_1,t)\Big[-\theta(t_2-t)\Big(B^>(t,t_2) - B^<(t,t_2)\Big)\Big].\end{aligned} \tag{2.89}$$

[21] We mentioned previously that to write $B^<$, both contour-times must have been projected back to real-times, but here let us slightly abuse the notation.

2.4.3 Advanced and retarded Green's functions

The above combinations of greater and lesser components appear equally often in NEGF. This leads us to introduce the advanced Green's function G^A and retarded Green's function G^R:

$$\begin{aligned} G^A(t_1,t_2) &= -\theta(t_2-t_1)\Big(G^>(t_1,t_2)-G^<(t_1,t_2)\Big) \\ &= +\frac{i}{\hbar}\theta(t_2-t_1)\left\langle\{d(t_1),d^\dagger(t_2)\}\right\rangle, \\ G^R(t_1,t_2) &= +\theta(t_1-t_2)\Big(G^>(t_1,t_2)-G^<(t_1,t_2)\Big) \\ &= -\frac{i}{\hbar}\theta(t_1-t_2)\left\langle\{d(t_1),d^\dagger(t_2)\}\right\rangle, \end{aligned} \tag{2.90}$$

where $\{\cdot,\cdot\}$ is the anticommutator. Using the shorthand notation (multiplication means appropriate convolution), we have:

$$C^< = A^R B^< + A^< B^A. \tag{2.91}$$

From the definition (2.90) we infer that one way to obtain the retarded projection is by calculating their lesser and greater projections. Therefore we will also need the greater projection, whose calculation is similar to the lesser:

$$C^> = A^R B^> + A^> B^A. \tag{2.92}$$

To obtain the retarded projection, we need to combine (2.91) and (2.92). For simplicity we shall drop the two-time dependences wherever possible:

$$\begin{aligned} &C^R(t_1,t_2) \\ &= \theta(t_1-t_2)\Big(C^>(t_1,t_2)-C^<(t_1,t_2)\Big) \\ &= \theta(t_1-t_2)\Big[\int_{\mathbb{R}}\mathrm{d}t\,\left(A^RB^>+A^>B^A\right)-\int_{\mathbb{R}}\mathrm{d}t\,\left(A^RB^<+A^<B^A\right)\Big] \\ &= \theta(t_1-t_2)\int_{\mathbb{R}}\mathrm{d}t\,\left[\theta(t_1-t)(A^>-A^<)(B^>-B^<)-\theta(t_2-t)(A^>-A^<)(B^>-B^<)\right]. \end{aligned} \tag{2.93}$$

On the other hand, with some patience we observe that:

$$\begin{aligned} \theta(t_1-t_2)\theta(t_2-t) &= \theta(t_1-t_2)\theta(t_1-t)\theta(t_2-t) \\ &= \theta(t_1-t_2)\theta(t_1-t)\Big(1-\theta(t-t_2)\Big) \\ &= \theta(t_1-t_2)\theta(t_1-t)-\theta(t_1-t_2)\theta(t_1-t)\theta(t-t_2) \\ &= \theta(t_1-t_2)\theta(t_1-t)-\theta(t_1-t)\theta(t-t_2). \end{aligned} \tag{2.94}$$

Therefore,

$$\theta(t_1-t_2)\left[\theta(t_1-t)-\theta(t_2-t)\right] = \theta(t_1-t)\theta(t-t_2) \tag{2.95}$$

and for the retarded projection we have:

$$\begin{aligned} C^R(t_1,t_2) &= \int_{\mathbb{R}} \mathrm{d}t\ \theta(t_1-t)\theta(t-t_2)(A^> - A^<)(B^> - B^<) \\ &= \int_{\mathbb{R}} \mathrm{d}t\ A^R(t_1,t)B^R(t,t_2). \end{aligned} \tag{2.96}$$

The advanced projection is obtained similarly. Using the shorthand notation, we have:

$$\begin{aligned} C^R &= A^R B^R \\ C^A &= A^A B^A. \end{aligned} \tag{2.97}$$

2.4.4 Projections of triple product

We are now ready to attack the case of triple product which appears in Dyson equation. Suppose we have four contour-ordered functions satisfying $D = ABC$, which means as usual:

$$D(\tau_1,\tau_2) = \int_{\mathcal{C}}\int_{\mathcal{C}} \mathrm{d}\tau \mathrm{d}\tilde{\tau}\ A(\tau_1,\tau)B(\tau,\tilde{\tau})C(\tilde{\tau},\tau_2). \tag{2.98}$$

To obtain the lesser projection, we first treat $E = AB$ as a contour-ordered function, then $D = EC$ and the projection rules for double product apply:

$$\begin{aligned} D^< &= E^R C^< + E^< C^A \\ &= (AB)^R C^< + (AB)^< C^A. \end{aligned} \tag{2.99}$$

Now we have another double product AB and the projection rules apply:

$$\begin{aligned} (AB)^R C^< + (AB)^< C^A &= A^R B^R C^< + \Big(A^R B^< + A^< B^A\Big) C^A \\ &= A^R B^R C^< + A^R B^< C^A + A^< B^A C^A. \end{aligned} \tag{2.100}$$

The retarded projection for a triple product is then trivial:

$$D^R = A^R B^R C^R. \tag{2.101}$$

These projection rules are collectively known as Langreth's rule or analytic continuation. We began with Dyson equation, discussed how to obtain its lesser/greater and retarded/advanced projections. These projections of Green's function are not completely independent, and it turns out that $G^<$ and G^R correspond respectively to particle number and spectral function. These two are the only ones that we need from G, at least in this project. Hence in the following, we shall bear in mind that our goal is to solve for $G^<$ and G^R.

2.5 Kadanoff-Baym equations

After projections into lesser and retarded components, Dyson equations are still integral equations. To facilitate Wigner transform, we need to convert them into integro-differential equations, known as the Kadanoff-Baym equations. Firstly, we return to the

retarded component of Dyson equation:

$$\begin{aligned} G^R(t_1,t_2) &= g^R(t_1,t_2) + \int\int \mathrm{d}t'\mathrm{d}t''\, g^R(t_1,t')\Sigma^R(t',t'')G^R(t'',t_2), \\ &= g^R(t_1,t_2) + \int\int \mathrm{d}t'\mathrm{d}t''\, G^R(t_1,t')\Sigma^R(t',t'')g^R(t'',t_2). \end{aligned} \tag{2.102}$$

Recall that the free retarded (and advanced) Green's function $g^{R/A}$ both satisfy:

$$\begin{aligned} \left(i\hbar\frac{\partial}{\partial t_1} - \varepsilon(t_1)\right) g^{R/A}(t_1,t_2) &= \delta_{t_2}(t_1), \\ \left(-i\hbar\frac{\partial}{\partial t_2} - \varepsilon(t_2)\right) g^{R/A}(t_1,t_2) &= \delta_{t_1}(t_2), \end{aligned} \tag{2.103}$$

which we write, symbolically:

$$\begin{aligned} g^{-1}g^{R/A} &= 1, \\ g^{R/A}g^{-1} &= 1. \end{aligned} \tag{2.104}$$

Then, using the equations for g^R, we have:

$$\begin{aligned} \left(i\hbar\frac{\partial}{\partial t_1} - \varepsilon(t_1)\right) G^R(t_1,t_2) &= \delta_{t_2}(t_1) + \int \mathrm{d}t''\, \Sigma^R(t_1,t'')G^R(t'',t_2), \\ \left(-i\hbar\frac{\partial}{\partial t_2} - \varepsilon(t_2)\right) G^R(t_1,t_2) &= \delta_{t_1}(t_2) + \int \mathrm{d}t'\, G^R(t_1,t')\Sigma^R(t',t_2), \end{aligned} \tag{2.105}$$

which shall be represented symbolically as follows:

$$\begin{aligned} g^{-1}G^R &= 1 + \Sigma^R G^R, \\ G^R g^{-1} &= 1 + G^R\Sigma^R. \end{aligned} \tag{2.106}$$

Their meanings should always be referred back to (2.105). We do the same for the lesser projection:

$$\begin{aligned} G^< &= g^< + g^<\Sigma^A G^A + g^R\Sigma^< G^A + g^R\Sigma^R G^< \\ &= g^< + G^<\Sigma^A g^A + G^R\Sigma^< g^A + G^R\Sigma^R g^< \end{aligned} \tag{2.107}$$

and notice that the free lesser Green's function $g^<$ is annihilated by the differential operators above:

$$\begin{aligned} \left(i\hbar\frac{\partial}{\partial t_1} - \varepsilon(t_1)\right) g^<(t_1,t_2) &= 0, \\ \left(-i\hbar\frac{\partial}{\partial t_2} - \varepsilon(t_2)\right) g^<(t_1,t_2) &= 0, \end{aligned} \tag{2.108}$$

which allows us to greatly simplify the lengthy expressions for $G^<$:

$$\begin{aligned} g^{-1}G^< &= \Sigma^< G^A + \Sigma^R G^<, \\ G^< g^{-1} &= G^<\Sigma^A + G^R\Sigma^<. \end{aligned} \tag{2.109}$$

Equations (2.106) and (2.109) are called the Kadanoff-Baym equations.

We now add the two equations in (2.106):

$$\{g^{-1}, G^R\} = 2 + \{\Sigma^R, G^R\} \tag{2.110}$$

with $[\cdot,\cdot]$ a symbolic commutator. As for the other two equations in (2.109), let us introduce the following functions to symmetrize the expressions:

$$\begin{cases} A & = i(G^R - G^A) \\ \operatorname{Re} G^R & = \dfrac{G^R + G^A}{2} \end{cases} \qquad \begin{cases} \Gamma & = i(\Sigma^R - \Sigma^A) \\ \operatorname{Re} \Sigma^R & = \dfrac{\Sigma^R + \Sigma^A}{2} \end{cases} \tag{2.111}$$

It should be stressed that, for the moment, we still do not have $(G^R)^* = G^A$ and therefore $\operatorname{Re} G^R$ should not yet be considered as the real part of G^R. Using these new variables and taking the difference of (2.109), we obtain:

$$[g^{-1}, G^<] = [\Sigma^<, \operatorname{Re} G^R] + [\operatorname{Re}\Sigma^R, G^<] + \frac{i}{2}\{\Sigma^<, A\} - \frac{i}{2}\{\Gamma, G^<\} \tag{2.112}$$

with $\{\cdot,\cdot\}$ a symbolic anticommutator. Equations (2.110) and (2.112) are only symbolic: g^{-1} acting on left/right refers to two different differentiation operators, while multiplications without g^{-1} mean convolutions.

2.6 Wigner transform

Before we begin, it is useful to remark that, had we been discussing equilibrium situation, we would have temporal translational invariance, allowing us to reduce the two-time dependence of the Green's functions to just one. This is not true for non-equilibrium problems, therefore one way to proceed further is by means of the so-called Wigner transform.

2.6.1 Definition

Since the Green's functions involve two instances of time, t_1 and t_2, we begin with a change of coordinates[22]:

$$\begin{cases} t & = \dfrac{t_1 + t_2}{2}, \\ s & = t_1 - t_2. \end{cases} \tag{2.113}$$

The Wigner transform of a function $h(t_1, t_2)$ is obtained as follows: we first consider it as a function $\tilde{h}$ in the new variables (s, t):

$$h(t_1, t_2) \longrightarrow \tilde{h}(s,t) = h\left(t + \frac{s}{2}, t - \frac{s}{2}\right), \tag{2.114}$$

then we perform a Fourier transform on the "fast variable" s:

$$\tilde{h}(s,t) \xrightarrow{\text{Fourier in } s} \mathscr{F}\{\tilde{h}\}(E,t) = \int \mathrm{d}s\; \tilde{h}(s,t) e^{+\frac{iEs}{\hbar}}. \tag{2.115}$$

[22]Sometimes called Wigner or centre-of-mass coordinates.

We use the symbol $\mathscr{W}$ to denote Wigner transformation and put a hat on top of a function to denote its Wigner transform:

$$h(t_1, t_2) \longrightarrow \hat{h}(E, t) := \mathscr{W}\{h\}(E, t) = \int \mathrm{d}s\ \tilde{h}(s, t) e^{+\frac{iEs}{\hbar}}. \tag{2.116}$$

2.6.2 Convolution under Wigner transform

Let us investigate the result of Wigner-transforming a convolution:

$$C(t_1, t_2) = \int \mathrm{d}t'\ A(t_1, t') B(t', t_2). \tag{2.117}$$

To this end, we first transform A, B into their respective Wigner coordinates:

$$\begin{aligned} A(t_1, t') &\longrightarrow A\left(t_1 - t', \frac{t_1 + t'}{2}\right), \\ B(t', t_2) &\longrightarrow B\left(t' - t_2, \frac{t' + t_2}{2}\right), \\ C(t_1, t_2) &\longrightarrow \tilde{C}(s, t) = C\left(t - s, \frac{t + s}{2}\right). \end{aligned} \tag{2.118}$$

For A and B, we modify further their second arguments:

$$\begin{aligned} \frac{t_1 + t'}{2} &= t + \frac{t' - t_2}{2}, \\ \frac{t' + t_2}{2} &= t - \frac{t_1 - t'}{2}. \end{aligned} \tag{2.119}$$

Given a sufficiently smooth function $g(x)$, we have:

$$\begin{aligned} g(x + a) &= g(x) + a \frac{\mathrm{d}}{\mathrm{d}x} g(x) + \frac{a^2}{2!} \frac{\mathrm{d}^2}{\mathrm{d}x^2} g(x) + \dots \\ &= \exp\left[a \frac{\mathrm{d}}{\mathrm{d}x}\right] g(x). \end{aligned} \tag{2.120}$$

Hence, generalised to two-variable:

$$\begin{aligned} A\left(t_1 - t', t + \frac{t' - t_2}{2}\right) &= A(t_1 - t', t) \exp\left[\frac{t' - t_2}{2} \frac{\overleftarrow{\partial}}{\partial t}\right], \\ B\left(t' - t_2, t - \frac{t_1 - t'}{2}\right) &= \exp\left[-\frac{t_1 - t'}{2} \frac{\overrightarrow{\partial}}{\partial t}\right] B(t' - t_2, t). \end{aligned} \tag{2.121}$$

where the arrow above the partial derivative indicates the direction on which it acts. When multiplied together, the operators $\exp[\dots]$ commute:

$$A(t_1, t') B(t', t_2) = A(t_1 - t', t) \exp\left[-\frac{t_1 - t'}{2} \frac{\overrightarrow{\partial}}{\partial t}\right] \exp\left[\frac{t' - t_2}{2} \frac{\overleftarrow{\partial}}{\partial t}\right] B(t' - t_2, t). \tag{2.122}$$

Let us define the following functions to simplify notation:

$$\begin{aligned}\bar{A}(t_a,t) &= A(t_a,t)\exp\left[-\frac{t_a}{2}\frac{\overrightarrow{\partial}}{\partial t}\right],\\ \bar{B}(t_b,t) &= \exp\left[\frac{t_b}{2}\frac{\overleftarrow{\partial}}{\partial t}\right]B(t_b,t).\end{aligned} \tag{2.123}$$

Then, when the LHS of (2.117) is regarded as a function of s,t, we have:

$$\tilde{C}(s,t) = \int \mathrm{d}t'\ \bar{A}(t_1-t',t)\bar{B}(t'-t_2,t) \tag{2.124}$$

For the sake of clarity, the $t-$dependence of functions will be indicated at subscript:

$$\begin{aligned}\bar{A}(t_1-t',t) &\longrightarrow \bar{A}_t(t_1-t'),\\ \bar{B}(t'-t_2,t) &\longrightarrow \bar{B}_t(t'-t_2).\end{aligned} \tag{2.125}$$

Thus we see the RHS of (2.124) is simply a convolution:

$$(\bar{A}_t * \bar{B}_t)(t_1-t_2) = \int \mathrm{d}t'\ \bar{A}(t_1-t',t)\bar{B}(t'-t_2,t). \tag{2.126}$$

Recalling that $s = t_1 - t_2$, we have:

$$C(t_1,t_2) = \tilde{C}(s,t) = (\bar{A}_t * \bar{B}_t)(s). \tag{2.127}$$

Since Fourier transform $\mathscr{F}$ converts convolution into multiplication, we thus see the advantage of performing Wigner transform:

$$\begin{aligned}\mathscr{W}\{C\}(E,t) &= \int \mathrm{d}s\ \tilde{C}(s,t)e^{+\frac{iEs}{\hbar}}\\ &= \mathscr{F}\{\tilde{C}\}(E,t)\\ &= \mathscr{F}\{\bar{A}_t\}(E)\mathscr{F}\{\bar{B}_t\}(E).\end{aligned} \tag{2.128}$$

We shall now calculate the Fourier transform. Since multiplying by a phase factor corresponds to shifting argument:

$$\mathscr{F}\{e^{\omega s}f(s)\}(E) = \mathscr{F}\{f\}(E - i\hbar\omega), \tag{2.129}$$

we have:

$$\begin{aligned}\mathscr{F}\{\bar{A}_t(t_a)\}(E) &= \mathscr{F}\left\{A_t(t_a)\exp\left[-\frac{t_a}{2}\frac{\overrightarrow{\partial}}{\partial t}\right]\right\}(E)\\ &= \hat{A}_t\left(E + \frac{i\hbar}{2}\frac{\overrightarrow{\partial}}{\partial t}\right)\\ \mathscr{F}\{\bar{B}_t(t_b)\}(E) &= \mathscr{F}\left\{\exp\left[\frac{t_b}{2}\frac{\overleftarrow{\partial}}{\partial t}\right]B_t(t_b)\right\}(E)\\ &= \hat{B}_t\left(E - \frac{i\hbar}{2}\frac{\overleftarrow{\partial}}{\partial t}\right)\end{aligned} \tag{2.130}$$

where we have denoted the Fourier transform (with respect to s) of A_t by $\hat{A}_t$. Finally, using again (2.120), we have:

$$\begin{aligned}\hat{A}_t\left(E+\frac{i\hbar}{2}\overrightarrow{\frac{\partial}{\partial t}}\right) &= \hat{A}_t(E)\exp\left[\overleftarrow{\frac{\partial}{\partial E}}\left(\frac{i\hbar}{2}\overrightarrow{\frac{\partial}{\partial t}}\right)\right] \\ \hat{B}_t\left(E-\frac{i\hbar}{2}\overleftarrow{\frac{\partial}{\partial t}}\right) &= \exp\left[\left(-\frac{i\hbar}{2}\overleftarrow{\frac{\partial}{\partial t}}\right)\overrightarrow{\frac{\partial}{\partial E}}\right]\hat{B}_t(E)\end{aligned} \tag{2.131}$$

Returning to (2.128), we get:

$$\begin{aligned}\mathscr{W}\{C\}(E,t) &= \hat{A}_t(E)\exp\left[\overleftarrow{\frac{\partial}{\partial E}}\left(\frac{i\hbar}{2}\overrightarrow{\frac{\partial}{\partial t}}\right)\right]\exp\left[\left(-\frac{i\hbar}{2}\overleftarrow{\frac{\partial}{\partial t}}\right)\overrightarrow{\frac{\partial}{\partial E}}\right]\hat{B}_t(E) \\ &= \hat{A}_t(E)\overleftrightarrow{\mathcal{G}}\hat{B}_t(E)\end{aligned} \tag{2.132}$$

where we have grouped the two operators into one:

$$\overleftrightarrow{\mathcal{G}} = \exp\left\{\frac{i\hbar}{2}\left[\overleftarrow{\frac{\partial}{\partial E}}\overrightarrow{\frac{\partial}{\partial t}} - \overleftarrow{\frac{\partial}{\partial t}}\overrightarrow{\frac{\partial}{\partial E}}\right]\right\}. \tag{2.133}$$

To summarize, we obtained the following rule for the Wigner transform of a convolution:

$$\int \mathrm{d}t'\; A(t_1,t')B(t',t_2) \xrightarrow{\text{Wigner}} \hat{A}(E,t)\overleftrightarrow{\mathcal{G}}\hat{B}(E,t). \tag{2.134}$$

2.7 First order gradient expansion

Thus far, the discussion above is exact and equally difficult as the original one, since the operator $\overleftrightarrow{\mathcal{G}}$ is quite complicated. We previously called $s = t_1 - t_2$ a "fast variable". Naturally, we wish to regard $t = \frac{t_1+t_2}{2}$ as a "slow variable". In other words, we assume that external driving agent is slowly varying in the time-scale t:

$$\left\|\frac{\partial}{\partial t}\right\| \sim \omega \ll 1 \tag{2.135}$$

in a suitable operator norm, and ω is some characteristic driving frequency. If we expand $\overleftrightarrow{\mathcal{G}}$ up to first order in $\frac{\partial}{\partial t}$, we obtain:

$$\overleftrightarrow{\mathcal{G}} \approx \mathbb{1} + \frac{i\hbar}{2}\left[\overleftarrow{\frac{\partial}{\partial E}}\overrightarrow{\frac{\partial}{\partial t}} - \overleftarrow{\frac{\partial}{\partial t}}\overrightarrow{\frac{\partial}{\partial E}}\right] \tag{2.136}$$

This approximation is called first-order gradient expansion. Recall that the equations of interest, the Kadanoff-Baym equations were modified to obtain (2.110) and (2.112). We shall now investigate the effect of Wigner transform, to first-order in gradient expansion, on such equations.

2.7.1 $\{\cdot,\cdot\}$ and $[\cdot,\cdot]$ under gradient expansion

We begin with the symbolic commutator and anticommutator that do not involve g^{-1}:

$$\begin{aligned}\mathscr{W}\Big\{[A,B]\Big\} &= \mathscr{W}\{AB-BA\}\\ &= \mathscr{W}\{AB\}-\mathscr{W}\{BA\}\\ &= A\overleftrightarrow{\mathcal{G}}B - B\overleftrightarrow{\mathcal{G}}A\\ &\approx \left\{\hat{A}\hat{B}+\frac{i\hbar}{2}\left[\frac{\partial\hat{A}}{\partial E}\frac{\partial\hat{B}}{\partial t}-\frac{\partial\hat{A}}{\partial t}\frac{\partial\hat{B}}{\partial E}\right]\right\}-\left\{\hat{B}\hat{A}+\frac{i\hbar}{2}\left[\frac{\partial\hat{B}}{\partial E}\frac{\partial\hat{A}}{\partial t}-\frac{\partial\hat{B}}{\partial t}\frac{\partial\hat{A}}{\partial E}\right]\right\}\\ &= i\hbar\{\hat{A},\hat{B}\}_{E,t}\end{aligned} \tag{2.137}$$

where we have used $\{\cdot,\cdot\}_{E,t}$ to denote the Poisson bracket between two functions of E and t. In the same manner we consider the Wigner transform of the symbolic anticommutator:

$$\begin{aligned}\mathscr{W}\Big\{\{A,B\}\Big\} &= \mathscr{W}\{AB\}+\mathscr{W}\{BA\}\\ &\approx \left\{\hat{A}\hat{B}+\frac{i\hbar}{2}\left[\frac{\partial\hat{A}}{\partial E}\frac{\partial\hat{B}}{\partial t}-\frac{\partial\hat{A}}{\partial t}\frac{\partial\hat{B}}{\partial E}\right]\right\}+\left\{\hat{B}\hat{A}+\frac{i\hbar}{2}\left[\frac{\partial\hat{B}}{\partial E}\frac{\partial\hat{A}}{\partial t}-\frac{\partial\hat{B}}{\partial t}\frac{\partial\hat{A}}{\partial E}\right]\right\}\\ &= 2\hat{A}\hat{B}\end{aligned} \tag{2.138}$$

This is similar to the result that Fourier transform converts convolution into multiplication.

2.7.2 g^{-1} under gradient expansion

We now turn to terms involving the "left/right inverse" of g, denoted by g^{-1}, which are just a symbol for two differential operators, cf. (2.103). Recall the transformation of $(t_1,t_2)\longrightarrow(s,t)$, which yields the following differentiation rules:

$$\begin{aligned}\frac{\partial}{\partial t_1} &= \frac{1}{2}\frac{\partial}{\partial t}+\frac{\partial}{\partial s}\\ \frac{\partial}{\partial t_2} &= \frac{1}{2}\frac{\partial}{\partial t}-\frac{\partial}{\partial s}\end{aligned} \tag{2.139}$$

For a function $h(t_1, t_2)$, we have, up to first order in gradient expansion:

$$\begin{aligned} g^{-1}h(t_1,t_2) &= \left(i\hbar\frac{\partial}{\partial t_1} - \varepsilon(t_1)\right) h(t_1,t_2) \\ &= \left(\frac{i\hbar}{2}\frac{\partial}{\partial t} + i\hbar\frac{\partial}{\partial s} - \varepsilon\left(t+\frac{s}{2}\right)\right)\tilde{h}(s,t) \\ &\approx \left(\frac{i\hbar}{2}\frac{\partial}{\partial t} + i\hbar\frac{\partial}{\partial s} - \varepsilon(t) - \dot{\varepsilon}(t)\frac{s}{2}\right)\tilde{h}(s,t) \\ h(t_1,t_2)g^{-1} &= \left(-i\hbar\frac{\partial}{\partial t_2} - \varepsilon(t_2)\right) h(t_1,t_2) \\ &= \left(-\frac{i\hbar}{2}\frac{\partial}{\partial t} + i\hbar\frac{\partial}{\partial s} - \varepsilon\left(t-\frac{s}{2}\right)\right)\tilde{h}(s,t) \\ &\approx \left(-\frac{i\hbar}{2}\frac{\partial}{\partial t} + i\hbar\frac{\partial}{\partial s} - \varepsilon(t) + \dot{\varepsilon}(t)\frac{s}{2}\right)\tilde{h}(s,t) \end{aligned} \tag{2.140}$$

Hence, the symbolic commutator and anticommutator involving g^{-1} simplify to give:

$$\begin{aligned} [g^{-1},h] &= \left(i\hbar\frac{\partial}{\partial t} - \dot{\varepsilon}(t)s\right) h(t_1,t_2) \\ \{g^{-1},h\} &= \left(2i\hbar\frac{\partial}{\partial s} - 2\varepsilon(t)\right) h(t_1,t_2) \end{aligned} \tag{2.141}$$

Recall that Wigner-transform is just rewriting in Wigner coordinates (s,t) then Fourier-transform the s variable. Therefore, we have:

$$\begin{aligned} s\ h_t(s) &\xrightarrow{\text{Fourier in } s} -i\hbar\frac{\partial}{\partial E}\hat{h}_t(E) \\ \frac{\partial}{\partial s}h_t(s) &\xrightarrow{\text{Fourier in } s} -\frac{i}{\hbar}E\hat{h}_t(E) \end{aligned} \tag{2.142}$$

where we write the $t-$dependence at subscript for more clarity. Thus, we have for the Wigner transform:

$$\begin{aligned} \mathscr{W}\Big\{[g^{-1},h]\Big\} &= i\hbar\left(\frac{\partial}{\partial t} + \dot{\varepsilon}(t)\frac{\partial}{\partial E}\right)\hat{h}_t(E) \\ \mathscr{W}\Big\{\{g^{-1},h\}\Big\} &= 2(E-\varepsilon(t))\hat{h}_t(E) \end{aligned} \tag{2.143}$$

We can manipulate a little bit the first equation above to make appear the Poisson bracket in (E,t):

$$\begin{aligned} \left(\frac{\partial}{\partial t} + \dot{\varepsilon}(t)\frac{\partial}{\partial E}\right)\hat{h}_t(E) &= \left[\frac{\partial}{\partial E}(E-\varepsilon(t))\frac{\partial}{\partial t} - \frac{\partial}{\partial t}(E-\varepsilon(t))\frac{\partial}{\partial E}\right]\hat{h}_t(E) \\ &= \{E-\varepsilon(t), \hat{h}_t(E)\}_{E,t} \end{aligned} \tag{2.144}$$

After all these derivations, we will now only work with Wigner-transformed functions. Hence we will drop the hat and simply write $h(E,t)$.

2.8 Solution for G^R

Equipped with the above considerations, we can solve for one of the quantity of interest, the retarded Green's function $G^R(E,t)$. Indeed, from (2.110) we have:

$$\begin{aligned} \mathscr{W}\Big\{\{g^{-1},G^R\}\Big\} &= 2+\mathscr{W}\Big\{\{\Sigma^R,G^R\}\Big\} \\ 2[E-\varepsilon(t)]G^R(E,t) &= 2+2\Sigma^R(E,t)G^R(E,t) \end{aligned} \tag{2.145}$$

which solves the retarded Green's function:

$$G^R(E,t)=\frac{1}{E-\varepsilon(t)-\Sigma^R(E,t)}. \tag{2.146}$$

This is Equation (2) of Esposito's article.

2.9 Solution for $G^<$

Applying Wigner transform on both sides of (2.112) and using rules (2.137) and (2.138), we obtain an equation of motion for the lesser Green's function $G^<$:

$$i\hbar\{E-\varepsilon,G^<\}=i\hbar\{\Sigma^<,\operatorname{Re}G^R\}+i\hbar\{\operatorname{Re}\Sigma^R,G^<\}+i\Sigma^<A-i\Gamma G^< \tag{2.147}$$

or upon some simplification:

$$\{E-\varepsilon-\operatorname{Re}\Sigma^R,G^<\}+\{\operatorname{Re}G^R,\Sigma^<\}=\frac{1}{\hbar}[\Sigma^<A-\Gamma G^<] \tag{2.148}$$

where we dropped the (E,t) dependences and stress that $\{\cdot,\cdot\}$ here means Poisson bracket with respect to (E,t). In order to proceed we shall admit the Kadanoff-Baym ansatz:

$$G^<(E,t)=iA(E,t)\phi(E,t) \tag{2.149}$$

Here, $\phi(E,t)$ is the occupation probability and $A(E,t)=-2\operatorname{Im}G^R(E,t)$ is the spectral function. Recall that in equations above, $\Sigma^{R,<}$ actually mean:

$$\Sigma^{R,<}(E,t)=\sum_{\nu=\{L,R\}}\Sigma^{R,<}_\nu(E,t) \tag{2.150}$$

that is, the retarded and lesser self-energy are sum of the self-energies of left and right reservoirs. Next, we will admit the following result:

$$\Sigma^<_\nu(E,t)=i\Gamma_\nu(E,t)f_\nu(E) \tag{2.151}$$

where $\Gamma_\nu(E,t)=-2\operatorname{Im}\Sigma^R_\nu(E,t)$ and

$$f_\nu(E)=\frac{1}{\exp\left[\beta_\nu(E-\mu_\nu)\right]+1} \tag{2.152}$$

is the Fermi-Dirac function of the $\nu=L,R$ bath. (2.148) then becomes:

$$\{E-\varepsilon-\operatorname{Re}\Sigma^R,iA\phi\}+\{\operatorname{Re}G^R,i\Gamma f\}=\frac{1}{\hbar}[(i\Gamma f)A-\Gamma(iA\phi)] \tag{2.153}$$

Using (2.150), we obtain the following equation:

$$\sum_{\nu=L,R} \{E - \varepsilon - \mathrm{Re}\,\Sigma_\nu^R, A\phi\} + \{\mathrm{Re}\,G^R, \Gamma_\nu f_\nu\} = \frac{1}{\hbar} \sum_{\nu=L,R} A\Gamma_\nu (f_\nu - \phi) \tag{2.154}$$

Finally, we invoke the Botermans-Malfliet approximation[23], which replaces[23] the Fermi-Dirac function in the second bracket by ϕ:

$$\{\mathrm{Re}\,G^R, \Gamma_\nu f_\nu\} \approx \{\mathrm{Re}\,G^R, \Gamma_\nu \phi\} \tag{2.155}$$

and obtain the following quantum kinetic equation:

$$\sum_{\nu=L,R} \{E - \varepsilon - \mathrm{Re}\,\Sigma_\nu^R, A\phi\} + \{\mathrm{Re}\,G^R, \Gamma_\nu \phi\} = \frac{1}{\hbar} \sum_{\nu=L,R} A\Gamma_\nu (f_\nu - \phi) \tag{2.156}$$

With $\hbar = 1$, this is Equation (3) of Esposito's article.

2.10 Self energy Σ and spectral function A

Before we conclude this chapter, let us say a few words about the self energy Σ and the spectral function A. First of all, with the diagrammatic analysis we obtained

$$\Sigma = \Sigma_L + \Sigma_R \tag{2.157}$$

that is to say the total self energy is the sum of individual one. From the structure of the tunneling Hamiltonian (2.4), we deduce that so long as the tunneling stays between dot and bath[24], we can have as many reservoirs as we wish. From the expressions for Σ_L and Σ_R, cf. (2.79) and (2.81), we see that the self energy tells us about the influence of the reservoirs on the dot[25]. It is customary to write for the retarded self energy of ν reservoir:

$$\Sigma_\nu^R(E,t) = \Lambda_\nu(E,t) - \frac{i\Gamma_\nu(E,t)}{2} \tag{2.158}$$

We will turn to the interpretations in a minute. Before that let us consider the spectral function:

$$A(E,t) = -2\mathrm{Im}\,G^R(E,t) \tag{2.159}$$

In the following, when a quantity has both (E,t) dependence, we will not write it at all. Using the solution for G^R, (2.146), we have:

$$A = \frac{\Gamma_L + \Gamma_R}{[E - \varepsilon(t) - (\Lambda_L + \Lambda_R)]^2 + \left(\frac{\Gamma_L + \Gamma_R}{2}\right)^2} \tag{2.160}$$

This is a Lorentzian centred at $\varepsilon + (\Lambda_L + \Lambda_R)$, with width $(\Gamma_L + \Gamma_R)$. The real part Λ_ν of the retarded self energy Σ_ν^R can be interpreted as the shift of the quantum dot energy level from ε, and the imaginary part Γ_ν as the broadening of the energy level, both due to its coupling to ν reservoir.

[23]This is justified because the difference $\{\mathrm{Re}\,G^R, \Gamma_\nu f_\nu - \Gamma_\nu \phi\}$ is of second order in gradient expansion.

[24]That is, no bath-bath tunneling.

[25]For instance, $\Sigma_L(\tau_1,\tau_2) = \sum_k \gamma_k(\tau_1) g_k^c(\tau_1,\tau_2)\gamma_k^*(\tau_2)$ involves the left bath free-electron Green's function g_k^c and the tunneling amplitudes γ_k.

Chapter 3

Thermodynamics of Quantum Dot

With the retarded Green's function (2.146) and the quantum kinetic equation (2.156), we are now in the position to discuss the thermodynamics of the single-level system connected to two reservoirs. The definitions below were introduced by Esposito [1], probably by reverse-engineering: integrate the quantum kinetic equation and define according to the similarity of each term to its weak-coupling counterpart. The equations involved are tedious but not difficult to derive. We omit the points already discussed in Esposito's article, but include some explanations and motivations that they did not provide. To begin with, let us introduce the following notations:

$$\begin{aligned} \Gamma &= \Gamma_L + \Gamma_R, \\ \Lambda &= \Lambda_L + \Lambda_R. \end{aligned} \tag{3.1}$$

One important point is the introduction of the renormalized spectral function:

$$\mathcal{A} = A\frac{\partial}{\partial E}\Big(E - \varepsilon(t) - \Gamma\Big) + \Gamma\frac{\partial}{\partial E}\Big(\mathrm{Re}\, G^R\Big) \tag{3.2}$$

which will be the weight used to define the thermodynamic variables as follows. The sequence of functions $\mathcal{A}_\Gamma$ is a candidate for Dirac delta in the limit $\Gamma \to 0$, ie. the weak coupling limit. This renormalized version, rather than the usual $A = -2\mathrm{Im}\, G^R$ spectral function, would yield equations of motion that mirror the ones in stochastic thermodynamics.

3.1 Particle number

The most immediate quantity that one can think of is probably the particle number. If we integrate with respect to energy divided by 2π, we obtain:

$$\frac{\mathrm{d}}{\mathrm{d}t}\int \frac{\mathrm{d}E}{2\pi}\mathcal{A}\phi = \sum_\nu \int \frac{\mathrm{d}E}{2\pi} A\Gamma_\nu(f_\nu(E) - \phi). \tag{3.3}$$

Recall that ϕ is the dot occupation density, f_ν is the Fermi-Dirac function for ν reservoir, Γ_ν is the coupling strength to ν reservoir. Thus in absence of A, the term $\Gamma_\nu(f_\nu - \phi)$ mirrors the rate of change of the system occupation probability due to transition to ν

reservoir. Therefore when summed over bath, integrated with weight A, it seems natural to interpret the result as the rate of particle flow to the system. This leads to defining

$$\mathcal{I}_\nu(t) = \int \frac{\mathrm{d}E}{2\pi} A\Gamma_\nu(f_\nu(E) - \phi) \tag{3.4}$$

as the particle current flowing into the dot. The integral at LHS of (3.3) is then interpreted as particle number in the dot:

$$\mathcal{N}(t) = \int \frac{\mathrm{d}E}{2\pi} \mathcal{A}\phi. \tag{3.5}$$

Before we proceed, the integrand of (3.4) will frequently appear, leading to its definition as (energy-resolved) current density:

$$C_\nu = A\Gamma_\nu(f_\nu(E) - \phi). \tag{3.6}$$

Thus, we have separated the total current density into the bath, reservoir by reservoir: $C = \sum_\nu C_\nu$. However, we can do better. For each C_ν, we can split it into two terms: one representing inflow from ν, another outflow to ν, so that the sum signifies the net flow to (or from, depending on the sign):

$$C_\nu = C_\nu^+ - C_\nu^-. \tag{3.7}$$

There is a myriad of ways to split this term, but if we regard $\big(1-f_\nu(E)\big)$ as the distribution function of hole in reservoir ν, then the following:

$$A\Gamma_\nu[\ \underbrace{f_\nu(E)}_{\text{Electron in } \nu}\ \underbrace{\big(1-\phi(E,t)\big)}_{\text{Hole in dot}} - \underbrace{\big(1-f_\nu(E)\big)}_{\text{Hole in } \nu}\ \underbrace{\phi(E,t)}_{\text{Electron in dot}}\ ] \tag{3.8}$$

mimics the Boltzmann collision term [30] describing a process after which (hole in ν and electron in dot) scatter into (electron in ν and hole in dot). Therefore, the particle current density from ν reservoir to the dot is defined as:

$$C_\nu^+ = A\Gamma_\nu f_\nu(1-\phi) \tag{3.9}$$

and the current flowing from dot to ν:

$$C_\nu^- = A\Gamma_\nu(1-f_\nu)\phi. \tag{3.10}$$

3.2 Energy

Equally important is of course the energy of the dot. If we multiply the quantum kinetic equation by E and integrate, we obtain:

$$\frac{\mathrm{d}}{\mathrm{d}t}\int \frac{\mathrm{d}E}{2\pi}\mathcal{A}\phi E = \sum_\nu \int \frac{\mathrm{d}E}{2\pi} EC_\nu - \int \frac{\mathrm{d}E}{2\pi}\phi\left[A\frac{\partial}{\partial t}\Big(E-\varepsilon(t)-\Gamma_\nu\Big) + \Gamma_\nu \frac{\partial}{\partial t}\operatorname{Re} G^R\right], \tag{3.11}$$

$\mathcal{A}\phi$ being the integrand of particle number, it is natural[1] to define energy as follows:

$$\mathcal{E}(t) = \int \frac{\mathrm{d}E}{2\pi}\mathcal{A}\phi E. \tag{3.12}$$

[1]Notice that the Hamiltonian of the dot, $\varepsilon d^\dagger d$, could also suggest a definition such as $\varepsilon\mathcal{N}$, i.e., energy level times the particle number. However looking at the spectral function, we see that the distribution in energy is not delta-peaked at ε but smeared around it. This is probably why $\varepsilon\mathcal{N}$ is not a good definition.

3.2.1 Energy current

C_ν being the current density, the first term at the RHS of (3.11) is interpreted as energy current from ν reservoir:

$$\mathcal{J}_\nu^E(t) = \int \frac{\mathrm{d}E}{2\pi} E C_\nu := \int \frac{\mathrm{d}E}{2\pi} C_\nu^E \tag{3.13}$$

with C_ν^E the energy current density. An analogy would be from electrodynamics, where

charge density	velocity		charge current density
ρ	$\vec{v}$	$=$	$\vec{J}$
$\updownarrow$	$\updownarrow$		$\updownarrow$
E	C_ν	$=$	C_ν^E
energy	particle current density		energy current density

In classical thermodynamics, given that after a process, our system of interest has its energy changed from E to $E + \Delta E$, we often wish to know further: which part of ΔE goes to work being done and heat being exchanged. This is of no exception here and we shall next discuss how to split $\mathcal{J}_\nu^E$ into a heat flux and work current.

3.2.2 Heat current

Defining heat is a persistent question in open quantum system. Entropy, on the contrary, is unambiguous as the Shannon-von Neumann entropy is pretty much universally accepted. In Esposito's previous works [24], with a master equation approach, they considered a quantum system weakly in contact with a thermal particle reservoir. In the spirit of linear irreversible thermodynamics, they split the rate of change of entropy into two parts: production $\dot{\mathcal{S}}_i$ and flow $\dot{\mathcal{S}}_e$. Next, by considering quasi-static dynamics, ie. system in equilibrium with bath at all instant, with detailed balance condition they obtained an expression to be satisfied for the rates of transition. When one demands the entropy flow $\dot{\mathcal{S}}_e$ to be that of Clausius' definition:

$$\mathrm{d}S = \frac{\delta Q_{\mathrm{rev}}}{T}, \tag{3.14}$$

then the rate of heat flow is identified as:

$$\text{Rate of change of probability} \times (\text{Energy} - \text{chemical potential}). \tag{3.15}$$

This is probably why, for non-weakly-coupled regime, Esposito defined heat current to be:

$$\mathcal{J}_\nu^Q(t) = \int \frac{\mathrm{d}E}{2\pi} C_\nu (E - \mu_\nu). \tag{3.16}$$

3.2.3 Work current

Drawing analogy with the First Law, in which energy change equals work plus heat, the work current is defined to be:

$$\begin{aligned} \mathcal{J}_\nu^N &= \mathcal{J}_\nu^E - \mathcal{J}_\nu^Q, \\ \mathcal{J}_\nu^N &= \mu_\nu \mathcal{I}_\nu. \end{aligned} \tag{3.17}$$

Since $\mathcal{I}_\nu$ represents the particle current, this $\mathcal{J}_\nu^N$ is interpreted as the work done in transferring particles. It must be emphasized that this work current is the "internal work". It is of great importance when we consider particle-exchange engine in Section 5.4, because there we wish to transfer particles against a bias. However, this is not quite the case when we consider a cyclic heat engine, in which we wish to perform "external work" (to be discussed immediately after). Hence, any energy expended that is not for the aforementioned purpose will lead to degradation of the performance of the heat engine.

3.2.4 External power

Having identified the energy, heat and work current, we notice that there is still a term in (3.11), namely:

$$-\int \frac{\mathrm{d}E}{2\pi}\phi\left[A\frac{\partial}{\partial t}\Big(E-\varepsilon(t)-\Gamma_\nu\Big)+\Gamma_\nu\frac{\partial}{\partial t}\operatorname{Re}G^R\right]. \tag{3.18}$$

At first glance, there is no reason why this should be the rate of external work done, apart from the requirement for (3.11) to be a First Law-like equation. However, in the wide band limit[2], the above expression becomes:

$$\int \frac{\mathrm{d}E}{2\pi}\mathcal{A}\phi\left[\dot{\varepsilon}(t)+\big(E-\varepsilon(t)\big)\frac{d_t\Gamma}{\Gamma}\right]=\mathcal{N}(t)\dot{\varepsilon}(t)+\int\frac{\mathrm{d}E}{2\pi}\mathcal{A}\phi\big(E-\varepsilon(t)\big)\frac{d_t\Gamma}{\Gamma}. \tag{3.21}$$

The first term on the RHS is similar to the quantum thermodynamics definition [25] of rate of work done[3]. The second term does not have good analogy in the weak-coupling

[2]Referring to the discussion of the retarded self energy in Subsection 2.10, the wide band limit is an approximation which consists in ignoring the energy-level shift:

$$\Lambda_\nu = 0 \tag{3.19}$$

and assuming the energy-level broadening Γ_ν to be uniform:

$$\Gamma_\nu(E,t)=\Gamma_\nu(t) \tag{3.20}$$

[3]For a generic quantum system we write its energy as

$$E=\sum_n \epsilon_n p_n \tag{3.22}$$

where n is state index, ϵ_n and p_n are respectively the energy and probability of the system in state n. If we grant the system time evolution and assume the validity of $E(t)=\sum_n \epsilon_n(t)p_n(t)$, then we have

$$\dot{E}(t)=\sum_n\big(\dot{\epsilon}_n(t)p_n(t)+\epsilon_n(t)\dot{p}_n(t)\big) \tag{3.23}$$

literature. However, looking at how the integrand involves E and the time-derivative of the coupling Γ, it seems plausible to interpret it as the power due to driving the coupling. Thus following Esposito we write the external power as:

$$\mathcal{P}_{\text{ext}} = \mathcal{N}(t)\dot{\varepsilon}(t) + \int \frac{\mathrm{d}E}{2\pi}\mathcal{A}\phi\big(E-\varepsilon(t)\big)\frac{d_t\Gamma}{\Gamma}. \tag{3.24}$$

3.3 Entropy

In the weak-coupling regime, the state space of a single-level quantum system is two-dimensional: empty $|0\rangle$ or occupied $|1\rangle$. Therefore, one way to characterize the entropy of the system is by using the Shannon entropy: $S = -[p_0 \ln p_0 + p_1 \ln p_1]$. Similarly, Esposito defined the energy-resolved Shannon entropy as:

$$\sigma = -k_B\big[\phi\ln\phi + (1-\phi)\ln(1-\phi)\big]. \tag{3.25}$$

Since the Poisson bracket obeys the chain rule:

$$\{\cdot, \sigma(\phi)\}_{E,t} = \{\cdot,\phi\}_{E,t}\frac{\mathrm{d}\sigma}{\mathrm{d}\phi} \tag{3.26}$$

by multiplying the quantum kinetic equation with $\frac{\mathrm{d}\sigma}{\mathrm{d}\phi}$ and integrate, one obtains the following equation:

$$\frac{\mathrm{d}}{\mathrm{d}t}\int\frac{\mathrm{d}E}{2\pi}\mathcal{A}\sigma = \sum_\nu\int\frac{\mathrm{d}E}{2\pi}\big(C_\nu^+ - C_\nu^-\big)\ln\frac{C^+}{C^-} + \sum_\nu\frac{\mathcal{J}_\nu^Q}{T_\nu}, \tag{3.27}$$

where S is identified as the total entropy of the quantum dot:

$$S(t) = \int\frac{\mathrm{d}E}{2\pi}\mathcal{A}\sigma \tag{3.28}$$

and the entropy flow rate from $\nu-$reservoir, reminiscent of Clausius' definition of entropy:

$$\dot{\mathcal{S}}_e^\nu(t) = \frac{\mathcal{J}_\nu^Q}{T_\nu} \tag{3.29}$$

and the entropy production rate:

$$\dot{\mathcal{S}}_i^\nu(t) = \int\frac{\mathrm{d}E}{2\pi}\big(C_\nu^+ - C_\nu^-\big)\ln\frac{C^+}{C^-} \geq 0. \tag{3.30}$$

Now, ϵ_n is the energy level and for the simplest case: a particle in a box, this is closely related to the width of the box. For a classical ideal gas performing work corresponds to changing the volume. Hence $\dot{\epsilon}_n(t)p_n(t)$ is identified as work exchange. Next, p_n is the occupation probability of each state n and together they describe the state of the quantum system. Classically, entropy also plays the role of characterising the state, thus $\epsilon_n(t)\dot{p}_n(t)$ is identified as the heat exchange.

Chapter 4

Quantum Kinetic Equation

Under the framework of NEGF and first-order gradient expansion, granted the wide band approximation, the problem is now characterized by the spectral function A, occupation probability ϕ, coupling strengths to $\nu-$reservoir Γ_ν, and the Fermi functions f_ν. In the previous chapter we discussed Esposito's thermodynamic definitions, which can be calculated from the above mentioned quantities. Now, recall that the spectral function A is related to the retarded Green's function whose solution turns out to be immediate, cf. (2.146), whereas the occupation probability ϕ, related to the lesser Green's function, is not yet solved, cf. (2.156). In this chapter we focus on solving this last equation: exactly and perturbatively. These are just mechanical so we will be brief.

4.1 Exact solution

With Poisson bracket, (2.156) looks compact and neat, but is not the operational one. Under the wide band limit, $\Gamma_\nu(E,t) = \Gamma_\nu(t)$ and $\mathrm{Re}\,\Sigma^R_\nu = 0$, so (2.156) (with $\hbar = 1$ and index ν implies summation) becomes:

$$\{E-\varepsilon, A\phi\} + \{\mathrm{Re}\,G^R, \Gamma_\nu\phi\} = A\Gamma_\nu(f_\nu - \phi). \tag{4.1}$$

It can be shown that

$$\{E-\varepsilon, A\} + \{\mathrm{Re}\,G^R, \Gamma_\nu\} = 0. \tag{4.2}$$

Therefore with the Leibniz rule of Poisson bracket, we obtain:

$$\{E-\varepsilon, \phi\}A + \{\mathrm{Re}\,G^R, \phi\}\Gamma_\nu = A\Gamma_\nu(f_\nu - \phi). \tag{4.3}$$

Using the relations

$$\begin{aligned}
\Gamma_\nu\partial_t \mathrm{Re}\,G^R &= A\dot{\varepsilon}\frac{(E-\varepsilon)^2 - (\frac{\Gamma_\nu}{2})^2}{(E-\varepsilon)^2 + (\frac{\Gamma_\nu}{2})^2} - \frac{A^2(E-\varepsilon)d_t\Gamma_\nu}{2}, \\
\Gamma_\nu\partial_E \mathrm{Re}\,G^R &= A\frac{(\frac{\Gamma_\nu}{2})^2 - (E-\varepsilon)^2}{(E-\varepsilon)^2 + (\frac{\Gamma_\nu}{2})^2},
\end{aligned} \tag{4.4}$$

(4.1) becomes:

$$\frac{A^2\Gamma_\nu}{2}\left[\frac{\partial}{\partial t} + \left(\dot{\varepsilon} + (E-\varepsilon(t))\frac{d_t\Gamma_\nu}{\Gamma_\nu}\right)\frac{\partial}{\partial E}\right]\phi(E,t) = A\Big[\Gamma_\nu f_\nu + \Gamma_\nu\phi(E,t)\Big] \tag{4.5}$$

or upon simplifying common factors:

$$\left[\frac{\partial}{\partial t}+\left(\dot{\varepsilon}+(E-\varepsilon(t))\frac{d_t\Gamma_\nu}{\Gamma_\nu}\right)\frac{\partial}{\partial E}\right]\phi=\frac{2}{A}\left[\frac{\Gamma_L f_L+\Gamma_R f_R}{\Gamma_L+\Gamma_R}-\phi\right]. \tag{4.6}$$

The above is a one-dimensional convection equation. We provide the solution in Appendix D. Denote

$$K(E,t)=2\left[\left(\frac{E-\varepsilon(0)}{\Gamma_\nu(0)}\right)^2+\frac{1}{4}\right]\Gamma_\nu(t) \tag{4.7}$$

and

$$g(E,t)=\frac{\Gamma_L(t)f_L\left(\varepsilon(t)+\frac{E-\varepsilon(0)}{\Gamma_\nu(0)}\Gamma_\nu(t)\right)+\Gamma_R(t)f_R\left(\varepsilon(t)+\frac{E-\varepsilon(0)}{\Gamma_\nu(0)}\Gamma_\nu(t)\right)}{\Gamma_L(t)+\Gamma_R(t)} \tag{4.8}$$

the exact solution for the occupation probability is given by:

$$\phi(E,t)=\phi(E,0)e^{-\int_0^t K(E,t')\mathrm{d}t'}+\int_0^t e^{-\int_{t'}^t K(E,t'')\mathrm{d}t''}K(E,t')g(E,t')\mathrm{d}t'. \tag{4.9}$$

One way to fix the initial condition $\phi(E,0)$ is to take the steady-state solution, a subject we will discuss in the next section.

4.2 Perturbative solution

The previous section shows how to solve analytically the quantum kinetic equation under the wide band approximation. However, the expression (4.9) probably does not serve much other than academic purpose. In the spirit of perturbation theory let us write:

$$\phi(E,t)=\phi^{(0)}(E,t)+\phi^{(1)}(E,t)+\cdots \tag{4.10}$$

where superscript indicates the order in some driving frequency ω.

4.2.1 Steady-state solution

When (4.10) is plugged back into (4.6), the zeroth order term is simply a non-equilibrium steady-state situation:

$$0=\frac{2}{A}\left[\frac{\Gamma_L(t)f_L(E)+\Gamma_R(t)f_R(E)}{\Gamma_L(t)+\Gamma_R(t)}-\phi^{(0)}(E,t)\right] \tag{4.11}$$

leading to a convex combination of the left/right Fermi functions as our steady-state solution:

$$\phi^{(0)}(E,t)=\frac{\Gamma_L(t)f_L(E)+\Gamma_R(t)f_R(E)}{\Gamma_L(t)+\Gamma_R(t)} \tag{4.12}$$

Notice that, zeroth order in driving frequency does not mean absence of time-dependence. As we see from the above expression, though we try to refrain from varying temperature nor chemical potential[1], we can very well drive the coupling strengths Γ_ν. In such a

[1] A large part of the formalism consists in having two reservoirs which are individually and separately in equilibrium. When temperature and chemical potential are allowed to change, it is not clear that the bath will still remain a bath.

situation, the zeroth order solution describes a time-dependent steady state. The difficulty of interpreting this oxymoron can be surmounted if we think of the quasi-static processes in classical thermodynamics, where on each point of a process, the system is always in equilibrium with some bath.

4.2.2 First-order solution

We plug the zeroth order solution back to (4.6). Since time-differentiating or multiplying with terms with time derivative will increase the order by one, up to first order in driving frequency, we have:

$$\left[\frac{\partial}{\partial t}+\left(\dot{\varepsilon}+(E-\varepsilon(t))\frac{d_t\Gamma_\nu}{\Gamma_\nu}\right)\frac{\partial}{\partial E}\right]\phi^{(0)}=-\frac{2}{A}\phi^{(1)} \tag{4.13}$$

yielding the following solution:

$$\phi^{(1)}(E,t)=-\frac{A(E,t)}{2}\left[\frac{\partial}{\partial t}+\left(\dot{\varepsilon}+(E-\varepsilon(t))\frac{d_t\Gamma_\nu}{\Gamma_\nu}\right)\frac{\partial}{\partial E}\right]\frac{\Gamma_L f_L+\Gamma_R f_R}{\Gamma_L+\Gamma_R} \tag{4.14}$$

Having obtained an exact and another perturbative solution for first-order (in driving frequency) quantum kinetic equation, one naturally asks whether it is possible to go one order higher. Unfortunately, the resulting expressions are too complicated for manipulation. Therefore, we refer to Appendix E for a discussion of second order gradient expansion.

Chapter 5

Steady-state Regime

In this chapter, we temporarily disregard the possibility of having external driving agents and focus on the steady-state regime. We first obtain expressions for the thermodynamic quantities defined in Chapter 3. Then, we identify thermodynamic forces and fluxes associated to temperature and chemical potential difference. Next, by considering small differences in temperature and chemical potential, we Taylor-expand expressions containing $\Delta\frac{1}{T}$ and $\Delta(-\frac{\mu}{T})$ and keep only the linear terms to identify Onsager kinetic coefficients. With these coefficients, Onsager reciprocal relation is shown to hold. These results are new but Esposito probably took them into considerations when defining his thermodynamic quantities. We then study a particle-exchange engine and show numerically the validity of Curzon-Ahlborn efficiency for small ΔT.

5.1 Currents and entropy

At steady state, the particle current density from the left reservoir is given by:

$$C_L(E) = \frac{A\Gamma_L\Gamma_R}{\Gamma_L+\Gamma_R}\big(f_L(E) - f_R(E)\big) \tag{5.1}$$

whereas for the right reservoir we have $C_R = -C_L$, leading to zero net particle current entering the dot:

$$\frac{d\mathcal{N}}{dt} = \int \frac{\mathrm{d}E}{2\pi}\big(C_L(E) + C_R(E)\big) = 0. \tag{5.2}$$

However, individually the current (say from left) is interesting:

$$\mathcal{J}_L^N = \int \frac{\mathrm{d}E}{2\pi}\frac{A\Gamma_L\Gamma_R}{\Gamma_L+\Gamma_R}\big(f_L(E) - f_R(E)\big) \tag{5.3}$$

where we recognize a Landauer-Büttiker-like expression [26] for a one-dimensional electron conduction, with A the number of modes, $\frac{\Gamma_L\Gamma_R}{\Gamma_L+\Gamma_R}$ the transmission probability, and $f_L(E) - f_R(E)$ the difference of Fermi distributions. Let us make a remark that this result for steady-state particle current is widely accepted in nanoscale transport [27][28]. This strengthens the evidence in favour for Esposito's definitions, since by means of NEGF and gradient expansion (which are also widely used [15][20]), we arrive at a standard result that is (5.3).

Next, the heat current from reservoir L is given by:

$$\mathcal{J}_L^Q = \int \frac{\mathrm{d}E}{2\pi}(E-\mu_L)\frac{A\Gamma_L\Gamma_R}{\Gamma_L+\Gamma_R}\big(f_L(E)-f_R(E)\big) \tag{5.4}$$

and finally the energy current from left bath:

$$\mathcal{J}_L^E = \int \frac{\mathrm{d}E}{2\pi}E\frac{A\Gamma_L\Gamma_R}{\Gamma_L+\Gamma_R}\big(f_L(E)-f_R(E)\big) \tag{5.5}$$

and we notice that these three currents satisfy:

$$\mathcal{J}_L^Q = \mathcal{J}_L^E + \mu_L\mathcal{J}_L^N. \tag{5.6}$$

Same results hold for the right bath and we shall not repeat them here. For a consistency check, the rate of change of dot energy in steady-state is indeed:

$$\frac{\mathrm{d}\mathcal{E}}{\mathrm{d}t} = \sum_{\nu=\{L,R\}} \mathcal{J}_\nu^Q + \mu_\nu\mathcal{J}_\nu^N = 0. \tag{5.7}$$

Turning to the entropy production rate contributed by left reservoir, we have:

$$\begin{aligned}\dot{\mathcal{S}}_i^L &= \int \frac{\mathrm{d}E}{2\pi}\big(C_L^+ - C_L^-\big)\ln\frac{C_L^+}{C_L^-} \\ &= \int \frac{\mathrm{d}E}{2\pi}\frac{A\Gamma_L\Gamma_R}{\Gamma_L+\Gamma_R}\big(f_L(E)-f_R(E)\big)\ln\frac{f_L(1-\phi)}{(1-f_L)\phi}.\end{aligned} \tag{5.8}$$

This expression cannot be further simplified, however when one considers the entropy production rate contributed by both baths:

$$\begin{aligned}\dot{\mathcal{S}}_i &= \dot{\mathcal{S}}_i^L + \dot{\mathcal{S}}_i^R \\ &= \int \frac{\mathrm{d}E}{2\pi}C_L\ln\frac{f_L(1-f_R)}{(1-f_L)f_R} \\ &= \int \frac{\mathrm{d}E}{2\pi}\Big[-\beta_L(E-\mu_L)C_L - \beta_R(E-\mu_R)C_R\Big] \\ &= -\frac{\mathcal{J}_L^Q}{T_L} - \frac{\mathcal{J}_R^Q}{T_R}.\end{aligned} \tag{5.9}$$

This is negative entropy flow from both baths, which when considered separately is nothing but Clausius' definition of entropy[1] for reversible heat flow. When combined, we verify that the rate of change of dot entropy is zero:

$$\frac{\mathrm{d}S}{\mathrm{d}t} = \sum_{\nu=\{L,R\}} \dot{\mathcal{S}}_i^\nu + \frac{\mathcal{J}_\nu^Q}{T_\nu} = 0. \tag{5.10}$$

[1]To be more precise, Clausius' definition involves the differential of entropy and the reversible heat, whereas here we have entropy *current* and heat *current*.

5.2 Near-equilibrium thermodynamics

Splitting the rate of change of entropy S of the single-level system into the production rate $\dot{\mathcal{S}}_i$ and the flow rate $\dot{\mathcal{S}}_e$:

$$\frac{\mathrm{d}S}{\mathrm{d}t} = \dot{\mathcal{S}}_i + \dot{\mathcal{S}}_e \tag{5.11}$$

is nowadays well-accepted. This dates back to Prigogine [29] and probably stems from the observation that for reversible processes, entropy, like most other quantities, is conserved. Thus, when we are close to equilibrium but not quite[2], it would be desirable to split the entropy change into a part $\dot{\mathcal{S}}_e$ that is conserved, and another part $\dot{\mathcal{S}}_i$ that generates entropy. Using classical thermostatics and imposing continuity equations, one can argue that the entropy production is given by:

$$\dot{\mathcal{S}}_i = \mathcal{F}_T \mathcal{J}^Q + \mathcal{F}_\mu \mathcal{J}^N \tag{5.12}$$

where $\mathcal{J}^Q$ ($\mathcal{J}^N$) is the heat (particle) current, and $\mathcal{F}_T = \Delta\frac{1}{T}$ ($\mathcal{F}_\mu = -\Delta\frac{\mu}{T}$) is the affinity[3] associated to temperature (chemical potential). Not surprisingly, Esposito's definitions are consistent with the above. Returning to (5.9) and using (5.6) we find:

$$\dot{\mathcal{S}}_i = \left(\frac{1}{T_L} - \frac{1}{T_R}\right)(-\mathcal{J}_L^E) + \left[-\left(\frac{\mu_L}{T_L} - \frac{\mu_R}{T_R}\right)\right](-\mathcal{J}_L^N). \tag{5.13}$$

The signs are kept this way, because by convention a positive current indicates flowing into the dot, thus a negative current means flowing to the bath. As another check, in absence of particle current, the second law implies that energy current flows down temperature gradient:

$$(\mathcal{J}_L^N = 0) \wedge (\dot{\mathcal{S}}_i \geq 0) \implies (-\mathcal{J}_L^E \geq 0 \text{ iff } \left(\frac{1}{T_L} - \frac{1}{T_R}\right) \geq 0). \tag{5.14}$$

5.3 Linear irreversible thermodynamics

Let us return to the discussion of thermodynamic forces ($\mathcal{F}_i$) and fluxes ($\mathcal{J}_i$). Intuitively, one wishes to regard the fluxes as responses to the forces. If such is the case, when the forces are weak, then a linear expansion is in place. Now, a difference in chemical potential generates particle flow, and there is no reason for this current to be decoupled from the energy flow, and vice versa. Thus phenomenologically, for small forces [30]:

$$\begin{bmatrix} -\mathcal{J}^N \\ -\mathcal{J}^E \end{bmatrix} = \begin{bmatrix} L_{NN} & L_{NE} \\ L_{EN} & L_{EE} \end{bmatrix} \begin{bmatrix} \mathcal{F}_\mu \\ \mathcal{F}_T \end{bmatrix}, \tag{5.15}$$

where we remind the presence of minus sign is because of the convention that negative current flows away from the dot. Arguing with detailed balance, Onsager [31] showed his famous reciprocal relation: $L_{NE} = L_{EN}$ for time-reversal invariant systems (eg. no

[2]Sometimes referred to as near-equilibrium and close-to-equilibrium.

[3]Also called thermodynamic forces, in the sense that negative entropy, $-S$ is like some trapping potential and when a system is deviated from the minimum of $-S$, these forces will attempt to restore the system to the minimum and they do so by inducing the fluxes to generate entropy.

magnetic field). Setting $k_B = 1$, our task is to determine the expression of $\mathcal{J}_L^N$ and $\mathcal{J}_L^E$ up to first order in $\mathcal{F}_T = \Delta\beta = \beta_L - \beta_R$ and $\mathcal{F}_\mu = \Delta(-\beta\mu) = -\beta_L\mu_L + \beta_R\mu_R$. After some elementary calculations, one obtains:

$$\begin{aligned}
L_{NN} &= \int \frac{\mathrm{d}E}{2\pi} A \frac{\Gamma_L\Gamma_R}{\Gamma_L+\Gamma_R} \left[4\cosh^2\left(\frac{\overline{\beta}E - \overline{\beta\mu}}{2}\right)\right]^{-1}, \\
L_{NE} &= \int \frac{\mathrm{d}E}{2\pi} EA \frac{\Gamma_L\Gamma_R}{\Gamma_L+\Gamma_R} \left[4\cosh^2\left(\frac{\overline{\beta}E - \overline{\beta\mu}}{2}\right)\right]^{-1}, \\
L_{EN} &= \int \frac{\mathrm{d}E}{2\pi} EA \frac{\Gamma_L\Gamma_R}{\Gamma_L+\Gamma_R} \left[4\cosh^2\left(\frac{\overline{\beta}E - \overline{\beta\mu}}{2}\right)\right]^{-1}, \\
L_{EE} &= \int \frac{\mathrm{d}E}{2\pi} E^2 A \frac{\Gamma_L\Gamma_R}{\Gamma_L+\Gamma_R} \left[4\cosh^2\left(\frac{\overline{\beta}E - \overline{\beta\mu}}{2}\right)\right]^{-1},
\end{aligned} \tag{5.16}$$

where we denoted $\overline{\beta} = \frac{\beta_L+\beta_R}{2}$ and $\overline{\beta\mu} = \beta_L\mu_L - \beta_R\mu_R$. Thus, we checked that Onsager reciprocal relation $L_{NE} = L_{EN}$ holds with Esposito's definitions. These matrix elements are called Onsager kinetic coefficients and here unfortunately the integrals cannot be further simplified.

5.4 Thermoelectric engine

Let us first analyse the title of this section, word by word. *Thermoelectricity* is the phenomenon in which heat and electricity (the flow of electrons) intertwine with each other, thanks to the presence of both temperature and voltage (chemical potential in our context) difference. *Engine* is a generic term designating energy-converting devices which utilize heat to perform work. By thermoelectric engine, we mean one which uses heat to overcome chemical potential barrier. More precisely, suppose $T_L > T_R$ but $\mu_L < \mu_R$. The temperature gradient drives heat from left to right, but particles tend to flow from right to left because of the chemical potential difference. However, heat and particle current are not independent, since when particles flow they carry with them energies. Thus we can hope to pump electrons against chemical potential by using heat. This device then qualifies to be called an engine[4]:

[4]Contrary to the cyclic heat engine that one encounters when studying Carnot cycle, this thermoelectric device is a particle-exchange heat engine. The working medium (quantum dot) does not undergo a cycle which exchanges heat and work at different stages. It takes in heat and perform work continuously in a steady state.

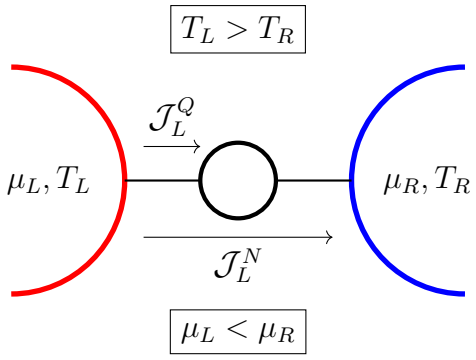

Figure 5.1: Thermoelectric engine: pumping electrons against chemical potential with heat.

5.4.1 Thermopower and thermoelectric efficiency

Generally speaking, we evaluate the performance of an engine based on its efficiency and power[5]. For our thermoelectric engine, the power is the rate of work done in transporting particles against the bias:

$$\mathcal{P} = (\mu_R - \mu_L)\mathcal{J}_L^N \tag{5.17}$$

whereas the efficiency is the output power, divided by the heat current needed to deliver it:

$$\eta_{TE} = \frac{\mathcal{P}}{\mathcal{J}_L^Q} \tag{5.18}$$

where $\mathcal{J}_L^N$ ($\mathcal{J}_L^Q$) is the particle (heat) current flowing from the left bath, as given by (5.3) and (5.4). Let us check the pertinence of these definitions. We refer to a situation depicted in Figure 5.1. Thus $\mu_R - \mu_L > 0$ and $\mathcal{J}_L^Q > 0$ (since it is entering the dot[6]), and the power $\mathcal{P}$ is positive. As for η_{TE}, we consider the difference of $\mathcal{P}$ and $\mathcal{J}_L^Q$:

$$\begin{aligned}\mathcal{P} - \mathcal{J}_L^Q &= (\mu_R - \mu_L)\int \frac{\mathrm{d}E}{2\pi} C_L - \int \frac{\mathrm{d}E}{2\pi}(E - \mu_L)C_L \\ &= \int \frac{\mathrm{d}E}{2\pi}(E - \mu_R)C_R \\ &= \mathcal{J}_R^Q \leq 0.\end{aligned} \tag{5.19}$$

Since heat is leaving from the dot to right as depicted in Figure 5.1. Thus $\eta_{TE} \leq 1$ as required.

5.4.2 Carnot efficiency

Allow us to make a historical detour to bring in the concept of Curzon-Ahlborn efficiency. In 1824, Carnot [9] ruled out all attempts to build a maximally efficient engine in which all

[5]Recently people have begun to study efficiency and power fluctuations [32][33], which also serve to characterize the performance.

[6]In absence of temperature gradient, $\mu_R > \mu_L$ implies $\mathcal{J}_L^Q < 0$, cf. (5.14). Thus in order for $\mathcal{J}_L^Q$ to be positive we need to either have a strong enough temperature gradient, or to properly position the energy level ε. Unfortunately we cannot provide explicit conditions because the expressions are not integrable.

heat is converted into work[7]. He demonstrated a universal upper bound to the efficiency of all cyclic heat engines, given by:

$$\eta_C = 1 - \frac{T_C}{T_H} \tag{5.20}$$

where T_H (T_C) is the temperature of the hot (cold) bath from (to) which heat is absorbed (discharged). In order to achieve this efficiency, it is necessary that the cycle be reversible and hence quasi-static[8]. Power is output work divided by operational time. To perform a quasi-static process, one needs to do it infinitely slowly. Therefore, even though Carnot engine is the most efficient one, with zero power, it is also the least practical one.

5.4.3 Curzon-Ahlborn efficiency

The above consideration motivated the study of finite-time Carnot cycles. One way to relax the quasi-static requirement is to allow heat transfers to take place in finite time, which Curzon and Ahlborn did [34]. They then proceeded to maximize the output power and showed that the efficiency at maximum power of their modified Carnot cycle is given by:

$$\eta_{CA} = 1 - \sqrt{\frac{T_C}{T_H}} \leq \eta_C. \tag{5.21}$$

Similar to η_C, the Curzon-Ahlborn efficiency is universal in that it does not depend on the working fluid nor the thermal conductivity[9]. Furthermore, it only depends on the temperature ratio $\frac{T_C}{T_H}$. If we express η_{CA} as a function of η_C, then since $\eta_C < 1$, we have:

$$\eta_{CA} = 1 - \sqrt{1 - \eta_C} \tag{5.22}$$

$$= \frac{\eta_C}{2} + \frac{\eta_C^2}{8} + \frac{\eta_C^3}{16} + O(\eta_C^4). \tag{5.23}$$

Interestingly, it was shown for a Brownian Carnot engine[10] and for a Feynman ratchet[36] that the efficiency at maximum power has the same expansion as in (5.23) up to second order in η_C.

5.5 Thermoelectric efficiency at maximum power

While studying the same model in weak-coupling regime, with master equation, Esposito showed that, when the temperature ratio $\frac{T_C}{T_H}$ is close to unity, the efficiency at maximum power of the thermoelectric engine (denoted by η_{TE}) as given in Figure 5.1 has an asymptotic expression identical to that of (5.21) up to second order in $\eta_C = 1 - \frac{T_C}{T_H}$:

$$\eta_{TE} = \frac{\eta_C}{2} + \frac{\eta_C^2}{8} + 0.077492\,\eta_C^3 + O(\eta_C^4). \tag{5.24}$$

[7]Nowadays called a perpetual motion machine of the second kind.

[8]A reversible process is necessarily quasi-static but the converse is not true.

[9]In the derivation of η_{CA}, one assumes a Fourier law of heat conduction between working medium and each reservoir. The thermal conductivities disappear in the final expression of efficiency at maximum power.

Thus, we ask if the thermoelectric efficiency at maximum power obeys similar expansion using the definitions in this project. We first need to maximize the power given by (5.17). Since in non-weak coupling, all integrals involved cannot be simplified, we can only resort to numerical calculations. Next, we remark that the integrals of interest involve seven parameters in total $(\varepsilon, \mu_L, \mu_R, T_L, T_R, \Gamma_L, \Gamma_R)$. While we can argue by symmetry to reduce them to five[10], a brute force optimization without considering the physical context is still impossible[11]. Hence, we adopt the following two different strategies:

(1) Fix the temperature and chemical potential of the hotter but negatively-biased bath: T_L, μ_L. Fix the total coupling strengths $\Gamma = \Gamma_L + \Gamma_R$ and set $\Gamma_L = \Gamma_R$.

(2) For each η_C, calculate the corresponding T_R.

(3) By varying ε and μ_R, maximize the power using either of:

   (a) "Weak-coupling optimization": Maximize the power with weak-coupling expressions[12]. Calculate efficiencies using strong-coupling expressions.

   (b) "Ordinary optimization": Maximize the power and calculate the efficiencies, both using strong-coupling expressions.

(4) Calculate the corresponding efficiency η with the optimizing values of ε and μ_R.

(5) Plot η against η_C.

5.5.1 Weak-coupling optimization

We first discuss the results with weak-coupling optimization. The units used are such that $\hbar = 1, k_B = 1$. This leaves a freedom of choice for, say, time, and if desired it can chosen for realistic values. For ease of reading we list the observations:

(i) For temperature ratio close to unity (ie. Carnot efficiency η_C close to zero), all curves coincide and thus from η_{CA} we infer that they all behave like:

$$\eta \approx \frac{\eta_C}{2} + \frac{\eta_C^2}{8} \tag{5.25}$$

for η_C sufficiently close to zero.

(ii) With naked eyes, the curves η_{TE}, $\Gamma = 0.1$ and $\Gamma = 1.0$ coincide perfectly. Thus for sufficiently weak coupling, the efficiency at maximum power is unchanged by the exact values of coupling. In fact, when zoomed in, $\Gamma = 1.0$ is below $\Gamma = 0.1$ which itself is below η_{TE}.

[10]The dot energy level ε, the left/right chemical potential $\mu_{L/R}$ enjoy translational invariance. This reduces the number of parameters by one. Furthermore, if we keep the total coupling strength $\Gamma_L + \Gamma_R$ fixed, the individual ones $\Gamma_{L/R}$ only affect the power by a multiplicative factor, thus we can set $\Gamma_L = \Gamma_R$.

[11]For example, if we let all five parameters to vary independently and freely, there is no solution to the power optimization, because the power can be made arbitrarily large by having sufficiently large temperature and chemical potential difference .

[12]This has been done by Esposito in [35].

(iii) At larger η_C, the curves start to deviate from each other. $\Gamma = 10.0$ always stays below $\Gamma = 0.1$ and $\Gamma = 1.0$, but is still above the exact Curzon-Ahlborn efficiency η_{CA}.

(iv) The $\Gamma = 40.0$ curve lies lowest among all. The efficiency decreases for large η_C. There is no proof to this but logically it is difficult to think of a machine whose efficiency does not follow monotonously its Carnot efficiency. We can understand this anomaly by considering $\Gamma = 40.0$ as having exceeded a critical coupling strength, beyond which the weak-coupling expressions simply differ too much from the non-weak coupling ones.

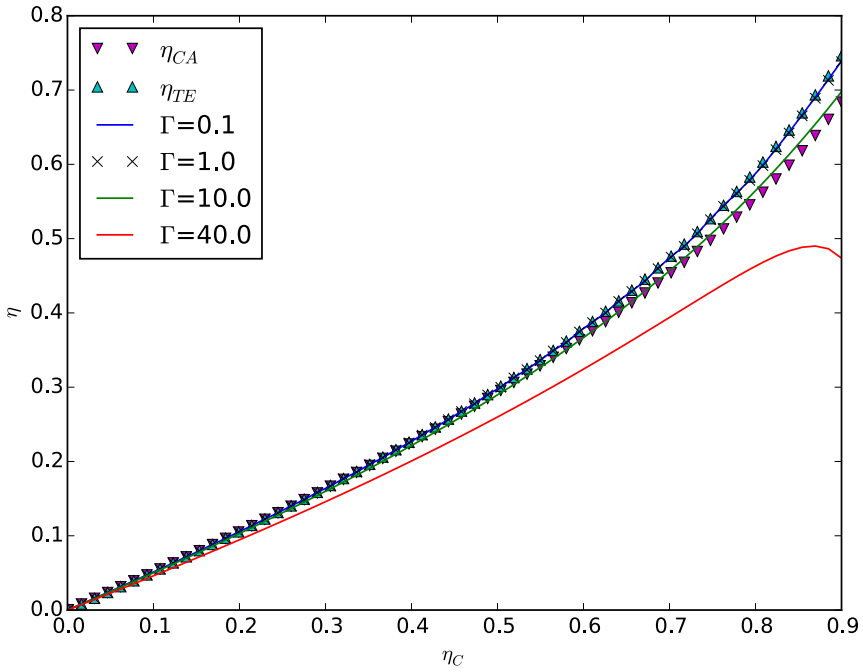

Figure 5.2: Efficiency at maximum power using weak-coupling optimization with fixed hot bath temperature. The parameters used are $\mu_L = 0$ and $T_L = 300.0$. Units used are such that $\hbar = 1$,$k_B = 1$.

5.5.2 Ordinary optimization

Contrary to the weak-coupling optimization, here for each data point, we optimize the strong-coupling expressions. We used a ready-made optimizer from SciPy called SLSQP (Sequential Least Squares Programming), which allows setting constraints[13] and require

[13]The constraints are: $\mu_R > \mu_L$ for consistency of the problem (transporting electrons from higher to lower chemical potential) and $\varepsilon > \frac{\beta_L\mu_L - \beta_R\mu_R}{\beta_L - \beta_R}$ (the centre of spectral function must be greater than the energy at which $f_L = f_R$). Note that this latter relation does not necessarily ensure the flow of electrons to be from left to right as desired. In particular when the hot bath temperature is too high and coupling strength too strong, there will be a significant backward flow of electrons and the optimization problem becomes ill-posed.

initial guesses. Naturally, one uses the weak-coupling optimized parameters as guesses. We first plot the results at fixed hot bath temperature for different total coupling strengths.

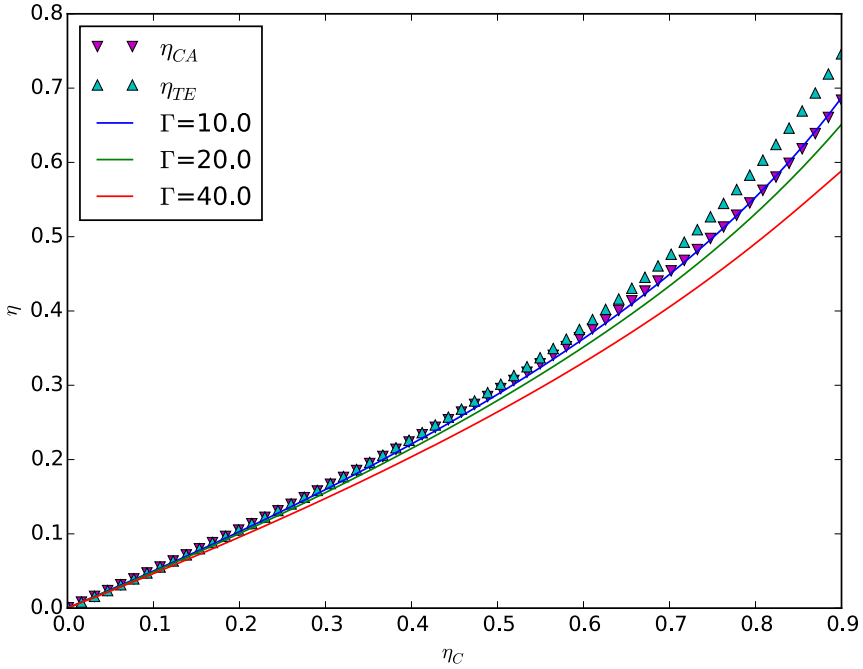

Figure 5.3: Efficiency at maximum power using ordinary optimization with fixed hot bath temperature. The parameters used are $\mu_L = 0$ *and* $T_L = 300.0$.

From the plot above, we see that the $\Gamma = 40.0$ curve is always monotonous even for large η_C. Compared to Figure 5.2, the curves for $\Gamma = 0.1$ and $\Gamma = 1.0$ are not shown because the results are not sensible[14]. Next, observe that the efficiency curves are shifted down as we increase the coupling strength. Thus strong coupling deteriorates the thermoelectric efficiency at maximum power. This is because maximizing power is finding the position at which electrons from both sides have the strongest urge to be moved. On the other hand, a larger coupling strength means allocating unnecessary bandwidth for the transport of electrons that are around the optimal position.

Finally, we plot also the results for fixed total coupling strength but different temperatures:

[14]The optimization problem becomes ill-posed because with coupling strength that is several orders of magnitude smaller than the temperature, by having chemical potential arbitrarily large the power can always be made larger.

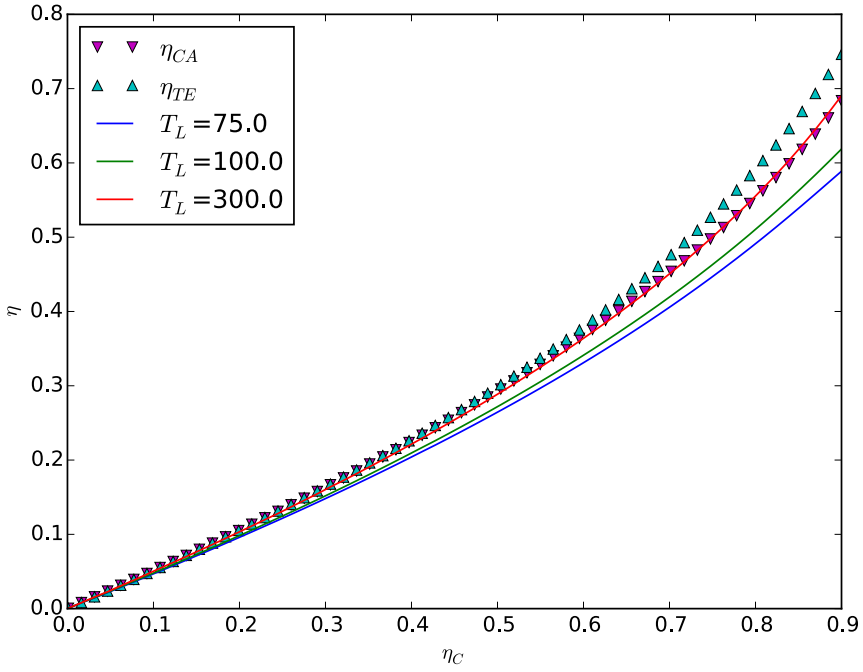

Figure 5.4: Efficiency at maximum power using ordinary optimization with fixed total coupling strength. The parameters used are $\mu_L = 0$ *and* $\Gamma = 10.0$.

Notice once again the validity of the expansion (5.25) since all curves including η_{CA} coincide for sufficiently small η_C. In particular, increasing the temperature of hot bath T_L shifts the efficiency curve upwards. One way to interpret this is, for a higher T_L, the Fermi function $f_L(E)$ is more smeared out around the chemical potential μ_L. Thus there is more search space for the optimizer to look for ε and μ_R. We conclude this chapter with the remark that the thermoelectric efficiency at maximum power is no longer a simple function of temperature ratio alone, as shown in Figure 5.3 and 5.4.

Chapter 6

Driven Quantum Dot

Having discussed steady-state thermoelectric engine, in this chapter we proceed to investigate the feasibility of a cyclic heat engine. We first recall several features of such engine. The name "cyclic" itself suggests that we need to allow for time-evolutions in our system. Among the plethora of possible modulations, we rule out a class by establishing a necessary condition for a non-trivial work extraction. Finally, while analysis on paper is not possible, we numerically implement one such engine.

6.1 Cyclic heat engine

By heat engine we mean a composite system consisting of two thermal[1] reservoirs T_H and T_C at different temperatures, a work reservoir W, and a working fluid S (single-level quantum dot for our model). The working fluid is always connected to the work reservoir and may be connected to both, either, or none of the thermal baths in the course of its operations. The tricky business in non-classical heat engine to identify properly the heat and work exchanged. In this project we follow Esposito's definitions, so that the external power[2] is $\mathcal{P}_{\text{ext}}$, heat from hot (cold) bath is $\mathcal{J}_L^Q$ ($\mathcal{J}_R^Q$) with the convention that $T_L = T_H > T_C = T_R$. By definition, the working fluid of a cyclic heat engine undergoes a cyclic process, so that after one cycle, heat is absorbed from T_H and discharged to T_C and work done to W.

[1] In our model, electrons are the carriers of energy, thus the reservoirs are thermal and particle.

[2] We have here a "black box" work reservoir, in that there is no mention of exactly how work is exchanged. One possible physical situation is an electric field, whose strength changes the energy level ε of the dot. If it results in a decrease of ε then work has been done to the external agent modulating the electric field strength.

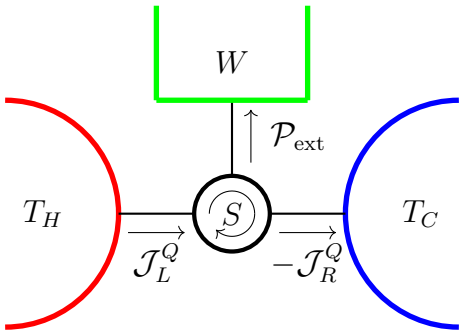

Figure 6.1: Cyclic heat engine: performing work by transferring heat.

For example, if we use classical ideal gas as a working fluid, then its pressure and volume p, V suffice to characterize its state, and we vary p, V in such a way to form a non-trivial closed loop[3] in the $p-V$ diagram. The work exerted would then be the area of the closed loop.

6.2 ε and Γ as state parameters

With $\mu_{L/R}, T_{L/R}, \varepsilon, \Gamma_{L/R}$, seven parameters in total, we choose to vary ε, the dot energy level, and $\Gamma = \Gamma_L + \Gamma_R$, the sum of the coupling strengths. Cyclicity means that we ought to choose periodic functions $\varepsilon(t)$ and $\Gamma(t)$, such that after one period, heat has transferred from hotter to colder bath, and work has been done to exterior. For simplicity, we choose the two protocols $\varepsilon(t)$ and $\Gamma(t)$ to be of the same period[4]. Then, the problem can be formulated as follows: on $\varepsilon - \Gamma$ plane[5], find periodic functions $\varepsilon(t)$ and $\Gamma(t)$ of the same period $\mathcal{T}$, such that after one period, they trace out a non-trivial closed loop, and if we compute

$$W = \int_0^{\mathcal{T}} \mathcal{P}_{\text{ext}}(t)\,\mathrm{d}t \tag{6.1}$$

that is the work after one cycle, we get a strictly negative number (so that work has been done by the system to exterior). Let us recall the expression of $\mathcal{P}_{\text{ext}}$ up to first order in driving frequency:

$$\begin{aligned}
\mathcal{P}_{\text{ext}} &= \int \frac{\mathrm{d}E}{2\pi} \mathcal{A}\phi^{(0)} \left[\dot{\varepsilon} + \frac{d_t\Gamma}{\Gamma}(E-\varepsilon)\right] \\
&= \int \frac{\mathrm{d}E}{2\pi} \left[\frac{\Gamma}{(E-\varepsilon)^2 + (\frac{\Gamma}{2})^2}\right]^2 \frac{\Gamma}{2} \frac{\Gamma_L f_L + \Gamma_R f_R}{\Gamma_L + \Gamma_R} \left[\dot{\varepsilon} + \frac{d_t\Gamma}{\Gamma}(E-\varepsilon)\right] \\
&= \int \frac{\mathrm{d}E}{2\pi} \frac{A^2\Gamma}{2} \frac{\Gamma_L f_L + \Gamma_R f_R}{\Gamma_L + \Gamma_R} \left[\dot{\varepsilon} + \frac{d_t\Gamma}{\Gamma}(E-\varepsilon)\right]
\end{aligned} \tag{6.2}$$

When we have proportional coupling:

$$\Gamma_R(t) = \lambda \Gamma_L(t) \tag{6.3}$$

[3]Non-trivial means that the loop does not reduce to a one-dimensional sector.
[4]They can be of different periods $\mathcal{T}_\varepsilon$ and $\mathcal{T}_\Gamma$, but their ratio must be a rational number.
[5]Strictly speaking it is the semi-half plane $\varepsilon - \Gamma^+$ since the coupling strength is non-negative.

with $\lambda > 0$ a time-independent constant, the above becomes:

$$\mathcal{P}_{\text{ext}} = \int \frac{\mathrm{d}E}{2\pi} \frac{A^2\Gamma}{2} \frac{f_L + \lambda f_R}{1+\lambda} \left[\dot{\varepsilon} + \frac{d_t\Gamma}{\Gamma}(E-\varepsilon) \right] \tag{6.4}$$

As for the total work done after one period we have:

$$\begin{aligned} W &= \int \frac{\mathrm{d}E}{2\pi} \left\{ \frac{f_L + \lambda f_R}{1+\lambda} \int_0^{\mathcal{T}} \mathrm{d}t \, \frac{A^2\Gamma}{2} \left[\dot{\varepsilon} + \frac{E-\varepsilon}{\Gamma}\dot{\Gamma} \right] \right\} \\ &= \int \frac{\mathrm{d}E}{2\pi} \left[\frac{f_L + \lambda f_R}{1+\lambda} \int_\gamma \frac{A^2\Gamma}{2} \mathrm{d}\varepsilon + \frac{A^2\Gamma}{2} \frac{E-\varepsilon}{\Gamma} \mathrm{d}\Gamma \right] \end{aligned} \tag{6.5}$$

where

$$\begin{aligned} \gamma : [0, \mathcal{T}] &\longrightarrow (\mathbb{R}, \mathbb{R}_+) \\ t &\longmapsto \big(\varepsilon(t), \Gamma(t)\big) \end{aligned} \tag{6.6}$$

is a protocol forming a non-trivial simple[6] closed loop. In writing the one-parameter t integral as a two dimensional (ε, Γ) line integral, we are considering A as a function of ε, Γ for each E:

$$A(E) = \frac{\Gamma}{(E-\varepsilon)^2 + (\frac{\Gamma}{2})^2} = A(\varepsilon, \Gamma) \tag{6.7}$$

A straightforward calculation shows that:

$$\frac{\partial}{\partial\varepsilon} \left[\frac{A(\varepsilon,\Gamma)^2\Gamma}{2} \frac{E-\varepsilon}{\Gamma} \right] = \frac{A(\varepsilon,\Gamma)^2}{2}(3 - A(\varepsilon,\Gamma)\Gamma) = \frac{\partial}{\partial\Gamma} \frac{A(\varepsilon,\Gamma)^2\Gamma}{2} \tag{6.8}$$

This is equivalent to saying:

(i) The vector field $(\frac{A(\varepsilon,\Gamma)^2\Gamma}{2}, \frac{A(\varepsilon,\Gamma)^2\Gamma}{2}\frac{E-\varepsilon}{\Gamma})$ has path-independent line integral.

(ii) $W = \int_\gamma \mathcal{P}_{\text{ext}}\, dt = 0$ for any closed loop γ.

The first item allows us to define the external work done as a state function of (ε, Γ):

$$W(\varepsilon, \Gamma) = \int \frac{\mathrm{d}E}{2\pi} \left[\frac{f_L + \lambda f_R}{1+\lambda} \int_A^B \frac{A^2\Gamma}{2} \mathrm{d}\varepsilon + \frac{A^2\Gamma}{2} \frac{E-\varepsilon}{\Gamma} \mathrm{d}\Gamma \right] \tag{6.9}$$

with $A = (\varepsilon_0, \Gamma_0)$ an arbitrary reference point and $B = (\varepsilon, \Gamma)$ the point of interest. Put it differently, given a protocol $(\varepsilon(t), \Gamma(t))$:

> *Under the proportional coupling condition* (6.3)*, the external work done between two instants t_i and t_f depends only on the two endpoints $P = (\varepsilon(t_i), \Gamma(t_i))$ and $Q = (\varepsilon(t_f), \Gamma(t_f))$, but not the way one traverses from P to Q.*

[6]Simple means the path is not self-intersecting.

This is rather peculiar and is in sharp contrast with classical situation where work done from one state to another depends largely on the path traversed. The second item tells us that for non-pathological periodic protocols $(\varepsilon(t), \Gamma(t))$, the work done after one period is always zero. In other words:

> *In order to design cyclic protocols such that after one period there is a non-zero work W being done, it is necessary that one breaks the proportional coupling condition* (6.3).

However, it must be stressed that the above conclusions only hold for equations of motion up to first order in driving frequency. After time integration over a period, the external work done actually becomes zeroth order. Unfortunately as shown in Appendix E, the quantum kinetic equation up to second order is too complicated to be handled. We thus focus only on first order equations (therefore zeroth order for time-integrated work done).

6.3 Four-stroke protocol for work extraction

Bearing in mind the necessity to break proportional coupling (6.3) for a non-trivial cyclic heat engine, we now discuss a simple case where the total coupling strength is kept fixed: $\Gamma = \Gamma_L(t) + \Gamma_R(t)$ with $\dot{\Gamma} = 0$. Then the rate of work done becomes:

$$\mathcal{P}_{\text{ext}} = \int \frac{\mathrm{d}E}{2\pi} \underbrace{\frac{\Gamma}{2}\left[\frac{\Gamma}{(E-\varepsilon(t))^2 + (\frac{\Gamma}{2})^2}\right]^2}_{\mathcal{A}(E,t)} \underbrace{\left[\frac{\Gamma_L(t)}{\Gamma} f_L + \left(1 - \frac{\Gamma_L(t)}{\Gamma}\right) f_R\right]}_{\phi^{(0)}(E,t)} \dot{\varepsilon}(t) \tag{6.10}$$

Thus by plotting along energy axis, we can investigate the effects of modulations on $\mathcal{A}$ and $\phi^{(0)}$. These are the terms that constitute the (energy) integrand of external power. When the total coupling strength Γ is fixed, the renormalised spectral function $\mathcal{A}$ does not change its width but moves its centre as we vary ε. On the other hand, the modulation of Γ_L changes the shape of the zeroth order probability distribution $\phi^{(0)}$:

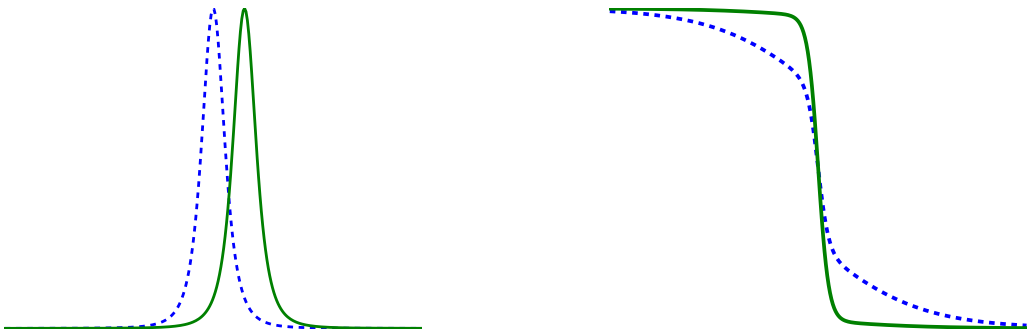

(a) *(b)*

Figure 6.2: (a) Changing the renormalised spectral function $\mathcal{A}$ by increasing dot energy level ε with total coupling strength Γ kept fixed. (b) Changing the steady-state distribution $\phi^{(0)}$ by decreasing hot bath coupling strength Γ_L. The transitions are represented from dashed to solid lines.

With the above in mind, we propose the following scheme that would allow us to obtain a negative time-integrated $\mathcal{P}_{\text{ext}}$ (work output):

(A) Decrease dot energy level ε. This leads to negative $\mathcal{P}_{\text{ext}}$ and hence work output W_{out} when integrated.

(B) Increase hot bath coupling strength Γ_L. This does not result in any exchange of work but will decrease the work that needs to be supplied later to restore the system to its initial state.

(C) Increase the dot energy level ε back to its initial value, this requires external work to be done on the dot W_{in}. If the parameters are appropriately tuned, we can expect to have $|W_{\text{in}}| < |W_{\text{out}}|$.

(D) Decrease the hot bath coupling strength Γ_L back to its initial value to start from step (A) again.

Schematically, the above can be summarised in the following flow chart:

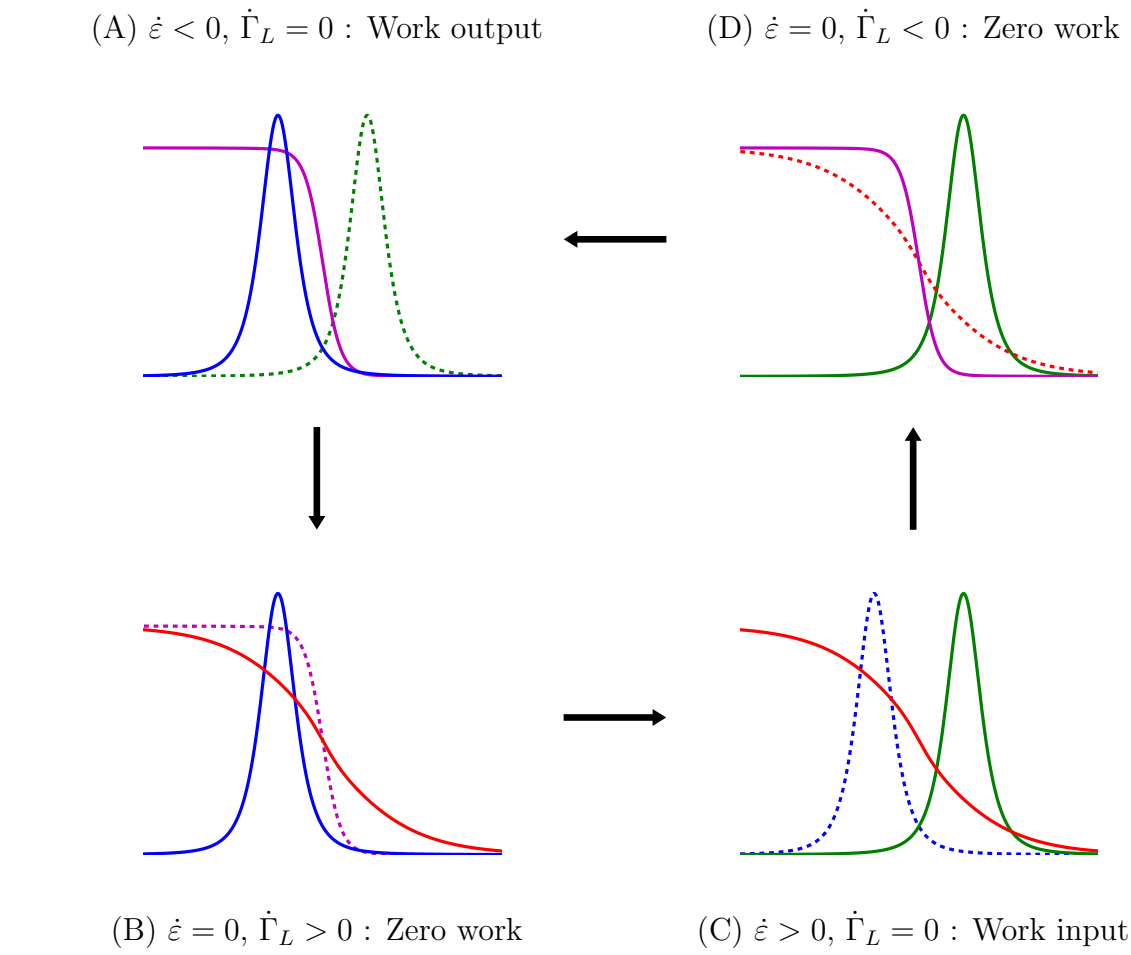

Figure 6.3: A possible realisation of quantum dot cyclic heat engine. Each process is represented by a dashed to solid line transition.

6.4 Fermi-smoothened trapezoidal driving

Graphically, one possible realisation of protocols $\varepsilon(t)$ and $\Gamma_L(t)$ is given by the following trapezoidal signal:

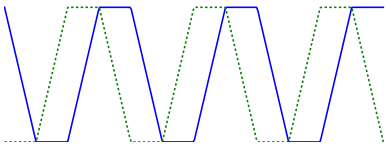

Figure 6.4: Trapezoidal control for work extraction. If we start from (A) as in Figure 6.3, then solid line is $\varepsilon(t)$ and dashed line $\Gamma_L(t)$.

However, in applying first order gradient expansion, we assumed regularity of all time-dependent functions so that they admit Taylor expansions and terms of order ∂_t^2 could be neglected for slow driving. The first derivative of trapezoidal signal is clearly discontinuous. One way to overcome this difficulty is by replacing the ramps with Fermi functions[7]:

$$K_{C,T}(t) = \begin{cases} 0 \\ C\left(\dfrac{4t}{T} - 1\right) \\ C \\ 4C\left(1 - \dfrac{t}{T}\right) \end{cases} \longrightarrow \begin{cases} 0 & ,t \in \left[0, \frac{T}{4}\right) \\ C\left(\exp\left[-80\left(\frac{t}{T} - \frac{3}{8}\right)\right] + 1\right)^{-1} & ,t \in \left[\frac{T}{4}, \frac{T}{2}\right) \\ C & ,t \in \left[\frac{T}{2}, \frac{3T}{4}\right) \\ C\left(\exp\left[80\left(\frac{t}{T} - \frac{7}{8}\right)\right] + 1\right)^{-1} & ,t \in \left[\frac{3T}{4}, T\right) \end{cases} \pmod{T}$$

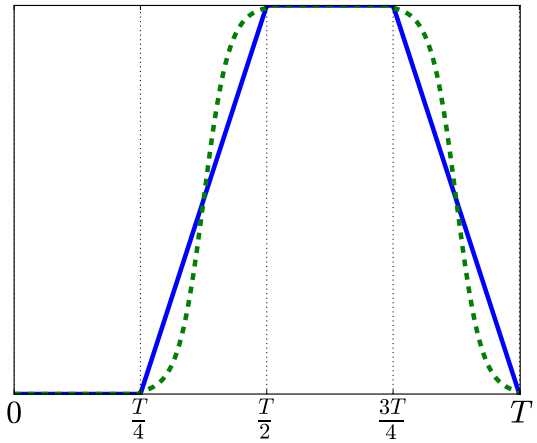

Figure 6.5: Smoothening trapezoidal signal with Fermi functions.

[7] In fact, there is a whole class of functions, collectively known as *sigmoid* functions, that allows us to smoothen the ramp. A sigmoid function admits two different asymptotic values at $\pm\infty$ and increases smoothly from one to another.

In choosing the factor 80 in the arguments of exponents, we approximate $\exp(-10) \approx 0$. It is worthwhile to mention that, by choosing protocols in which $\dot{\Gamma} = 0$, the expression for external power is then:

$$\mathcal{P}_{\text{ext}}(t) = \dot{\varepsilon}(t)\mathcal{N}(t) \tag{6.11}$$

with $\mathcal{N}(t)$ the particle number. This allows us to have a nice analogy with ideal gas heat engine, where the (infinitesimal) work done is given by pdV. In particular, we can draw a $\mathcal{N} - \varepsilon$ diagram, in which the area enclosed gives the total external work:

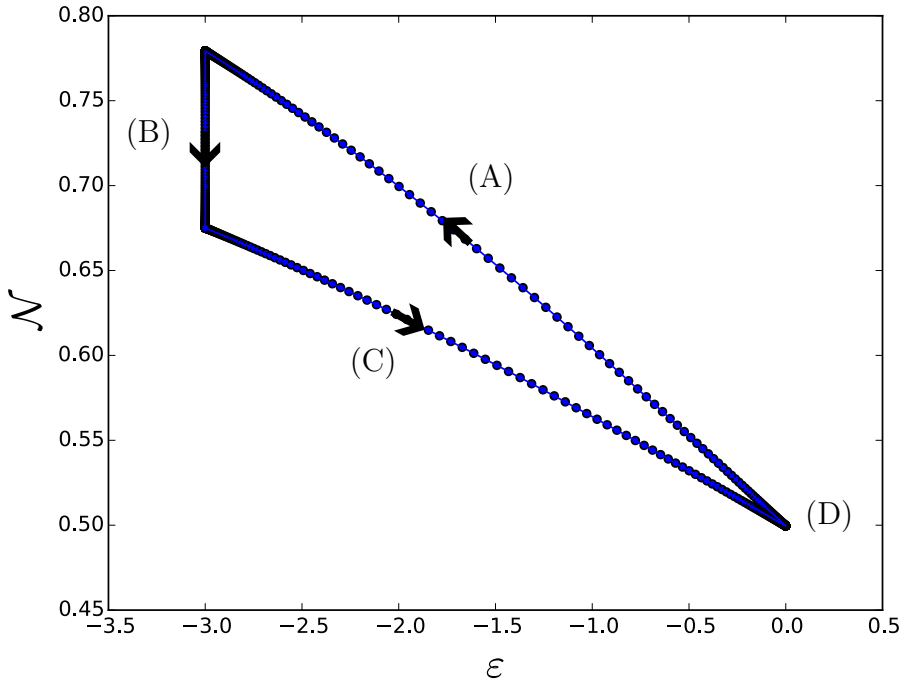

Figure 6.6: $\mathcal{N} - \varepsilon$ diagram analogous to ideal gas $p - V$ diagram. Area enclosed is the external work done. The protocols are $\varepsilon(t) = -3.0 + K_{\epsilon_0,T_0}(t)$ and $\Gamma_L(t) = K_{\Gamma_0,T_0}(t + \frac{T_0}{4})$, with parameters $\epsilon_0 = 3.0$, $\Gamma_0 = 5.0$, $T_0 = \frac{1}{\omega}$, $\omega = 0.01$, $T_L = 10.0$, $T_R = 1.0$, $\mu_R = \mu_L = 0$. Each process is labelled as illustrated in Figure 6.3.

For ordinary ideal gas engine, stroke (D) usually restores the pressure back to some higher value. Here, for quantum dot heat engine using the protocols as mentioned in the description of Figure 6.6, stroke (D) is degenerate to just a point. This can be understood by referring back to Figure 6.3, where process (D) decreases hot bath coupling strength Γ_L but does not alter significantly the particle number $\mathcal{N}$. Though we cannot prove this, by adjusting parameters, it is found that if one insists on having a non-degenerate stroke (D), then the resulting $\mathcal{N} - \varepsilon$ diagram will become doubly-connected. That is, for stroke (D) to be not just a point, there is a point $(\mathcal{N}, \varepsilon)$ that must be crossed.

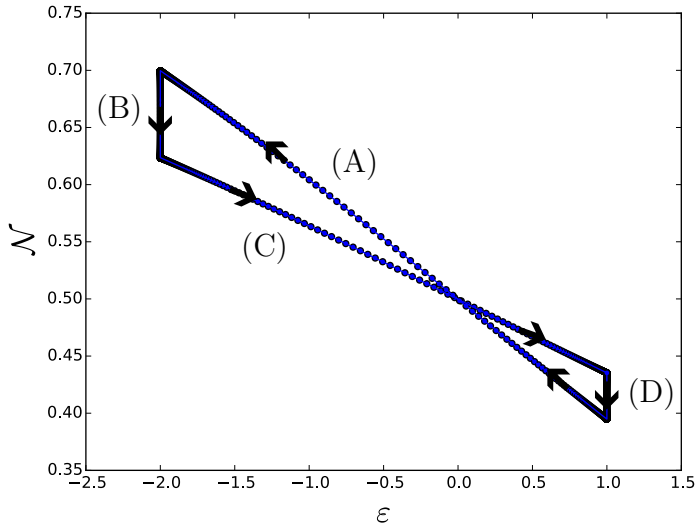

Figure 6.7: Path-crossing for non-degenerate stroke (D). The net work done is the difference of areas of the two connected regions. The protocols are $\varepsilon(t) = 1.0 + K_{\epsilon_0,T_0}(t)$ *and* $\Gamma_L(t) = K_{\Gamma_0,T_0}(t + \frac{T_0}{4})$*, with parameters* $\epsilon_0 = -3.0$*,* $\Gamma_0 = 5.0$*,* $T_0 = \frac{1}{\omega}$*,* $\omega = 0.01$*,* $T_L = 10.0$*,* $T_R = 1.0$*,* $\mu_R = \mu_L = 0$*.*

By increasing the amplitude of the modulation of coupling strength, this crossed point gets shifted and the areas enclosed decrease, leading to lower work output as shown:

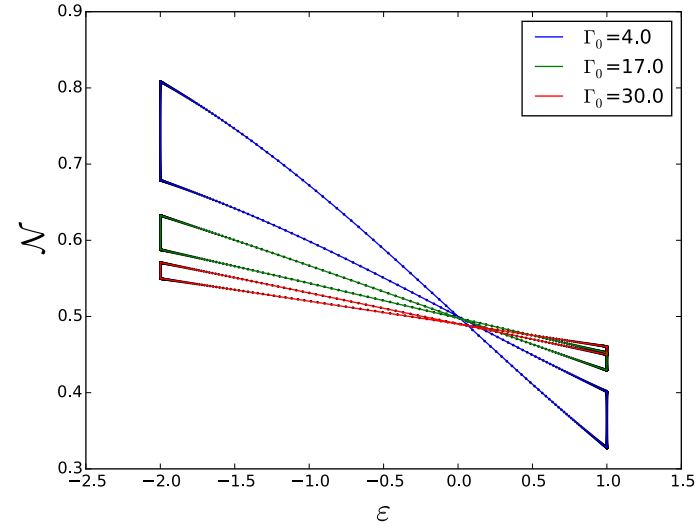

Figure 6.8: Coupling strength shifts the crossed point and decreases the area (therefore work output). Same protocol and parameters as in Figure 6.7 except for Γ_0 *which varies from 4.0 to 30.0.*

One can draw the same state diagram for the broadened dot energy $\mathcal{E} - \varepsilon$ and entropy $\mathcal{S} - \varepsilon$. The latter is not particularly illuminating so we will not show it here. For the $\mathcal{E} - \varepsilon$ diagram we have:

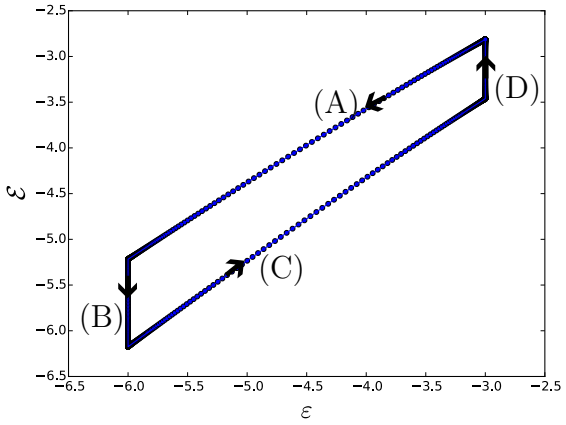

Figure 6.9: $\mathcal{E} - \varepsilon$ diagram of the system. Strokes (B) and (D) show how energy can be changed by tuning coupling strength Γ_L without changing the dot energy level. The protocols and parameters are the same as in Figure 6.6.

If anything, it serves as a reminder that in non-weak coupling regime, the dot energy $\mathcal{E}$ is no longer sharply-defined at its level ε but is smeared around it. Thus even when the dot level ε is unchanged, by modulating the coupling strength Γ_L (strokes (B) and (D)), one could still change the dot energy $\mathcal{E}$. Another observation is how Figure 6.9 bears a strong resemblance to state diagrams of classical four-stroke engine.

Next, instead of visualising the state variables individually with ε, we plot all three of them together:

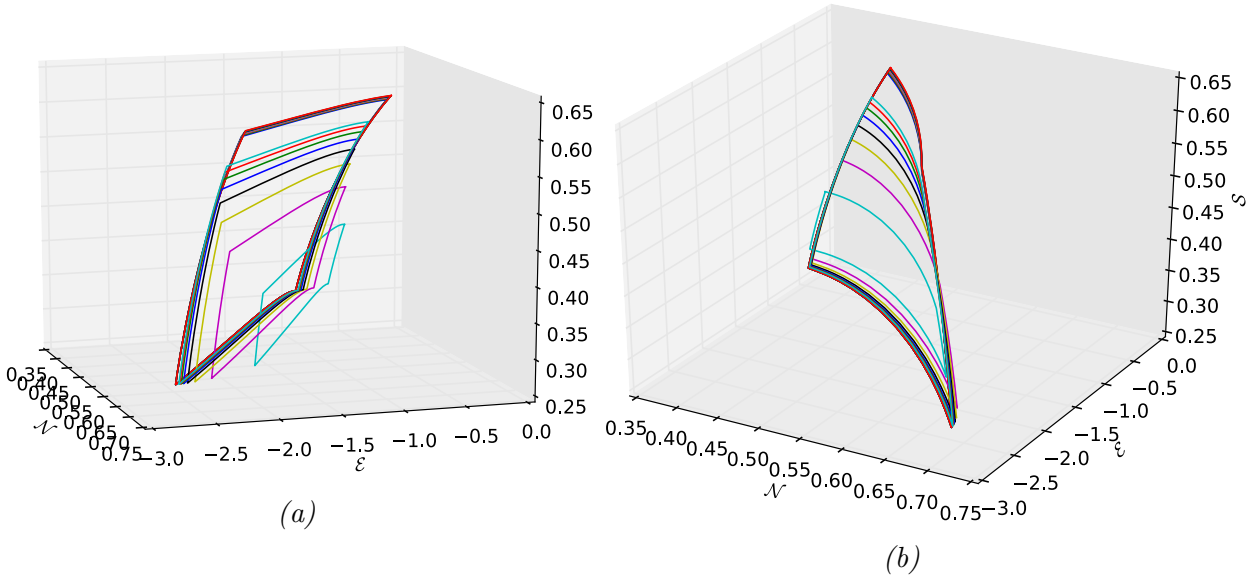

Figure 6.10: Three dimensional plots of particle number $\mathcal{N}$, dot energy $\mathcal{E}$ and dot entropy $\mathcal{S}$. The different curves are obtained by varying hot bath temperature T_L. The hot bath temperature T_L varies from 2.0 to 10.0, then from 30.0 to 50.0. The protocols and parameters are the same as in Figure 6.6.(a) Front view. (b) Back view.

We observe a limiting behaviour of the cycles as we increase the hot bath temperature T_L. This is not surprising because a large T_L corresponds to a more smeared out steady-state distribution $\phi^{(0)}$. Thus when other parameters $(\Gamma_L, \varepsilon, \mu)$ are kept fixed, further increasing T_L will only affect slightly the integrals $\mathcal{N}, \mathcal{E}, \mathcal{S}$.

Finally, we address the performance of the cyclic heat engine under the Fermi-smoothened protocol. We plot the total output work $W_{\text{out}} = -\int_0^{\mathcal{T}} \mathcal{P}_{\text{ext}}(t)\,\mathrm{d}t$ as a function of η_C:

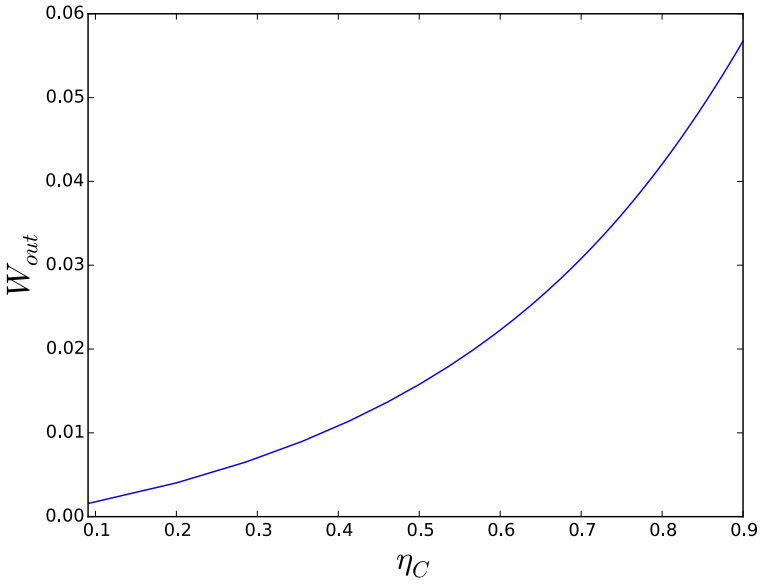

Figure 6.11: Total output work as a function of $\eta_C(T_L) = 1 - \frac{T_R}{T_L}$ *with cold bath temperature fixed at* $T_R = 1.0$. *The protocols and all parameters except* T_L *are the same as in Figure 6.6.*

However, total output work is not a good characterisation of engine performance. In fact, when designing the protocol, our only intention was to extract as much work as possible, regardless of the time spent nor the heat required. If we plot $\mathcal{P}_{\text{ext}}$ as a function of t:

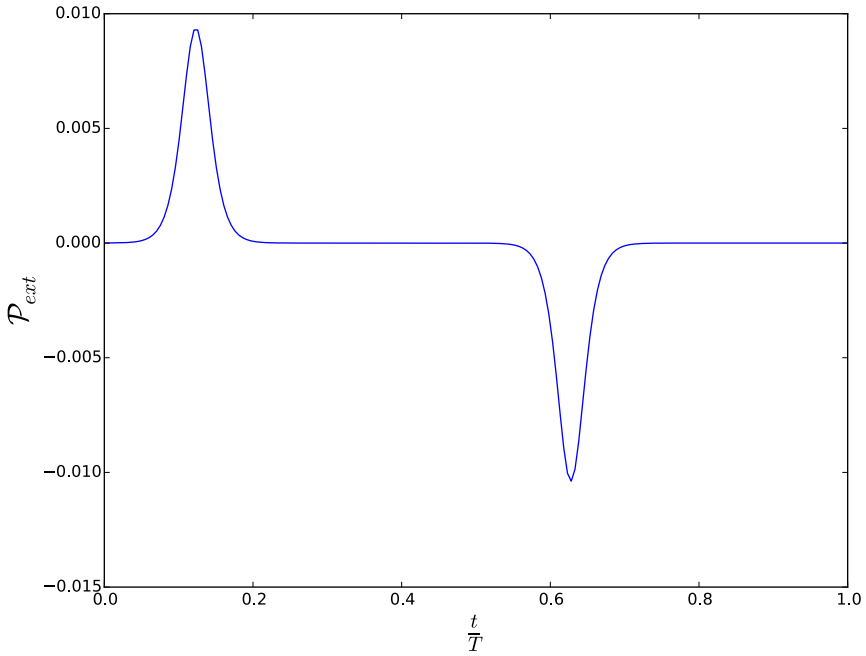

Figure 6.12: Rate of external power $\mathcal{P}_{ext}$ as a function of (period-normalised) time $\frac{t}{T}$. The protocols and all parameters are the same as in Figure 6.6.

we see that two halves of total time are spent not having any change to $\mathcal{P}_{\text{ext}}$. They correspond to strokes (B) and (D), where we modulate Γ_L in order to reduce input work and increase output work. Therefore, the proposed protocol aims at increasing net output work at the cost of reduced power. Figure 6.11 verifies the work extraction ability of our proposed protocol, which greatly resembles classical stroke engines. Furthermore, the extracted work increases with temperature ratio $\frac{T_L}{T_R}$, in accordance with Carnot's analogy[8].

6.5 Sinusoidal modulations

In the previous subsection, we observed that the stationary portions of Fermi control as illustrated in Figure 6.5 allows for a stroke-like engine but reduces the power. Here, we take the protocols in Figure 6.4 and replace them by sinusoidals:

$$\begin{aligned} \varepsilon(t) &= 2.0 + 4.0\sin^2[\omega t], \\ \Gamma_L(t) &= 5.0 - 4.0\sin^2[\omega(t+\varphi)], \end{aligned} \tag{6.12}$$

with $\omega = 0.01$ and $\varphi = \dfrac{\pi}{4\omega}$:

[8] In his *Réflexions*[9] the great thermodynamicist compared the motive power (work in present day terminology) of heat to that of waterfall, in which the temperature difference is compared to the height of a waterfall in providing motive power.

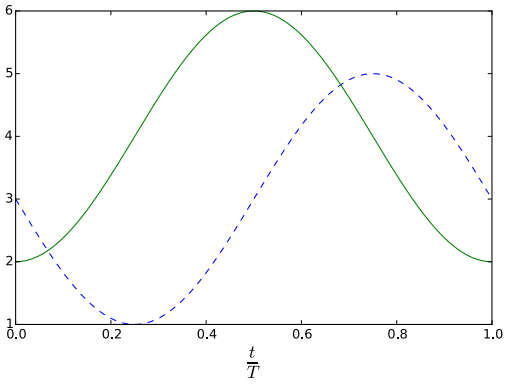

Figure 6.13: Sinusoidal controls given by (6.12) *as a function of period-normalised time* $\frac{t}{T}$ *with* $T = \frac{\pi}{\omega}$. *Solid line is* $\varepsilon(t)$ *and dashed line* $\Gamma_L(t)$.

Next, with this control, fixing $\mu_L = \mu_R = 0$ and $T_R = 1.0$, we plot the efficiency:

$$\eta = \frac{-W_{\text{out}}}{Q_{\text{in}}} = \frac{-\int_0^T \mathcal{P}_{\text{ext}}(t)\,\mathrm{d}t}{\int_0^T \mathcal{J}_L^Q(t)\,\mathrm{d}t} \tag{6.13}$$

as a function of $\eta_C(T_L) = 1 - \frac{T_R}{T_L}$:

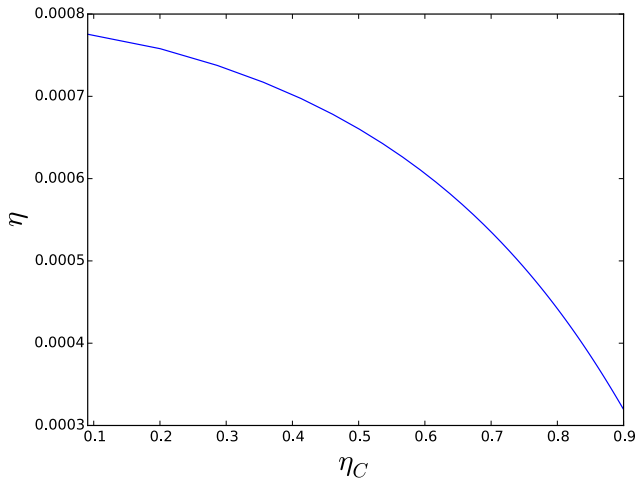

Figure 6.14: Efficiency η *as a function of Carnot efficiency* $\eta_C(T_L)$ *using sinusoidal controls* (6.12) *and parameters* $\mu_L = \mu_R = 0$ *and* $T_R = 1.0$.

The above plot is, to say the least, disturbing, for classically one expects the engine efficiency to increase with η_C, which is the theoretical maximum efficiency, should the engine be operating reversibly in a Carnot cycle[9]. If we plot W_{out} and Q_{in} separately as functions of η_C:

[9]Of course, we are not dealing with a classical engine, and in particular isolated adiabatic and isothermal processes cannot be defined. In fact, one of the major goals of quantum or nanothermodynamics is to study parallels or differences with their classical macroscopic counterparts.

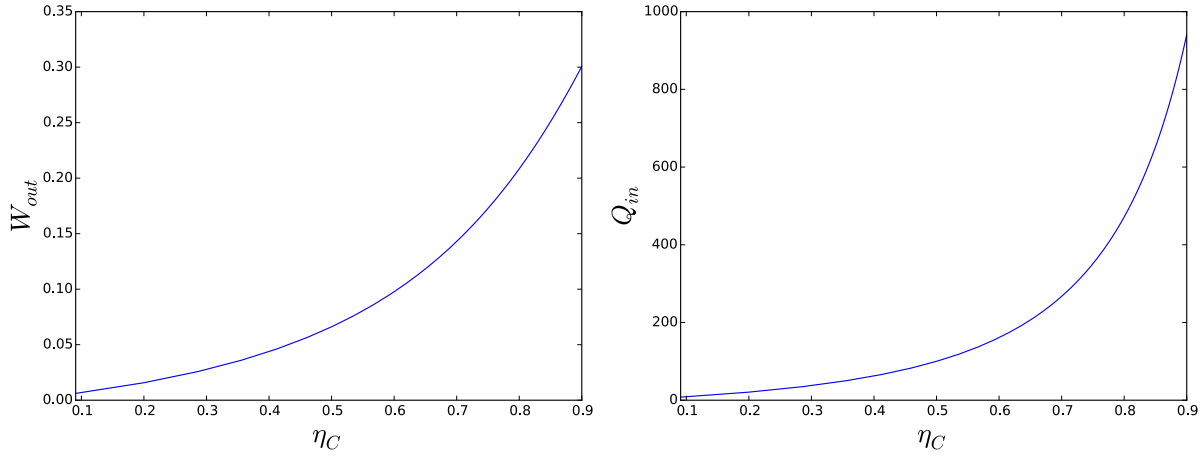

(a) *(b)*

Figure 6.15: (a) W_{out} and (b) Q_{in} as functions of η_C using sinusoidal controls (6.12) *and parameters $\mu_L = \mu_R = 0$ and $T_R = 1.0$.*

we see that luckily the work output and heat input are still monotonous with hot bath temperature T_L (as a function of η_C). This is because as we increase T_L, we need to extend the E integration axis and the spectral function picks up more contributions to the integrals. On the other hand, the problem of η decreasing with η_C can be seen from Figure 6.15 since Q_{in} increases way too fast for W_{out} to catch up. This in fact can be justified from their expressions:

$$\begin{aligned} W_{\text{out}} &= \int_0^T \mathcal{P}_{\text{ext}}\,\mathrm{d}t = \int_0^T \mathrm{d}t \int \frac{\mathrm{d}E}{2\pi} \underbrace{\mathcal{A}(E,t)}_{\propto E^{-4}} \underbrace{\phi^{(0)}(E,t)}_{\propto e^{-\beta_{L/R}|E|}} \dot{\varepsilon}(t), \\ Q_{\text{in}} &= \int_0^T \mathcal{J}_L^Q(t)\,\mathrm{d}t = \int_0^T \mathrm{d}t \int \frac{\mathrm{d}E}{2\pi} \underbrace{A(E,t)(E-\mu_L)}_{\propto E^{-1}} \underbrace{\big(f_L(E) - \phi(E,t)\big)}_{\propto e^{-\beta_{L/R}|E|}} \Gamma_L(t), \end{aligned} \tag{6.14}$$

where the asymptotic behaviours are for large $|E|$. Thus increasing T_L allows the (energy) integrands of both W_{out} and Q_{in} to pick up more contributions, with the former at a rate which is E^{-3} slower. Worse still, to obtain the total work and heat we need integrate over time which spans from $t = 0$ to $t = T = \frac{\pi}{\omega} = 100\pi$. Thus the difference gets further amplified for large time since at each time-step W_{out} and Q_{in} will increase at different speed.

Finally, notice that the argument above does not specify the type of modulations. Thus we have seen that using definition (6.13) as the efficiency η for our cyclic engine, we expect a decrease of η as the corresponding Carnot efficiency η_C increases via an increase of hot bath temperature T_L.

Summary

In this project, by following the literature, we provided detailed derivations in Chapter 2 for the retarded Green's function and the quantum kinetic equation in Esposito's article [1]. Tracing back some of his other articles [24], we then motivated the definitions of proposed thermodynamic variables in Chapter 3.

Under the wide-band approximation, taking into account all possible modulations, we solved analytically and perturbatively the quantum kinetic equation in Chapter 4. Though they are not used, we also obtained perturbative solutions up to second order in Appendix E.

Next, we obtained expressions for the thermodynamic variables in absence of time-dependent driving in Chapter 5 and checked the validity of Onsager reciprocal relation. We also studied the efficiency of a thermoelectric engine operating at maximum power, and showed graphically that in non-weak coupling, the efficiency is reduced for greater coupling strength.

Finally, for the case of driven quantum dot, we proved the impossibility of doing work if a certain proportional coupling is not broken. Then, we proposed protocols that mimic classical stroke engines. We plotted some state diagrams, in particular, a $\mathcal{N} - \varepsilon$ diagram that is analogous to the classical ideal gas engine $p - V$ diagram.

To summarize, we have extended Esposito's studies on the single-level quantum dot by considering steady-state regime and proposing protocols for it to operate as a cyclic heat engine. The next thing to do would be to consider more involved models: a double dot, a linear chain, or a central system with Coulomb interaction. Alternatively, it is very speculative but one might hope to replace (or supplement) gradient expansion with Floquet-Fourier analysis since both involve time-driving and the latter is abundant in the literature [27][37][38].

Let us thus conclude this thesis with Einstein's thought on thermodynamics [39]:

> *A theory is the more impressive the greater the simplicity of its premises, the more different kinds of things it relates, and the more extended its area of applicability. Therefore the deep impression that classical thermodynamics made upon me. It is the only physical theory of universal content which I am convinced will never be overthrown, within the framework of applicability of its basic concepts.*

Appendix A

Moving S-matrices into $\mathcal{T}_t\Big\{ \dots \Big\}$

In this appendix we justify the passage from (1.27):

$$\begin{aligned} &G_\Phi(t_1,t_2)\\ =&-\frac{i}{\hbar}\left\langle\Phi_I(+\infty)\right| S(+\infty,t_0)\mathcal{T}_t\Big\{S(t_0,t_1)a_I(t_1)S(t_1,t_2)a_I^\dagger(t_2)S(t_2,t_0)\Big\}S(t_0,-\infty)\left|\Phi_I(-\infty)\right\rangle \end{aligned}$$

to (1.28):

$$\begin{aligned} &G_\Phi(t_1,t_2)\\ =&-\frac{i}{\hbar}\left\langle\Phi_I(+\infty)\right| \mathcal{T}_t\Big\{S(+\infty,t_1)a_I(t_1)S(t_1,t_2)a_I^\dagger(t_2)S(t_2,-\infty)\Big\}\left|\Phi_I(-\infty)\right\rangle \end{aligned}$$

First, observe that there are three time instants (t_0,t_1,t_2) inside $\mathcal{T}_t$. It is convenient to regard t_0 as the time beyond which we start to study our system: $t_0 \le \min(t_1,t_2)$. Therefore, only two cases: $t_0 \le t_1 \le t_2$ or $t_0 \le t_2 \le t_1$ are possible. We first consider the latter case. $\mathcal{T}_t$ does nothing, and the operators inside the braket become:

$$\begin{aligned} &S(+\infty,t_0)\mathcal{T}_t\Big\{S(t_0,t_1)a_I(t_1)S(t_1,t_2)a_I^\dagger(t_2)S(t_2,t_0)\Big\}S(t_0,-\infty)\\ =&S(+\infty,t_0)S(t_0,t_1)a_I(t_1)S(t_1,t_2)a_I^\dagger(t_2)S(t_2,t_0)S(t_0,-\infty)\\ =&S(+\infty,t_1)a_I(t_1)S(t_1,t_2)a_I^\dagger(t_2)S(t_2,-\infty) \end{aligned} \tag{A.1}$$

Since we are in the case $t_1 \ge t_2 \ge t_0$, the scattering matrix $S(+\infty,t_1)$ contains terms whose time argument is always greater than those to the right of it. Similarly, $S(t_2,-\infty)$ contains terms whose time argument is always less than those to the left of it. Put it differently: the operators are already time-ordered, so we have

$$\begin{aligned} &S(+\infty,t_1)a_I(t_1)S(t_1,t_2)a_I^\dagger(t_2)S(t_2,-\infty)\\ =&\mathcal{T}_t\Big\{S(+\infty,t_1)a_I(t_1)S(t_1,t_2)a_I^\dagger(t_2)S(t_2,-\infty)\Big\} \end{aligned} \tag{A.2}$$

Turning to the case $t_2 \geq t_1 \geq t_0$, we have

$$\begin{aligned}
&S(+\infty, t_0)\mathcal{T}_t\Big\{S(t_0,t_1)a_I(t_1)S(t_1,t_2)a_I^\dagger(t_2)S(t_2,t_0)\Big\}S(t_0,-\infty)\\
=&S(+\infty, t_0)\mathcal{T}_t\Big\{a_{\mathcal{H}}(t_1)a_{\mathcal{H}}^\dagger(t_2)\Big\}S(t_0,-\infty)\\
=&S(+\infty, t_0)\Big\{-a_{\mathcal{H}}^\dagger(t_2)a_{\mathcal{H}}(t_1)\Big\}S(t_0,-\infty)\\
=&S(+\infty, t_0)\Big\{-S(t_0,t_2)a_I^\dagger(t_2)S(t_2,t_1)a_I(t_1)S(t_1,t_0)\Big\}S(t_0,-\infty)\\
=&-S(+\infty,t_2)a_I^\dagger(t_2)S(t_2,t_1)a_I(t_1)S(t_1,-\infty)
\end{aligned} \tag{A.3}$$

Again, this last line is already time-ordered, leading to

$$\begin{aligned}
&-S(+\infty,t_2)a_I^\dagger(t_2)S(t_2,t_1)a_I(t_1)S(t_1,-\infty)\\
=&-\mathcal{T}_t\Big\{S(+\infty,t_2)a_I^\dagger(t_2)S(t_2,t_1)a_I(t_1)S(t_1,-\infty)\Big\}
\end{aligned} \tag{A.4}$$

We demonstrate that after some manipulations, (A.4) will become identical to (A.2). Indeed, switching back to Heisenberg picture and using the fact that fermionic operators anticommute under $\mathcal{T}_t$:

$$\begin{aligned}
&-\mathcal{T}_t\Big\{S(+\infty,t_2)a_I^\dagger(t_2)S(t_2,t_1)a_I(t_1)S(t_1,-\infty)\Big\}\\
=&\mathcal{T}_t\Big\{-S(+\infty,t_0)S(t_0,t_2)a_I^\dagger(t_2)S(t_2,t_1)a_I(t_1)S(t_1,t_0)S(t_0,-\infty)\Big\}\\
=&\mathcal{T}_t\Big\{-S(+\infty,t_0)a_{\mathcal{H}}^\dagger(t_2)a_{\mathcal{H}}(t_1)S(t_0,-\infty)\Big\}\\
=&\mathcal{T}_t\Big\{S(+\infty,t_0)a_{\mathcal{H}}(t_1)a_{\mathcal{H}}^\dagger(t_2)S(t_0,-\infty)\Big\}\\
=&\mathcal{T}_t\Big\{S(+\infty,t_1)a_I(t_1)S(t_1,t_2)a_I^\dagger(t_2)S(t_2,-\infty)\Big\}
\end{aligned} \tag{A.5}$$

Hence, referring back to (1.27), for both cases, we can safely put the far-future and distant-past scattering matrices inside $\mathcal{T}_t$:

$$\begin{aligned}
&G_\Phi(t_1,t_2)\\
=&-\frac{i}{\hbar}\left\langle\Phi_I(+\infty)\right|\mathcal{T}_t\Big\{S(+\infty,t_1)a_I(t_1)S(t_1,t_2)a_I^\dagger(t_2)S(t_2,-\infty)\Big\}\left|\Phi_I(-\infty)\right\rangle
\end{aligned} \tag{A.6}$$

Appendix B

Familiarizing with $\mathcal{T}_t$ and $\mathcal{T}_\tau$

In this appendix, we describe the actions of $\mathcal{T}_t$ and $\mathcal{T}_\tau$ on more than two operators.

B.1 Actions of $\mathcal{T}_t$

When more than two operators are acted upon by $\mathcal{T}_t$, its action is to be applied recursively. To illustrate this point, we denote

$$A_i = A_i(t_i)$$

We then have

$$\begin{aligned}
&\mathcal{T}_t\{A_1 \dots A_k \dots A_n\} \\
&= (-1)^{k-1} A_k \, \mathcal{T}_t\{A_1 \dots A_{k-1} A_{k+1} \dots A_n\} \\
&= (-1)^{k-1} A_k \, (-1)^{m-1} A_m \, \mathcal{T}_t\{A_1 \dots A_{k-1} A_{k+1} \dots A_{m-1} A_{m+1} \dots A_n\} \\
&= \dots
\end{aligned}$$

where we have assumed that $t_k > t_m > t_i, \ \forall i \neq m, k$. In the hope of providing further clarity, we consider three operators A_1, A_2, A_3 with $t_1 < t_2 < t_3$. We have

$$\begin{aligned}
\mathcal{T}_t\{A_1 A_2 A_3\} &= (-1)^2 A_3 \, \mathcal{T}_t\{A_1 A_2\} \\
&= A_3 \, [(-1) A_2 A_1] \\
&= -A_3 A_2 A_1
\end{aligned}$$

For the first line, A_3 is moved twice to the leftmost position and out from $\mathcal{T}_t$, incurring a $(-1)^2$ factor, whereas for the second line, we simply apply the definition of $\mathcal{T}_t$ acting on only two operators.

B.2 Actions of $\mathcal{T}_\tau$

Let us now consider the case of three contour-times, τ_1, τ_2, τ_3:

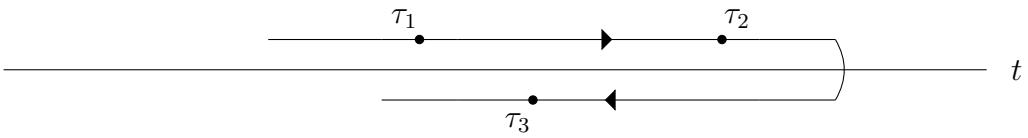

Figure B.1: A contour on which τ_1, τ_2, τ_3 are located.

Clearly, $\tau_3 \succ \tau_2 \succ \tau_1$. Hence, on three fermionic operators A, B, C, the action of $\mathcal{T}_\tau$ is given by:

$$\begin{aligned}
&\mathcal{T}_\tau\Big\{A(\tau_1)B(\tau_2)C(\tau_3)\Big\} \\
&= \mathcal{T}_\tau\Big\{A(\tau_1)[-C(\tau_3)B(\tau_2)]\Big\} && \text{Swap } B, C \text{ with a minus sign} \\
&= -\mathcal{T}_\tau\Big\{[-C(\tau_3)A(\tau_1)]B(\tau_2)\Big\} && \text{Swap } A, C \text{ with a minus sign} \\
&= +\mathcal{T}_\tau\Big\{C(\tau_3)[-B(\tau_2)A(\tau_1)]\Big\} && \text{Swap } A, B \text{ with a minus sign} \\
&= -\mathcal{T}_\tau\Big\{C(\tau_3)B(\tau_2)A(\tau_1)\Big\} \\
&= -C(\tau_3)B(\tau_2)A(\tau_1) && \text{All operators are now contour-ordered}
\end{aligned}$$

Finally, as mentioned previously, two equal contour times are not comparable. Therefore, as in the case for time-ordering, the order of two operators at equal contour time is unchanged by $\mathcal{T}_\tau$. Using Figure B.1 as example, with four fermionic operators A, B, C, D, we have:

$$\begin{aligned}
\mathcal{T}_\tau\Big\{A(\tau_1)B(\tau_2)C(\tau_3)D(\tau_1)\Big\} &= \mathcal{T}_\tau\Big\{A(\tau_1)[-C(\tau_3)B(\tau_2)]D(\tau_1)\Big\} \\
&= -\mathcal{T}_\tau\Big\{[-C(\tau_3)A(\tau_1)]B(\tau_2)D(\tau_1)\Big\} \\
&= +\mathcal{T}_\tau\Big\{C(\tau_3)[-B(\tau_2)A(\tau_1)]D(\tau_1)\Big\} \\
&= -C(\tau_3)B(\tau_2)\mathcal{T}_\tau\Big\{A(\tau_1)D(\tau_1)\Big\} \\
&= -C(\tau_3)B(\tau_2)A(\tau_1)D(\tau_1)
\end{aligned} \tag{B.1}$$

From these, one can inductively deduce the action of $\mathcal{T}_\tau$ for an arbitrary number of operators.

Appendix C

Extending a contour to $+\infty^{\pm}$

We show that the scattering matrix $\mathcal{S}_C(\tau_0^-, \tau_0^+)$ in

$$G(\tau_1, \tau_2) = -\frac{i}{\hbar}\left\langle \mathcal{T}_\tau\Big\{ d_I(\tau_1) d_I^\dagger(\tau_2) \mathcal{S}_C(\tau_0^-, \tau_0^+)\Big\}\right\rangle_0 \tag{C.1}$$

can be transformed to $\mathcal{S}_{C_{\text{ext}}}(\tau_0^-.\tau_0^+)$, where C is the following contour[1]:

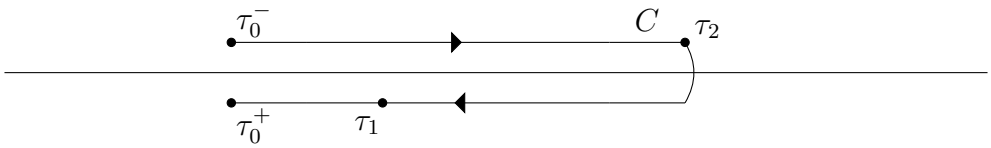

Figure C.1: A general contour C.

and C_{ext} is the same contour extended to $+\infty^{\pm}$:

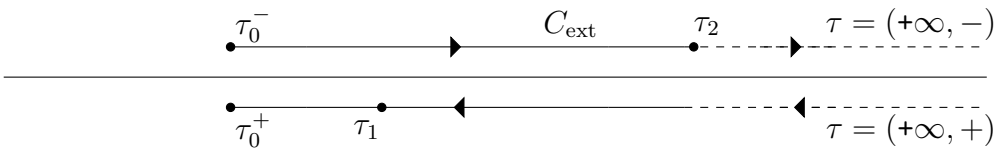

Figure C.2: An extended contour C_{ext} from Figure C.1.

In other words, we intend to show that:

$$\mathcal{T}_\tau\Big\{ d_I(\tau_1) d_I^\dagger(\tau_2) \mathcal{S}_C(\tau_0^-, \tau_0^+)\Big\} = \mathcal{T}_\tau\Big\{ d_I(\tau_1) d_I^\dagger(\tau_2) \mathcal{S}_{C_{\text{ext}}}(\tau_0^+, \tau_0^-)\Big\} \tag{C.2}$$

First of all, suppose $\tau_1 \succ \tau_2$. We begin with the RHS, and to fix idea we choose τ_1, τ_2 as located on Figure C.2:

$$\begin{aligned} &\mathcal{T}_\tau\Big\{ d_I(\tau_1) d_I^\dagger(\tau_2) \mathcal{S}_{C_{\text{ext}}}(\tau_0^+, \tau_0^-)\Big\} \\ =&\mathcal{T}_\tau\Big\{ d_I(\tau_1) d_I^\dagger(\tau_2) \Big[\mathcal{S}(\tau_0^+, \tau_1)\mathcal{S}(\tau_1, +\infty^+)\mathcal{S}(+\infty^-, \tau_2)\mathcal{S}(\tau_2, \tau_0^-)\Big]\Big\} \\ =&\mathcal{S}(\tau_0^+, \tau_1) d_I(\tau_1)\mathcal{S}(\tau_1, +\infty^+)\mathcal{S}(+\infty^-, \tau_2) d_I^\dagger(\tau_2)\mathcal{S}(\tau_2, \tau_0^-) \end{aligned} \tag{C.3}$$

[1]We mentioned in Subsection 2.2.2 that it does not matter whether τ_2 lies on upper or lower branch since for both cases $\tau_1 \succ \tau_2$, but in order to write a proof we here fix τ_2 on the upper branch.

Here comes a good opportunity to investigate the meaning of a scattering matrix admitting contour times as arguments. Consider the two $\mathcal{S}-$matrices sandwiched between $d_I(\tau_1)$ and $d_I^\dagger(\tau_2)$. For $\mathcal{S}(+\infty^-,\tau_2)$, since both $+\infty^-$ and τ_2 are on the upper branch, we have:

$$\begin{aligned}
\mathcal{S}(+\infty^-,\tau_2) &= \mathcal{T}_\tau \exp\left[-\frac{i}{\hbar}\int_\gamma V_I(\tau)\,\mathrm{d}\tau\right] && \gamma \text{ is the path } \tau_2 \to +\infty^- \\
&= \mathcal{T}_t \exp\left[-\frac{i}{\hbar}\int_{t_2}^{+\infty} V_I(s)\,\mathrm{d}s\right] && \text{Along } \gamma \text{ every contour times lie on the same branch} \\
&= S(+\infty,t_2) && \text{The definition of a real-time } S-\text{matrix}
\end{aligned}$$

where, the first line is the formal definition (which serves only manipulations) of a contour-time scattering matrix, whereas the second line is its operationnal definition (which, in principle, can be computed). For the same reason, the other $\mathcal{S}-$matrix is given by:

$$\mathcal{S}(\tau_1,+\infty^+) = \mathcal{T}_t \exp\left[-\frac{i}{\hbar}\int_{+\infty}^{t_1} V_I(s)\,\mathrm{d}s\right] \tag{C.4}$$

Therefore the product of these two can be simplified:

$$\begin{aligned}
\mathcal{S}(\tau_1,+\infty^+)\mathcal{S}(+\infty^-,\tau_2) &= \left\{\mathcal{T}_t \exp\left[-\frac{i}{\hbar}\int_{+\infty}^{t_1} V_I(s)\,\mathrm{d}s\right]\right\}\left\{\mathcal{T}_t \exp\left[-\frac{i}{\hbar}\int_{t_2}^{+\infty} V_I(s)\,\mathrm{d}s\right]\right\} \\
&= S(t_1,+\infty)S(+\infty,t_2) \\
&= S(t_1,t_2) \\
&= \mathcal{T}_t \exp\left[-\frac{i}{\hbar}\int_{t_2}^{t_1} V(s)\,\mathrm{d}s\right] \\
&= \mathcal{T}_\tau \exp\left[-\frac{i}{\hbar}\int_{\tilde\gamma} V(\tau)\,\mathrm{d}\tau\right] \\
&= \mathcal{S}(\tau_1,\tau_2)
\end{aligned}$$

where $\tilde\gamma$ is the path $\tau_2 \to \tau_1$ as in Figure C.1. Equation (C.3) then becomes:

$$\begin{aligned}
&\mathcal{T}_\tau\Big\{d_I(\tau_1)d_I^\dagger(\tau_2)\mathcal{S}_{C_{\text{ext}}}(\tau_0^+,\tau_0^-)\Big\} \\
&= \mathcal{S}(\tau_0^+,\tau_1)d_I(\tau_1)\mathcal{S}(\tau_1,+\infty^+)\mathcal{S}(+\infty^-,\tau_2)d_I^\dagger(\tau_2)\mathcal{S}(\tau_2,\tau_0^-) \\
&= \mathcal{S}(\tau_0^+,\tau_1)d_I(\tau_1)\mathcal{S}(\tau_1,\tau_2)d_I^\dagger(\tau_2)\mathcal{S}(\tau_2,\tau_0^-) \\
&= \mathcal{T}_\tau\Big\{\mathcal{S}(\tau_0^+,\tau_1)d_I(\tau_1)\mathcal{S}(\tau_1,\tau_2)d_I^\dagger(\tau_2)\mathcal{S}(\tau_2,\tau_0^-)\Big\} \\
&= \mathcal{T}_\tau\Big\{d_I(\tau_1)d_I^\dagger(\tau_2)\left[\mathcal{S}(\tau_0^+,\tau_1)\mathcal{S}(\tau_1,\tau_2)\mathcal{S}(\tau_2,\tau_0^-)\right]\Big\} \\
&= \mathcal{T}_\tau\Big\{d_I(\tau_1)d_I^\dagger(\tau_2)\mathcal{S}_C(\tau_0^+,\tau_0^-)\Big\}
\end{aligned} \tag{C.5}$$

Thus for $\tau_1 \succ \tau_2$ with τ_1 on the lower and τ_2 on the upper branch (as in Figure C.1), identity (C.2) is true. The proofs for five other possibilities follow in the same manner and it would not be useful to write them all here.

Appendix D

Exact Solution of First Order Quantum Kinetic Equation

We provide a detailed solution of the first order quantum kinetic equation (4.6):

$$\left[\frac{\partial}{\partial t} + \left(\dot{\varepsilon} + (E - \varepsilon(t))\frac{d_t\Gamma_\nu}{\Gamma_\nu}\right)\frac{\partial}{\partial E}\right]\phi = \frac{2}{A}\left[\frac{\Gamma_L f_L + \Gamma_R f_R}{\Gamma_L + \Gamma_R} - \phi\right] \tag{D.1}$$

First, let

$$v(E,t) = \dot{\varepsilon} + (E - \varepsilon(t))\frac{d_t\Gamma_\nu}{\Gamma_\nu} \tag{D.2}$$

and

$$s(E,t) = \frac{2}{A}\left[\frac{\Gamma_L f_L + \Gamma_R f_R}{\Gamma_L + \Gamma_R} - \phi\right] \tag{D.3}$$

We then have

$$\left[\frac{\partial}{\partial t} + v(E,t)\frac{\partial}{\partial E}\right]\phi(E,t) = s(E,t) \tag{D.4}$$

Suppose $z = \phi(E,t)$ is a solution. If we now consider a function $w(t,E,z) = \phi(E,t) - z$, then the two dimensional surface $w = 0$ yields the function we seek, $z = \phi(E,t)$. The advantage of going one dimension higher is that we can write (4.6) as:

$$\begin{bmatrix} 1 & v(E,t) & s(E,t) \end{bmatrix} \cdot \begin{bmatrix} \frac{\partial\phi}{\partial t} & \frac{\partial\phi}{\partial E} & -1 \end{bmatrix} = 0 \tag{D.5}$$

The second vector in the dot product is nothing but the gradient of w:

$$\nabla w(t,E,z) = \begin{bmatrix} \frac{\partial\phi}{\partial t} & \frac{\partial\phi}{\partial E} & -1 \end{bmatrix} \tag{D.6}$$

Therefore, suppose we have a curve

$$\begin{aligned} \gamma : \mathbb{R} &\longrightarrow \mathbb{R}^3 \\ \lambda &\longmapsto \begin{bmatrix} t(\lambda) & E(\lambda) & z(\lambda) \end{bmatrix} \end{aligned} \tag{D.7}$$

such that its tangent vector satisfies

$$\begin{aligned}\frac{\mathrm{d}t(\lambda)}{\mathrm{d}\lambda} &= 1\\ \frac{\mathrm{d}E(\lambda)}{\mathrm{d}\lambda} &= v(\lambda) = v(E(\lambda), t(\lambda))\\ \frac{\mathrm{d}z(\lambda)}{\mathrm{d}\lambda} &= s(\lambda) = s(E(\lambda), t(\lambda))\end{aligned} \tag{D.8}$$

Then, (D.5) is saying that the curve $\gamma(\lambda)$ is always perpendicular to ∇w. Thus if we choose the initial condition $\gamma(\lambda = 0)$ such that it lies on the surface $w = 0$, then the curve stays on the surface for all $\lambda > 0$. Since $z = \phi$ on $w = 0$, solving for the third component of $\gamma(\lambda)$ is therefore tantamount to solving for ϕ. Hence, we seek to solve (D.8) subject to the initial condition

$$\begin{aligned}t(\lambda = 0) &= 0\\ E(\lambda = 0) &= E_0\\ z(\lambda = 0) &= \phi(E_0, 0)\end{aligned} \tag{D.9}$$

The first component is easy: $t(\lambda) = \lambda$. Next, using prime $'$ to denote $\frac{\mathrm{d}}{\mathrm{d}\lambda}$, with the result $t = \lambda$ we have for the second component:

$$\begin{aligned}E'(\lambda) &= \varepsilon'(\lambda) + (E(\lambda) - \varepsilon(\lambda))\frac{\Gamma_\nu'(\lambda)}{\Gamma_\nu(\lambda)}\\ E(\lambda) - \varepsilon(\lambda) &= \frac{E(0) - \varepsilon(0)}{\Gamma_\nu(0)}\Gamma_\nu(\lambda)\end{aligned} \tag{D.10}$$

As for the last component, denote $g = \frac{\Gamma_L f_L + \Gamma_R f_R}{\Gamma_L + \Gamma_R}$. Recalling that we start from the surface $w = 0$ to ensure $z = \phi$. Thus we need to solve the following first order inhomogeneous ordinary differential equation:

$$\frac{\mathrm{d}\phi(\lambda)}{\mathrm{d}\lambda} = \frac{2}{A(\lambda)}(g(\lambda) - \phi(\lambda)) \tag{D.11}$$

with initial condition $\phi(\lambda = 0) = \phi(E(\lambda = 0), t(\lambda = 0))$. This is doable and we provide the solution:

$$\phi(\lambda) = \phi(0)\exp\Big[-\int_0^\lambda \frac{2}{A(\mu)}\mathrm{d}\mu\Big] + \int_0^\lambda \left(\exp\Big[-\int_\mu^\lambda \frac{2}{A(\alpha)}d\alpha\Big]\right)\frac{2}{A(\mu)}g(\mu)\mathrm{d}\mu \tag{D.12}$$

Now we must revert to the original variables E, t. Earlier we denoted $E(\lambda) = E_0$ to avoid confusion, but this "initial energy" is really just an arbitrary point on energy axis: $E_0 \to E$. Thus for the spectral function $A(\lambda) = A(E(\lambda), t(\lambda))$, we have:

$$\begin{aligned}A(E(\lambda), t(\lambda)) &= \frac{\Gamma_\nu(\lambda)}{(E(\lambda) - \varepsilon(\lambda))^2 + (\frac{\Gamma_\nu}{2})^2}\\ &= \left[\left(\frac{E - \varepsilon(0)}{\Gamma_\nu(0)}\right)^2 + \frac{1}{4}\right]^{-1}\frac{1}{\Gamma_\nu(t)}\end{aligned} \tag{D.13}$$

As for the Fermi functions:

$$f_\nu(E(\lambda)) = f_\nu\left(\varepsilon(t) + \frac{E-\varepsilon(0)}{\Gamma_\nu(0)}\Gamma_\nu(t)\right) \tag{D.14}$$

Denote

$$K(E,t) = 2\left[\left(\frac{E-\varepsilon(0)}{\Gamma_\nu(0)}\right)^2 + \frac{1}{4}\right]\Gamma_\nu(t) \tag{D.15}$$

and

$$g(E,t) = \frac{\Gamma_L(t) f_L\left(\varepsilon(t) + \frac{E-\varepsilon(0)}{\Gamma_\nu(0)}\Gamma_\nu(t)\right) + \Gamma_R(t) f_R\left(\varepsilon(t) + \frac{E-\varepsilon(0)}{\Gamma_\nu(0)}\Gamma_\nu(t)\right)}{\Gamma_L(t) + \Gamma_R(t)} \tag{D.16}$$

we thus obtain an explicit expression for the occupation probability:

$$\phi(E,t) = \phi(E,0)e^{-\int_0^t K(E,t')\mathrm{d}t'} + \int_0^t e^{-\int_{t'}^t K(E,t'')\mathrm{d}t''} K(E,t')g(E,t')\mathrm{d}t' \tag{D.17}$$

Appendix E

Second Order Gradient Expansion

In this appendix we discuss second order gradient expansion. We need to return to (2.134) and expand the operator $\overleftrightarrow{\mathcal{G}}$ to second order in $\frac{\partial}{\partial t}$, for the symbolic commutator, anticommutator, as well as for g^{-1}. Here we reintroduce $\hbar$ to keep track of dimensional consistency. Since the procedure is similar as discussed in Section 2.7, we only list the results:

$$\mathscr{W}(\{g^{-1},h\}) = \left[2(E-\varepsilon(t)) + \frac{\hbar^2}{4}\ddot{\varepsilon}(t)\partial_E^2\right] h(E,t) \tag{E.1}$$

$$\mathscr{W}([g^{-1},h]) = i\hbar(\partial_t + \dot{\varepsilon}(t)\partial_E)h(E,t) \tag{E.2}$$

$$\mathscr{W}(\{A,B\}) = 2AB - \frac{\hbar^2}{4}(\partial_E^2 A\,\partial_t^2 B + \partial_t^2 A\,\partial_E^2 B) \tag{E.3}$$

$$\mathscr{W}([A,B]) = i\hbar\{A,B\}_{E,t} + \frac{\hbar^2}{2}(\partial_t A\,\partial_E A\,\partial_t B\,\partial_E B) \tag{E.4}$$

Next, we directly invoke wide-band approximation, so that $\Sigma^R = -\frac{i\Gamma}{2}$ and $\partial_E\Gamma = 0$.

E.1 Second order retarded Green's function

We apply the new rules to (2.145) to obtain the following equation for the retarded Green's function:

$$\frac{\hbar^2}{8}\left(\ddot{\varepsilon} - \frac{i\ddot{\Gamma}}{2}\right)\partial_E^2 G^R = 1 - \left(E - \varepsilon + \frac{i\Gamma}{2}\right)G^R \tag{E.5}$$

Writing $G^R(E,t) = G^{R(0)}(E,t) + G^{R(1)}(E,t) + G^{R(2)}(E,t)$, we find that:

$$G^{R(0)} = \frac{1}{E - \varepsilon(t) + \frac{i\Gamma}{2}} \tag{E.6}$$

$$G^{R(1)} = 0 \tag{E.7}$$

$$G^{R(2)} = -\frac{\hbar^2}{8}\frac{\ddot{\varepsilon} - \frac{i\ddot{\Gamma}}{2}}{E - \varepsilon + \frac{i\Gamma}{2}}\partial_E^2 G^{R(0)} \tag{E.8}$$

E.2 Second order quantum kinetic equation

As above, we apply the new rules to the Kadanoff-Baym equation for $G^<$ under the wide band limit. Invoking again the Kadanoff-Baym ansatz $G^< = iA\phi$ and bearing in mind that to second order the Botermans-Malfliet approximation is no longer valid, we obtain the following equation for ϕ:

$$\begin{aligned}&(\partial_t + \dot{\varepsilon}\partial_E)(A\phi) + (\partial_E \mathrm{Re}\, G^R)\dot{\Gamma} f - (\partial_t \mathrm{Re}\, G^R)(\partial_E f)\Gamma + \frac{\hbar}{2}(\partial_t \mathrm{Re}\, G^R)(\partial_E \mathrm{Re}\, G^R)(\Gamma f)\dot{\Gamma}\partial_E f \\ &= \frac{1}{\hbar}\Gamma A(f-\phi) - \frac{\hbar}{8}\Big[\Gamma(\partial_E^2 f)(\partial_t^2 A) + f\ddot{\Gamma}\partial_E^2 A - \ddot{\Gamma}\partial_E^2(A\phi)\Big]\end{aligned} \tag{E.9}$$

where we remind that when Γ and f appear together they must be summed over reservoirs. For completeness, we list here the perturbative solutions for $\phi(E,t) = \phi^{(0)}(E,t) + \phi^{(1)}(E,t) + \phi^{(2)}(E,t)$, even though we will not be using them due to their complexities:

$$\phi^{(0)} = \frac{\Gamma_L f_L + \Gamma_R f_R}{\Gamma_L + \Gamma_R} \tag{E.10}$$

$$\begin{aligned}\phi^{(1)} = -\frac{\hbar}{\Gamma}\Bigg\{ & A\left[\frac{1}{4} - \left(\frac{E-\varepsilon}{\Gamma}\right)^2\right]\Big[(\dot{\Gamma_L}\Gamma_R - \dot{\Gamma_R}\Gamma_L)(f_L - f_R) + \dot{\varepsilon}(\Gamma_L\partial_E f_L + \Gamma_R \partial_E f_R)\Big] \\ & + \frac{A\dot{\Gamma}}{2\Gamma}(E-\varepsilon)(\Gamma_L\partial_E f_L + \Gamma_R\partial_E f_R) + (\partial_t + \dot{\varepsilon}\partial_E)\phi^{(0)}\Bigg\}\end{aligned} \tag{E.11}$$

where $A = A^{(0)} = -2\mathrm{Im}\, G^{R(0)}$. The reason that it does not agree with (4.14) is because for expressions accurate to second order in ∂_t, one could not apply the Botermans-Malfliet approximation. As for $\phi^{(2)}$ we have:

$$\begin{aligned}\phi^{(2)} = -\frac{\hbar}{A\Gamma}\Bigg\{ & (\partial_t A + \dot{\varepsilon}\partial_E)\phi^{(1)} + A(\partial_t + \dot{\varepsilon}\partial_E)\phi^{(1)} \\ & + \frac{\hbar}{2}\Big(\partial_t \mathrm{Re}\, G^R\Big)\Big(\partial_E \mathrm{Re}\, G^R\Big)(\Gamma_L f_L + \Gamma_R f_R)(\dot{\Gamma_L}\partial_E f_L + \dot{\Gamma_R}\partial_E f_R) \\ & - \frac{\hbar}{8}\Big[(\Gamma_L\partial_E^2 f_L + \Gamma_R\partial_E^2 f_R)\partial_t^2 A + (\ddot{\Gamma_L} f_L + \ddot{\Gamma_R} f_R)\partial_E^2 A - \partial_t^2\Gamma\partial_E^2\big(A\phi^{(0)}\big)\Big]\Bigg\}\end{aligned} \tag{E.12}$$

Finally, we conclude this Appendix with the following remark: when $\overleftrightarrow{\mathcal{G}}$ is expanded up to first order in ∂_t, we had a convection equation, cf. (4.6). Interestingly, when we keep ∂_t up to second order, we obtain a drift-diffusion equation (E.9), since the only derivatives (acting on ϕ) involved are ∂_t, ∂_E and ∂_E^2.

Bibliography

[1] M. Esposito, M. Ochoa, and M. Galperin. *Quantum Thermodynamics: A Nonequilibrium Greens Function Approach*. Phys. Rev. Lett. 114, 080602 (2015).

[2] A.B. Pippard. *Elements of Classical Thermodynamics: For Advanced Students of Physics*. Cambridge University Press. ISBN-13: 978-0521091015 (1957).

[3] U. Seifert. *Stochastic thermodynamics, fluctuation theorems and molecular machines*. Rep. Prog. Phys. 75 126001 (2012).

[4] F. Brandão, M. Horodecki, N. Ng, J. Oppenheim, and S. Wehner. *The second laws of quantum thermodynamics*. PNAS 112 (11) pp. 3275-3279 (2015).

[5] M. Esposito, M. Ochoa, and M. Galperin. *Nature of heat in strongly coupled open quantum systems*. Phys. Rev. B 92, 235440 (2015).

[6] E. Fermi. *Thermodynamics*. Dover Publications. ISBN-13: 080-0759603619 (1956).

[7] C. Truesdell, S. Bharatha. *The Concepts and Logic of Classical Thermodynamics as a Theory of Heat Engines*. Springer Berlin Heidelberg. DOI: 10.1007/978-3-642-81077-0 (1977).

[8] D. R. Owen. *A First Course in the Mathematical Foundations of Thermodynamics*. Springer New York. DOI: 10.1007/978-1-4613-9505-8 (1984).

[9] S. Carnot. *Réflexions sur la puissance motrice du feu et sur les machines propres à développer cette puissance*. (French) [*Reflections on the motive power of fire*]. Bachelier (Paris). ARK:/12148/btv1b86266609 (1824).

[10] T. Schmiedl, U. Seifert. *Efficiency at maximum power: An analytically solvable model for stochastic heat engines*. EPL 81 20003 (2008).

[11] H.T. Quan, Y-x. Liu, C.P. Sun and F. Nori. *Quantum Thermodynamic Cycles and quantum heat engines*. Phys. Rev. E 76. 031105 (2007).

[12] J. Jaramillo, M. Beau and A. del Campo. *Quantum Supremacy of Many-Particle Thermal Machines*. arXiv:1510.04633v3 (2016).

[13] M. Azimi, L. Chotorlishvili, S. K. Mishra, T. Vekua, W. Hübner, and J. Berakdar. *Quantum Otto heat engine based on a multiferroic chain working substance*. New Journal of Physics 16 063018 (2014).

[14] S. Carroll. *Spacetime and Geometry: An Introduction to General Relativity*. Pearson. ISBN-13: 978-0805387322 (2003).

[15] H. Haug, A-P. Jauho. *Quantum Kinetics in Transport and Optics of Semiconductors*. Springer-Verlag Berlin Heidelberg. DOI:10.1007/978-3-540-73564-9 (2008).

[16] J. Rammer. *Quantum Transport Theory (Frontiers in Physics)*. Westview Press. ISBN-13: 978-0813342849 (2004).

[17] L.G. Molinari. *Another proof of Gell-Mann and Low's theorem*. J. Math. Phys. 48, 052113 (2007).

[18] J.-S. Wang, J. Wang, J.T. Lü. *Quantum thermal transport in nanostructures*. The European Physical Journal B, Volume 62, Issue 4, pp. 381-404 (2008).

[19] G. Stefanucci, R. van Leeuwen. *Nonequilibrium Many-Body Theory of Quantum Systems: A Modern Introduction*. Cambridge University Press. ISBN-13: 978-0521766173 (2013).

[20] T. Kita. *Introduction to Nonequilibrium Statistical Mechanics with Quantum Field Theory*. Prog. Theor. Phys. 123 (4): 581-658 (2010).

[21] A.L. Fetter, J.D. Walecka. *Quantum Theory of Many-Particle Systems*. Dover Publications. ISBN-13: 978-0486428277 (2003).

[22] J.-S. Wang, B. K. Agarwalla, H. Li, and J. Thingna. *Nonequilibrium Greens function method for quantum thermal transport*. Front. Phys. 9, 673 (2014).

[23] W. Botermans, R. Malfliet. *Quantum transport theory of nuclear matter*. Physics Reports Volume 198, Issue 3, pp. 115-194 (1990).

[24] C. Van den Broeck, M. Esposito. *Ensemble and trajectory thermodynamics: A brief introduction*. Elsevier. Physica A: Statistical Mechanics and its Applications, Volume 418, pp. 616 (2015).

[25] R. Kosloff. *Quantum Thermodynamics: A Dynamical Viewpoint*. Entropy, 15(6), pp. 2100-2128. DOI:10.3390/e15062100 (2013).

[26] S. Datta. *Electronic Transport in Mesoscopic Systems*. Cambridge University Press. ISBN-13: 978-0521599436 (1997).

[27] T. Dittrich, P. Hänggi, G.-L. Ingold, B. Kramer, G. Schön and W. Zwerger. *Quantum Transport and Dissipation*. Wiley-VCH. ISBN-13: 978-3527292615 (1998).

[28] H. D. Cornean, A. Jensen and V. Moldoveanu. *A rigorous proof of the LandauerBüttiker formula*. J. Math. Phys. 46, 042106 (2005).

[29] D. Kondepudi, I. Prigogine. *Modern Thermodynamics: From Heat Engines to Dissipative Structures, 2nd Edition*. John Wiley & Sons Inc. ISBN-13: 978-1118371817 (2014).

[30] N. Pottier. *Nonequilibrium Statistical Physics: Linear Irreversible Processes*. Oxford University Press. ISBN-13: 978-0199556885 (2009).

[31] S.R. De Groot, P. Mazur. *Non-Equilibrium Thermodynamics*. Dover Publications. ISBN-13: 978-0486647418 (2011).

[32] G. Verley, T. Willaert, C. Van den Broeck, and M. Esposito. *Universal theory of efficiency fluctuations*. Phys. Rev. E 90, 052145 (2014).

[33] M. Campisi. *Fluctuation relation for quantum heat engines and refrigerators*. J. Phys. A: Math. Theor. 47 245001 (2014).

[34] F.L. Curzon, B. Ahlborn. *Efficiency of a Carnot engine at maximum power output*. American Journal of Physics, Volume 43, Issue 1, pp. 22-24 (1975).

[35] M. Esposito, K. Lindenberg and C. Van den Broeck. *Thermoelectric efficiency at maximum power in a quantum dot*. EPL 85 60010 (2009).

[36] Z.C. Tu. *Efficiency at maximum power of Feynman's ratchet as a heat engine*. J. Phys. A: Math. Theor. 41 312003 (2008).

[37] G.B. Cuetara, A. Engel and M. Esposito. *Stochastic thermodynamics of rapidly driven systems*. New J. Phys. 17 055002 (2015).

[38] A. Agarwal, D. Sen. *Equation of motion approach to non-adiabatic quantum charge pumping*. J. Phys.: Condens. Matter 19 046205 (2007).

[39] P. A. Schilpp. *Albert Einstein, Philosopher-Scientist: The Library of Living Philosophers Volume VII*. Open Court. ISBN-13: 979-0875482865 (1998).